

**NOVEL ANTIMICROBIAL PEPTIDE COATING TO PREVENT CATHETER-  
ASSOCIATED URINARY TRACT INFECTIONS**

by

Joey Chor Yee Lo

B.Sc., The University of British Columbia, 2012

A THESIS SUBMITTED IN PARTIAL FULFILLMENT OF  
THE REQUIREMENTS FOR THE DEGREE OF

MASTER OF SCIENCE

in

THE FACULTY OF GRADUATE AND POSTDOCTORAL STUDIES  
(Experimental Medicine)

THE UNIVERSITY OF BRITISH COLUMBIA

(Vancouver)

December 2015

© Joey Chor Yee Lo, 2015

## Abstract

**Introduction:** Urinary catheters provide ideal surfaces for bacterial biofilm formation, being a major factor for hospital-acquired infections. With increased antibiotic resistance, there is a push for non-antibiotic-based measures to prevent catheter-associated urinary tract infections (CAUTI). I pursue the use of polymer-linked, broad-spectrum, host-defense-based antimicrobial peptides (AMPs) as novel catheter coatings. Here, I present the efficacy of tethered AMPs against common uropathogens both *in vitro* and *in vivo*.

**Materials and Methods:** Peptides E6, Tet20, Tet26, and Kai13 were linked to surfaces using polymer brushes PDMA, PMPC, and PMPDSAH. All peptides were chosen based on their antimicrobial activity and biocompatibility as suggested by previously published papers. Antimicrobial activity of each coating was determined *in vitro* via colony counts 6 hours post-exposure to uropathogens. The *in vivo* efficacy of AMP coatings was also tested using a clinically relevant CAUTI mouse model; bladders of mice were catheterized percutaneously under ultrasound guidance, and 50  $\mu$ L of 5E+5 CFU/mL *P. aeruginosa* was instilled. Indwelling polyurethane catheters and urine were collected after 7 days for examination of bacterial adherence and growth.

**Results:** The most effective peptide-brush combination was E6-PDMA, decreasing bacterial adhesion and planktonic growth by up to 94.1% and 63.8%, respectively based on *in vitro* data. *In vivo* results look even more promising; the coating decreased bacterial adhesion by up to 99.9958% and planktonic growth by 99.8660% in comparison to untreated mice.

**Conclusions:** Based on our *in vitro* and *in vivo* data, E6-PDMA coatings may effectively prevent CAUTI. Further testing of these novel coatings against more common uropathogens as well as tests to confirm the safety of such coatings will be important.

## Preface

Joey Chor Yee Lo was involved in designing, conducting, and analysing the research data under the direct guidance of Dr. Dirk Lange with assistance from the Kizhakkedathu lab and the Hancock lab at The University of British Columbia. Specifically, Dr. Kai Yu from the Kizhakkedathu lab was responsible for the making of the peptide coatings used throughout the project. Dr. Igor Moskalev from the Vancouver Prostate Centre also provided assistance and guidance for all animal work performed.

Some data presented in this thesis were published by Joey in the following articles:

Lo, Joey and Dirk Lange, Current and Potential Applications of Host-Defense Peptides and Proteins in Urology, *BioMed Research International*, Volume 2015, Article ID 189016, 9 pages, 2015.

Lo, Joey, Dirk Lange, and Ben H. Chew, Ureteral Stents and Foley Catheters-Associated Urinary Tract Infections: The Role of Coatings and Materials in Infection Prevention. *Antibiotics* **2014**, 3(1) 87-97.

All animal work conducted for this study was approved by The University of British Columbia Animal Care Committee. Animal Care Service's Rodent Biological and Husbandry training course was completed through the UBC Animal Care Centre (certificate # RBH-272-12). Animal Care Service's Principles of Rodent Anesthesia course was completed through the UBC Animal Care Centre (certificate # RA-128-12). Animal Care Service's Principles of Rodent Surgery training course was completed through the UBC Animal Care Centre (certificate # RSx-94-12). Animal work ethics training was completed and met the requirements of the Canadian Council of Animal Care/National Institutional Animal User Training Program (CCAC, certificate # 4588-13).

## Table of Contents

Abstract .....	ii
Preface.....	iii
Table of Contents .....	iv
List of Tables .....	viii
List of Figures .....	ix
List of Abbreviations .....	xi
Acknowledgements .....	xiii
Chapter 1: Introduction .....	1
1.1 Catheter-associated urinary tract infections .....	1
1.1.1 Catheters: What they are and how they are used .....	1
1.1.2 Contamination by bacteria .....	4
1.1.3 Symptoms of urinary tract infections.....	5
1.1.4 Bacterial adhesion and biofilm formation.....	5
1.1.5 Major uropathogens involved .....	7
1.1.6 Mechanisms of adhesion.....	8
1.2 Prevention of CAUTI: .....	11
1.2.1 Limiting their use, proper hygiene procedures, and alternatives .....	11
1.2.2 Antimicrobial implant coatings .....	13
1.3 Novel antimicrobial peptides as an alternative to conventional antibiotics.....	17

1.3.1	Antimicrobial peptides: What are they? .....	17
1.3.2	General properties of AMPs and their mechanisms of action for membrane disruption .....	19
1.3.3	Ability of AMPs to target intracellular components and processes.....	22
1.3.4	Synthesis of AMPs with further modifications.....	23
1.3.5	Using AMPs to prevent CAUTI .....	23
1.3.6	Challenges faced by AMPs .....	24
1.3.7	Optimizing the peptide coating: The use of polymer brushes .....	25
1.3.8	Assessment of polymer-peptide coatings in past literature.....	28
1.3.9	The optimal polymer-peptide coating .....	30
1.4	Thesis objective: Investigating the use of novel antimicrobial peptide coating to prevent catheter-associated urinary tract infections.....	31
Chapter 2: Methods.....		32
2.1	<i>In vitro</i> studies.....	32
2.1.1	Large-scale activity screening of tethered AMPs using nanoparticles .....	32
2.1.1.1	Synthesis of polymer-AMP coated nanoparticles.....	32
2.1.1.2	Temporary storage of peptide-coated nanoparticles .....	34
2.1.1.3	<i>In vitro</i> testing of polymer-AMPs-coated, polymer-coated, and uncoated NPs .....	35
2.1.1.3.1	Bacterial strains.....	35
2.1.1.4	Antimicrobial testing of AMPs tethered to NPs .....	35
2.1.1.4.1	Determining bacterial concentration via luminescence .....	37
2.1.1.4.2	Determining bacterial concentration via colony forming units (CFU) counts .....	37
2.1.2	Testing tethered AMPs using polyurethane catheters.....	37

2.1.2.1	Preparing catheter pieces for coating .....	37
2.1.2.2	Synthesis of brush-AMP coating onto modified 18G PU catheter pieces .....	38
2.1.2.3	Bacteria and <i>in vitro</i> testing of coating 18G PU catheters.....	38
2.1.2.4	Antimicrobial testing of AMP tethered 18G PU catheters <i>in vitro</i> .....	39
2.1.2.5	Determining bacterial adherence on coated and uncoated polyurethane catheters...	39
2.1.2.6	Determining bacterial planktonic growth/survival when co-incubated with coated and uncoated polyurethane catheters .....	39
2.2	<i>In vivo</i> studies .....	40
2.2.1	Transurethral catheterization model .....	40
2.2.1.1	Bacterial strain, culture medium and animals.....	40
2.2.1.2	Modification of catheters .....	40
2.2.1.3	Day 0: Transurethral catheterization and bacterial instillation .....	41
2.2.1.4	Daily monitoring.....	44
2.2.1.5	Day 5: Assessment of urinary tract infection and bacterial adhesion and biofilm formation.....	44
2.2.2	Percutaneous catheterization model.....	44
2.2.2.1	Bacterial strain, culture medium and animals.....	44
2.2.2.2	Modification of catheter.....	45
2.2.2.3	Coating 24G PU catheters for <i>in vivo</i> testing.....	45
2.2.2.4	Day 0: Percutaneous catheter implantation.....	46
2.2.2.5	Day 1: Bacterial instillation into rodent bladder .....	48
2.2.2.6	Days 1 and 7: IVIS® Lumina imaging to confirm presence of bacteria .....	48
2.2.2.7	Daily monitoring.....	48

2.2.2.8 Day 7: Assessment of urinary tract infection and bacterial adhesion and biofilm formations .....	49
2.2.2.9 Performing percutaneous catheterization on rats .....	49
2.3 Statistical analysis .....	49
Chapter 3: Results .....	50
3.1 Surface-tethered AMPs are less effective than free-floating counterparts .....	50
3.2 PDMA results in better antimicrobial activity than PMPC and PMPDSAH when conjugated to selected peptides .....	51
3.3 Tethered E6 is more potent than tethered Tet20 .....	54
3.4 PDMA-E6 coated PU catheters significantly reduces both bacterial adhesion and planktonic bacterial growth <i>in vitro</i> .....	56
3.5 Ultrasound-guided percutaneous catheterization model is a more reliable CAUTI model than the transurethral catheterization model .....	59
3.6 Coated and uncoated 4mm-long, 24G polyurethane catheters successfully implanted percutaneously into mice bladder.....	62
3.7 Antimicrobial activity of PDMA-E6-coated implants is observed <i>in vivo</i> 7 days post-instillation.....	68
Chapter 4: Discussion .....	70
Chapter 5: Conclusion and Future Directions.....	82
References .....	83

## List of Tables

Table 1. Three main types of urinary catheters.....	2
Table 2. Clinical signs presented by asymptomatic versus symptomatic UTI patients.....	5
Table 3. Different types of antimicrobial implant coatings used to prevent bacterial adhesion and subsequent UTI.....	15
Table 4. Recently synthesized AMPs .....	23
Table 5. Summary of AMPs used in combination with low-fouling surface coatings .....	28
Table 6. Name and amino acid sequence of peptides tested using NPs .....	34
Table 7. Bacterial strains used to test peptide-coated nanoparticles.....	35



## List of Figures

Figure 1. A Foley catheter .....	3
Figure 2. The main categories of AMPs based on their size, AA composition, and conformational structures .....	19
Figure 3. The three most commonly-discussed models of membrane disruption by AMPs .....	21
Figure 4. Increasing the density of peptides loaded onto implant surfaces using co-polymer brushes .....	26
Figure 5. Two general techniques used to apply polymers (and AMPs) onto implant surfaces....	27
Figure 6. Co-polymer brushes tested <i>in vitro</i> .....	33
Figure 7. Synthesis of polymer brushes on NPs followed by conjugation of AMPs .....	34
Figure 8. Spot plating method allowing for large-scale screening of antimicrobial activity.....	36
Figure 9. Preparing catheter pieces for coating .....	38
Figure 10. Modification of 18G PU catheter .....	41
Figure 11. Transurethral catheter implantation into rat bladder .....	43
Figure 12. Modification of 24G I.V. PU catheter for <i>in vivo</i> testing.....	45
Figure 13. Ultrasound-guided percutaneous catheter implantation into mouse bladder .....	47
Figure 14. CFU counts of different brush-peptide samples co-incubated with bacteria .....	52
Figure 15. Relative luminescence readings of different brush-peptide samples co-incubated with bacteria.....	53
Figure 16. Comparison in bactericidal properties between PDMA-E6 and PDMA-Tet20 .....	55
Figure 17. Effect of PDMA- and PDMA-E6-coated polyurethane catheters on bacterial adherence and planktonic growth of <i>P. aeruginosa</i> .....	57

Figure 18. Effect of PDMA- and PDMA-E6-coated polyurethane catheters on bacterial adherence and planktonic growth of <i>S. saprophyticus</i> .....	58
Figure 19. The Sprague Dawley rat’s urethral opening (meatus) appears to lead to both the urethra and a dead-end groove.....	60
Figure 20. Amount of bacteria recovered via CFU counts from implanted catheters, and rodent urine from <i>S. aureus</i> -infect and uninfected control rats .....	61
Figure 21. IVIS® images of mice bearing either uncoated or coated catheter .....	63
Figure 22. Bioluminescence readings measured for untreated and treated mice using the IVIS® Lumina .....	64
Figure 23. Ultrasound images of bladders of mice with uncoated or coated implant pieces (1 day post-bacterial instillation) .....	65
Figure 24. Ultrasound images of bladders of mice with uncoated or coated implant pieces (4 days post-bacterial instillation) .....	66
Figure 25. Ultrasound images of bladders of mice with uncoated or coated implant pieces (7 days post-bacterial instillation) .....	67
Figure 26. Antimicrobial activity of PDMA-E6-coated catheters <i>in vivo</i> .....	69
Figure 27. Amino acid sequence of peptides E6 and Tet20 .....	72
Figure 28. Illustration of the relative size of bacteria in comparison to 1 mm-long catheter pieces and NPs .....	74
Figure 29. Hypothesized outcome of when AMPs of peptide-brush coatings come in contact with live bacteria and released LTA .....	77

## List of Abbreviations

AA	Amino acid
AMPs	Antimicrobial peptides
BM2	Basal medium 2
CAUTI	Catheter-associated urinary tract infections
CFU	Colony forming units
LB	Lysogeny broth
LPS	Lipopolysaccharide
LTA	Lipoteichoic acids
MDA	Multi-drug resistant
NPs	Nanoparticles
O/N	Overnight
PAM	Polyacrylamide
PAPMA	Poly N-(3-aminopropyl) methacrylamide
PBS	Phosphate buffered saline
PDMA	Poly (N,N-dimethylacrylamide)
PDMA-co-APMA	Poly(N,N-dimethylacrylamide)-co-N-(3-Aminopropyl)methacrylamide
PEG	Polyethylene glycol
PHPMA	Poly(N-hydroxypropyl methacrylamide)
PMPC-co-APMA	Poly(2-methacryloyloxyethyl phosphorylcholine)-co-N-(3-Aminopropyl)methacrylamide

PMPDSAH-co-APMA	poly(3-methacryloylamido)propyl)-N,N-dimethyl(3-sulfopropyl)ammonium hydroxide)-co-N-(3-Aminopropyl) methacrylamide
PS	Polystyrene
PSBMA	Poly(N-sulfobetaine methacrylamide)
PVP	Polyvinylpyrrolidone
ROI	Region of interest
RT	Room temperature
Si	Silicone
SI-ATRP	Surface-initiated atom transfer radical polymerization
THP	Tamm-Horsfall protein
Ti	Titanium
Ti-wires	Titanium wires
UBC	University of British Columbia
UTI	Urinary tract infection

## Acknowledgements

Being part of the UBC Experimental Medicine Program been a journey filled with both joy and frustration, but nonetheless, it has been a great learning experience for me. Through this program, I learned to appreciate the amount of time and effort involved in discovering new research findings and the determination put forth by individuals to solve the truth behind the unknown. It has taught me that bitter paths may open doors to the sweetest roads, a notion that I will carry with me as I continue to work through the different challenges in life.

First and foremost, I would like to thank Dr. Dirk Lange for being not only my supervisor, but also my personal mentor. Without your continual support and guidance, this project could not have advanced. Many thanks to my committee members, Dr. Jayachandran Kizhakkedathu and Dr. Ben Chew, for their guidance and scientific input. I would like to express my deepest gratitude to Dr. Kai Yu's effort in coating all surface materials tested in this study; without your hard work, this project would not have been feasible. Dr. Igor Moskalev, you are an expert when it comes to animal work, and I could not have asked for a better trainer than you. With your unwavering patience and outstanding guidance, I finally learned how to perform percutaneous bladder implantation independently! Special thanks to the Hancock lab, Brooks lab, Straus lab, Devine lab, and Wang lab for their support and scientific inputs.

Adrienne, David, Olga, Ulli, Martin, Claudia, Justin, and all JBRC colleagues, thanks for contributing to the lively and positive atmosphere at the lab; your presence really brought a lot of smiles and laughter to the workplace! Thanks to all VPC staffs as well for providing me with the support, knowledge, and resources that allowed me to grow as an individual.

Lastly, a big THANK YOU to my mom, dad, and brother for their unconditional love and support, and to my boyfriend, Kerwin, for pushing me forward and teaching me to always strive for the very best.

# **CHAPTER 1: INTRODUCTION**

## **1.1 Catheter-associated urinary tract infections**

Catheter-associated urinary tract infections (CAUTI) are one of the most common sources of health care acquired infections, accounting for up to 80% of these infections; urinary catheters account for approximately 20% of health-care acquired bacteremia cases in acute care facilities and over 50% in long term care facilities [1, 2]. As of 2008, treatment of these hospital-acquired infections are no longer eligible for reimbursement from the US Centres for Medicare and Medicaid Services, as they are considered to be preventable [3]. With direct treatment of CAUTI amounting to over \$350 million per year, it is crucial to prevent such infections [1]. Urinary catheters are hollow tubes used to facilitate the drainage of urine from the bladder to out the body, and are often used after treatment for kidney stones; since these are foreign bodies within the urinary tract system, they can also often lead to urinary tract infection. Current strategies to reduce CAUTI have been mostly unsuccessful and it remains a clinical problem.

### **1.1.1 Catheters: What they are and how they are used**

To understand CAUTI, it is important to understand what urinary catheters are, and how they can lead to infections.

Urinary catheters are devices that help drain the bladder. Common reasons for their recommended use by healthcare providers include:

- Urinary retention (inability to urinate)
- Monitoring urine output during hospitalization
- Urinary incontinence (inability to control urination)

- Post-surgery of the prostate or genitals
- Medical conditions such as spinal cord injury, multiple sclerosis, or dementia [4]

Three main types of urinary catheters are available. These include indwelling catheters, condom catheters, and intermittent self-catheters [4, 5]. General descriptions of each can be found in Table 1.

**Table 1.** Three main types of urinary catheters.

Type of catheter:	Reason or when to use:	How it works:
<b>Indwelling</b>	A catheter that is left inside the bladder for short term or long term drainage	<ul style="list-style-type: none"> <li>• Catheter is inserted through the urethra and into the bladder. Urine is collected by emptying bladder contents into a drainage bag [6].</li> <li>• Newer types of catheters have a valve which allows urine to flow out [6].</li> </ul>
<b>Condom</b>	Can be used by men with urinary incontinence	<ul style="list-style-type: none"> <li>• A condom-like device with a tubing that connects it to a drainage bag is placed over the penis. Hence, no tube needs to be inserted into the penis [5].</li> <li>• Requires daily replacement [5]</li> </ul>
<b>Intermittent</b>	Used when the patient does not want to carry a drainage bag around. Allows the bladder to fill naturally and then get emptied intermittently Reduces the risk of CAUTI	<ul style="list-style-type: none"> <li>• Caregiver or patient themselves insert catheter into the urethra to drain the bladder and removes the device afterwards [6].</li> <li>• Can be performed once or several times a day [6].</li> </ul>

Since indwelling catheters are left inside the urethra for the longest duration out of the 3 types of catheters described in Table 1, it is the main type of catheter associated with infections [6]. The most common type of indwelling urinary catheter used is the Foley catheter, as presented in Figure 1.

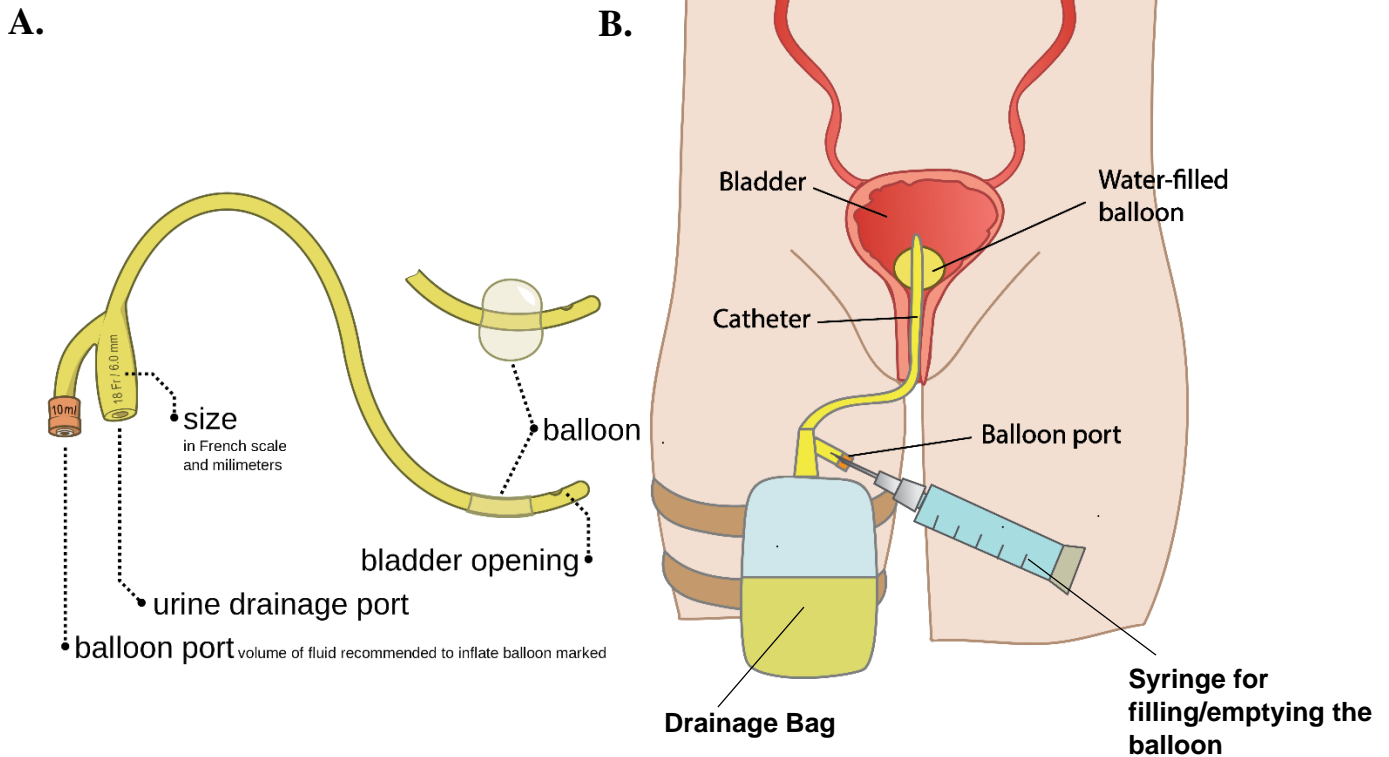


**Figure 1.** A Foley catheter; (A) An overview of the parts of a Foley catheter and (B) a diagram depicting an inserted, indwelling catheter. Note: Fig. 1A was a diagram found under Wikipedia Commons.

When inserting a Foley catheter, it is important to do so as aseptically as possible, using sterile equipment at all times and cleansing the peri-urethral mucosa with cleansing solution prior to insertion of the catheter [7]. Upon insertion, lubricant is often used to aid the insertion of the device through the urethra and into the bladder. Once inside the bladder, the balloon (see Fig. 1A) is inflated via the balloon port using an appropriate amount of sterile liquid based on balloon size. This helps prevent the catheter from slipping out after insertion. The urine drainage port is typically connected to a drainage bag where urine is collected. Figure 1B shows how a Foley catheter looks when inserted into a female's bladder. To remove an indwelling catheter, the



balloon is first drained using a syringe connected to the balloon port (Fig. 1B inset) before the catheter is gently pulled out [7].

### **1.1.2 Contamination by bacteria**

Although a urinary catheter connected directly to a drainage bag is considered to be a 'closed' catheter system (as opposed to an 'open-catheter system' where indwelling catheters are connected to collecting tubes drained into open buckets by the bedside), usage of the device can still become contaminated with bacteria [5].

Upon insertion of a catheter, organisms around the urethral opening can be carried into the bladder, leading to bacteriuria, a condition where bacteria is found within the normally sterile urine. In addition, as the attached drainage bag becomes filled with urine, the bag's drainage tube needs to be opened to decant the accumulated fluid. If the lumen of the tube becomes contaminated with bacteria, organisms may enter the drainage bag and ascend into the bladder through the indwelling catheter, again leading to bacteriuria. Unfortunately, even with meticulous efforts in maintaining the closed system, the microscopic gap between the external wall of the indwelling catheter and the urethral mucosa still offers opportunity for bacteria to enter the bladder. In fact, this small gap is considered to be the most common route of entry for uropathogens [5].

Once bacteria are introduced into the body, they can grow and multiply, eventually leading to a urinary tract infection if not effectively treated.

### 1.1.3 Symptoms of urinary tract infections

The presence of a urinary tract infection (UTI) can be either symptomatic or asymptomatic [8]. However, most cases are asymptomatic, and are defined as bacteriuria based mainly on the presence of  $\geq 10^5$  colony forming units (CFU) per milliliter (mL) of bacteria within the patient's urine specimen [8]. Suspicion of a UTI in these cases often arise due to abnormal cloudiness and/or scent of urine without the experience of pain upon urination [8]. In contrast, symptomatic UTI is often accompanied by fever, localized pain within the urinary tract, and hematuria [8]. Other symptoms include urination or flank pain, frequency, urgency, and increased incontinence [8]. Some of the differences in clinical signs presented by asymptomatic versus symptomatic UTI patients are listed in Table 2 [8].

**Table 2.** Clinical signs presented by asymptomatic versus symptomatic UTI patients.

Asymptomatic UTI	Symptomatic UTI
<ul style="list-style-type: none"><li>• Cloudiness or murkiness in urine</li><li>• Foul or strong odor in urine</li><li>• No voiding symptoms</li></ul>	<ul style="list-style-type: none"><li>• Fever</li><li>• Urinary tract obstruction</li><li>• Urinary retention</li><li>• Hematuria</li><li>• Acute lower tract infection (frequency, dysuria, urgency, increased incontinence)</li><li>• Acute pyelonephritis (fever, flank pain, tenderness)</li></ul>

### 1.1.4 Bacterial adhesion and biofilm formation

In order to develop effective mechanisms to decrease the incidence of CAUTI, the pathogenesis of implant-associated infection, which involves interactions between the pathogen, the implant surface, and the host, must be understood [9]. When sterile urinary catheters are

inserted into the human body, components in urine, blood, or surrounding tissue, such as polysaccharides, ions, and glycoproteins, are deposited on the surface of the device [1, 10] forming an urinary conditioning film. Considering that the conditioning film components have varying physical characteristics, their deposition alters the surface properties of the implants, allowing various planktonic bacteria to adhere to the surface via multiple mechanisms including electrostatic interactions and bacterial adhesins [11, 12]. These free-floating bacteria may have entered the urinary bladder upon insertion of the catheter, or may have been a result from movement of the implant while indwelling [13].

The initial interaction between bacteria and device surface is reversible as it is driven by weak hydrophobic and electrostatic forces [14]. However, over time, the adherence becomes irreversible due to the binding of bacterial adhesins, such as fimbriae or pili, to their target molecules on the device surface as well as bacterial exopolysaccharide secretion, resulting in the formation of a biofilm [15].

Biofilms are highly structured and actively growing bacterial communities that consist of multiple bacterial layers protected by a thick exopolysaccharide layer [9, 14]. The presence of this thick protective layer combined with the fact that the phenotypes and metabolic functions of the embedded bacteria are modified, result in biofilms being significantly more resistant to antimicrobial drugs or disturbances than their planktonic counterparts [16]. This resistance is further complicated by the fact that antimicrobial agents cannot penetrate sufficiently through the exopolysaccharide layer towards the underlying bacteria as well as the strength with which it holds the community together [17]. In addition, organisms growing within a biofilm tend to have a slower rate of growth, allowing them to be more resistant to the effects of many antimicrobial agents which are only effective against actively-growing bacteria [18]. These embedded bacteria

are also phenotypically different from their planktonic counterparts for which numerous antimicrobial agents have been developed against, hence causing the drugs to fail at eradicating organisms within the biofilm [18]. Quorum sensing, a process in which bacteria communicate with one another through the use of signalling molecules, is also prevalent in biofilms; bacteria within the film are able to sense the external environment, communicate with adjacent cells, and transfer genetic information and plasmids between each other. As such, bacteria in a well-established biofilm have been shown to survive in antibiotic concentrations up to 1000-fold higher than the minimal inhibitory concentration for their planktonic counterparts [14, 19]. This helps provide a reservoir where viable organisms can continue to cause infection and encrustation (caused by infection with urease-producing bacteria), potentially leading to blockage of the catheter [20, 21].

As the biofilm becomes more developed, the expansion of the biofilm to “unpopulated” areas of the catheters is facilitated by the detachment of bacterial cells from the biofilm followed by subsequent conversion back into planktonic, or free-swimming state. Diffusion of these planktonic bacteria to unpopulated areas of the surface results in the initiation of new biofilm formation [22].

### **1.1.5 Major uropathogens involved**

Device associated infections in urology are complicated by the fact that the majority of uropathogens are able to form these complex biofilm communities including both gram-positive and gram-negative bacteria, as well as yeast [19, 23-26].

The most commonly isolated strains associated with uropathogenic biofilms are *Escherichia coli*, *Enterococcus faecalis*, and *Pseudomonas aeruginosa*, with *Proteus mirabilis*,

and *Staphylococcus aureus* considered to be the strongest biofilm formers among uropathogens [27]. *P. mirabilis* biofilms are further complicated by the fact that they express urease, an enzyme capable of hydrolyzing urea up to 10 times faster than the rate of other bacterial species. This process generates ammonia, which rapidly increases the alkalinity of urine significantly, creating an environment that promotes formation of hydroxyapatite and struvite crystals, resulting in a significant encrustation of the device surface [28]. Aside from promoting further bacterial adhesion and biofilm formation, these encrustations also block the catheter lumen often resulting in complete device failure [1, 14].

#### **1.1.6 Mechanisms of adhesion**

The first step to biofilm formation is bacterial adhesion; interaction between the uropathogen and the surface of an indwelling device allows the organism to escape from being drained out the body by the flow of urine [29]. This is an important step in allowing the bacteria to colonise, internalise, and persist inside the host's urinary tract system, and to potentially cause infection [29]. This adhesion and colonization process is usually aided by the presence of a conditioning film, which is formed by the deposition of surrounding urine, blood, and tissue components onto the indwelling device's surface, and is often mediated by pathogenic outer membrane structures known as adhesins. The adhesins are able to recognize and bind to specific receptor moieties on the host cell surface, allowing the bacterium to colonize. Examples of such receptor moieties include oligosaccharide residues of glycoprotein or glycolipid receptors, collagen, and fibronectin [29].

Bacterial adhesins are also present in many forms, such as surface structures and proteins (pili, fimbriae, flagella) [30]. Since both the pathogen and the host cell or catheter surface

biomaterial are often negatively charged, bacterial cells often experience repulsive forces from host or implant surfaces. This can be overcome through the development of specialized cell surface structures where the adhesin is located at the tip of hair-like filamentous surface appendages known as the fimbriae or pili, which can be found on both gram-positive and gram-negative bacteria. An example of such an uropathogen that utilises this type of extended adhesin is *E. coli*. The bacterium possesses several virulence factors allowing it to adhere to both indwelling catheter surfaces and to host cells. One such virulence factor is the Type I pili, which are present in most *E. coli* strains, particularly on uropathogenic strains [30]. Another example is protein fimH, which is found on many different uropathogens as part of the pilus for adhesion, including *E. coli* and *Klebsiella pneumoniae*. FimH binds to mannose-containing molecules such as Tamm-Horsfall protein (THP), which is the most abundant protein in the urine and is often found bound to indwelling ureteral devices. Interestingly, THP is normally part of the host urinary mechanism for preventing bacterial adhesion to bladder cells; the urinary protein contains mannose moieties and has high affinity for mannose-binding *E. coli* species, inhibiting bacterial adhesion and colonization to host bladder cells by binding onto the bacterial cells which gets drained out with the urine. However, when indwelling medical devices are present, THP acts as a facilitator of bacterial adhesion where catheter-bound THP acts as an anchor for bacterial cells to bind to, allowing bacteria to colonize the implant's surface [30]. Similarly, *P. mirabilis* and *P. aeruginosa* have also been found to bind THP, although via an adhesin that is different from FimH [30].

Several other adhesins discovered in *E. coli* have also been found to potentially play a role in attaching to urinary catheter surfaces. This includes members of the Dr adhesin family, which bind to integrins and type IV collagen [30]. Likewise, the Ace adhesin from *E. faecalis*

and adhesins from *S. aureus* and *Staphylococcus epidermidis* are also capable of binding to collagen as well as to other extracellular matrix components that can attach to indwelling catheter surfaces [30]. Indeed, with the broad range of adhesins expressed by bacteria, which in turn are capable of binding to various different receptors found deposited on implant surfaces as well as on host cells, it is of no surprise CAUTI remain to be a common problem at hospitals worldwide.

The problems brought by the presence of various bacterial adhesins are further complicated by the ability of uropathogens to alter the expression of surface structures. This includes lipopolysaccharide, exopolysaccharide, and capsular polysaccharide which assist in the attachment of bacterial cells to indwelling medical devices. This is made possible by the ability of bacteria to become attracted to the hydrophilic polymer coating which is commonly found on urinary catheters intended for a smoother, more comfortable insertion by increasing lubricity; initially, bacteria adhere to the hydrophilic coating via weak hydrophobic and electrostatic forces [14], however irreversible adherence soon follows as bacterial adhesins bind to their target molecules on the device surface along with bacterial exopolysaccharide secretion, resulting in the formation of nascent clusters which eventually mature into multi-layer biofilms [30]. An example of such interaction involves the unique surface characteristics of *P. aeruginosa* which allow the bacterium to bind to both hydrophilic and hydrophobic surfaces. When A-band lipopolysaccharide is expressed, the bacterium possesses a hydrophobic surface. This is in contrast to when B-band lipopolysaccharide is expressed, which gives the pathogen a hydrophilic surface. Hence, by expressing either the A-band or the B-band lipopolysaccharides, the bacterium is able to switch between binding to hydrophilic or hydrophobic surfaces, allowing it

to adhere via interaction with urine components which bind to indwelling ureteral catheters and other polymer surfaces [30].

A similar mechanism for the flexibility in bacterial surface characteristics can be found in *E. faecalis*, where subpopulations of bacteria are capable of expressing different surface charges. This allows for adhesion of bacteria to a broad range of surface materials. Past studies have found such heterogeneous strains to bind better to hydrophilic surfaces than strains that do not possess this capability [30].

When there is an absence of a conditioning film, bacteria can still bind directly to indwelling surfaces through the secretion of extracellular polymeric substances, such as DNA, proteins, and polysaccharides. The secretion of such substances allow the bacteria to directly adhere to the surfaces without the aid of conditioning films, adhesins, or changes in bacterial surface structures [31].

Once adhered, bacteria can grow and develop biofilms on indwelling implant surfaces. These biofilms can play an important role in urinary tract infections as well as in serious systemic infections known as urosepsis [32].

## **1.2 Prevention of CAUTI**

### **1.2.1 Limiting their use, proper hygiene procedures, and alternatives**

One foremost strategy for CAUTI prevention is to avoid the use of indwelling catheters. Past studies have shown that at least 21% and up to 55.7% of urinary catheters are placed in patients unnecessarily [33]. Since CAUTI develop through the use of catheters, decreasing the use of this device would significantly lower the prevalence rate of associated infections. Hence, written policies and criteria for indwelling catheterization have been made to limit the use of



unnecessary urinary catheters [34]. However, ensuring that all healthcare providers are following such indications is also important [35, 36].

In addition to reducing the use of catheters, limiting the duration of catheterization is also important [33]. Past studies have suggested that simply relying on physicians' orders for catheter removal may not be adequate; Saint *et al.* found 28% of physicians were unaware of their patients being catheterized [37]. With nurse-driven interventions and computerized physician order entry systems, however, the use of urinary catheters and the durations of use have been effectively lowered [34]. For instance, a systemic review and meta-analysis found reduction of the mean catheterization duration by 37% and CAUTI by 52% when urinary catheter reminder systems and stop orders were used [38].

Once an indwelling catheter is deemed necessary, aseptic catheter insertion and maintenance are necessary to help prevent CAUTI. For instance, insertion should be performed by trained healthcare professionals using aseptic techniques and instruments. While cleansing the meatus prior to insertion is recommended, daily meatal cleansing with antiseptic post-insertion may increase rates of infection in comparison to routine care with soap and water. Sterile lubricants are also recommended for insertion. Once inserted, maintaining a closed catheterization system is also important, as opening the system would increase chances of introducing contaminants into the body.

Using alternatives to indwelling urinary catheters, such as the condom and intermittent catheters listed in Table 1, have also demonstrated a decrease in bacteriuria, symptomatic UTI, or death [39]. For condom catheter users this effect was observed primarily in men without dementia. Less experienced pain compared to indwelling catheters has also been reported by

some users [39, 40]. Similar findings have also been reported with the use of intermittent catheters in patients of post-hip or knee surgery [41]. When combining intermittent catheterization with the use of a portable bladder ultrasound scanner, the need for indwelling catheters may be reduced [35, 42].

### **1.2.2 Antimicrobial implant coatings**

While improved hygiene procedures as well as limiting catheter usage have helped decreased the incidence of CAUTI, it has not been completely prevented. As such it is crucial to develop strategies that will specifically inhibit the adhesion and growth of uropathogens. Conventional treatment has been the use of broad-spectrum antibiotics [20, 43]. However, while the use of prophylactic antibiotics could be an effective way to kill potential intruders of the urinary tract prior to their adhesion to the device surface, it increases the development of further resistance and will not prevent the attachment and biofilm formation of uropathogens that are already resistant. In fact, the development of resistance against conventional antibiotics by pathogenic bacteria occurs regularly, such that between the 1950s to the 2000s, there was an alarming 57% increase in the prevalence of multi-drug resistant (MDR) bacteria, with more resistance observed towards drugs that had been used for humans and animals for the longest time [44-46].

With sporadic emergences of new MDR pathogens becoming a leading cause of nosocomial infections, and with the lack of novel, effective antibiotics, there is an urgent need to discover alternative drugs to control bacterial infections [46]. In addition, because biofilms are exceedingly difficult to disrupt compared to their planktonic counterparts, it is best to prevent the entire adhesion process prior to the development of biofilms for the treatment of CAUTI. Hence,

other approaches to prevent the initial bacterial attachment to surfaces need to be developed further, as this would prevent the bacteria from being retained in the urinary tract environment, being flushed back out by normal urinary flow.

To date, several new approaches have been attempted; one of the most promising approaches involves modification of the biomaterial surface of urinary implants [1, 10, 47]. Table 3 lists some of the antimicrobial implant coatings that have been studied to prevent bacterial adhesion and subsequent UTI (Table 3) [48]. Full details regarding each coating is described by Lo and Lange in a recent review article [48].

**Table 3.** Different types of antimicrobial implant coatings used to prevent bacterial adhesion and subsequent urinary tract infections.

Type of Coating	Description	Pros	Cons
<b>Antibiotics</b>	<ul style="list-style-type: none"> <li>Conventional treatment coated on implants</li> <li>Specific mode of action [49]</li> <li>Can be eluting or non-eluting [48]</li> </ul>	<ul style="list-style-type: none"> <li>A very well-studied treatment</li> </ul>	<ul style="list-style-type: none"> <li>Resistance developed by MDR strains of bacteria</li> </ul>
<b>Triclosan</b>	<ul style="list-style-type: none"> <li>A ubiquitous compound that affects the stability of bacterial cell walls [48]</li> </ul>	<ul style="list-style-type: none"> <li>Affects both gram-positive and gram-negative bacteria [50-52]</li> <li>Widespread use for the past 40 years has not produced resistant strains [49]</li> <li>Effectiveness shown <i>in vivo</i> [52]</li> </ul>	<ul style="list-style-type: none"> <li>Coating was no match against the extensive biofilm formation when used in patients [53]</li> <li>Triclosan was never FDA approved due to it potentially leading to antibiotic resistance although none has been shown [54]</li> </ul>
<b>Silver</b>	<ul style="list-style-type: none"> <li>Silver ions are capable of modifying bacterial cell walls and membranes, as well as inhibit bacterial genome replication [48]</li> </ul>	<ul style="list-style-type: none"> <li>Effective broad-spectrum antimicrobial agent at low concentrations [8]</li> </ul>	<ul style="list-style-type: none"> <li>Inflexible nature of silver implants cause abdominal pain in patients [48]</li> <li>Silver-coated and silver-impregnated catheters show variable effectiveness among studies [17]</li> <li>Argyria may result from prolonged usage [10]</li> </ul>
<b>Hydrogel</b>	<ul style="list-style-type: none"> <li>A hydrophilic, cross-linked polymer capable of absorbing large volumes of liquid forming a thin layer of water on coated device, preventing conditioning film formation [48]</li> </ul>	<ul style="list-style-type: none"> <li>Prevents conditioning film formation, which may decrease biofilm formation</li> <li>Associated with less urethral irritation and inflammation [55]</li> </ul>	<ul style="list-style-type: none"> <li>Highly variable results [55]</li> <li>Recent study suggested presence on conditioning film do not increase bacterial adhesion and colonization [56]</li> </ul>
<b>Polyvinylpyrrolidone (PVP)</b>	<ul style="list-style-type: none"> <li>A hydrophilic, water-soluble polymer with excellent lubricant properties which result in a soft, smooth and non-adhesive implant surface [48]</li> </ul>	<ul style="list-style-type: none"> <li>Shown to reduce adherence of <i>E. faecalis</i> and device encrustation <i>in vitro</i> compared to uncoated catheters [57]</li> <li>Has low toxicity, chemical stability, and good biocompatibility [58]</li> </ul>	<ul style="list-style-type: none"> <li>When applied to a substrate by simple coating methods, PVP layer may easily detach, making them unsuitable for long-term applications [58]</li> <li>Improved methods of immobilizing PVP is needed [58]</li> </ul>
<b>Heparin</b>	<ul style="list-style-type: none"> <li>A highly sulfated glycosaminoglycan, often used as an anticoagulant with the highest negative charge density amongst all known biologic molecules [48]</li> </ul>	<ul style="list-style-type: none"> <li>Has shown great clinical performance in vascular catheters [48]</li> <li>Shown to result in no detectable biofilm formation or encrustation for up to 6 weeks under clinical trials [59, 60]</li> <li>Strong electronegativity believed to repel microorganisms [59-61]</li> </ul>	<ul style="list-style-type: none"> <li>Recent <i>in vitro</i> study showed no decrease in bacterial adhesion to heparin-coated stents [62]</li> <li>Interaction of material and urine is not as beneficial as they are in blood, making heparin a poor coating for urinary biomaterials [63]</li> </ul>

Type of Coating	Description	Pros	Cons
<b>Hyaluronic Acid</b>	<ul style="list-style-type: none"> <li>Hyaluronic acid is a type of glycosaminoglycan [64]</li> <li>An inhibitor of nucleation, growth, and aggregation of salts [65]</li> </ul>	<ul style="list-style-type: none"> <li>Coating is associated with increased hydration, decreased adsorption of proteins, and decreased bacterial adhesion [48]</li> <li>Promising results obtained <i>in vitro</i> [65]</li> </ul>	<ul style="list-style-type: none"> <li>Efficacy in clinical setting remains to be determined [65]</li> </ul>
<b>Gendine</b>	<ul style="list-style-type: none"> <li>A novel antiseptic that contains Gentian Violet and chlorhexidine [14]</li> </ul>	<ul style="list-style-type: none"> <li>Shown to be more effective than silver hydrogel-coatings in terms of bacterial adhesion <i>in vivo</i> [48]</li> </ul>	<ul style="list-style-type: none"> <li>Larger animal studies needed to validate efficacy and safety [66]</li> </ul>
<b>Chitosan</b>	<ul style="list-style-type: none"> <li>Natural cationic, biodegradable polysaccharide and a weak polyelectrolyte [22, 67]</li> <li>A non-toxic biopolymer obtained via chitin deacetylation [22, 67]</li> </ul>	<ul style="list-style-type: none"> <li>Broad-spectrum activity against bacteria [22, 67]</li> <li>Hypothesised to result in leaky cell membranes [48]</li> </ul>	<ul style="list-style-type: none"> <li>Due to its poorly soluble nature, chitosan has had limited capabilities for its use as a catheter coating [35]</li> </ul>
<b>Low-Energy Surface Acoustic Waves</b>	<ul style="list-style-type: none"> <li>Transmitted directly to indwelling devices via a portable actuator generating piezoelectric vibrations between frequencies of 100 to 200 kHz [68]</li> <li>Waves cover the entire surface, generating a virtual vibrating coat [68]</li> </ul>	<ul style="list-style-type: none"> <li>Disrupts formation of biofilms [48]</li> <li>Results confirmed using <i>in vivo</i> rabbit model [14, 68]</li> </ul>	<ul style="list-style-type: none"> <li>To maintain the vibrating coating, elastic waves would need to be continuously delivered throughout the implantation process, which may be complicated by the fact that patients would be required to carry a portable actuator with them at times [68]</li> </ul>
<b>Salicylic Acid-Releasing Polyurethane Acrylate Polymers</b>	<ul style="list-style-type: none"> <li>A metabolite of aspirin, known to have various effects on bacteria [69]</li> </ul>	<ul style="list-style-type: none"> <li>Under aqueous environments, the coating hydrolyses and releases salicylic acid, which has been shown to inhibit biofilm formation, possibly via inhibition of bacterial quorum sensing [48]</li> </ul>	<ul style="list-style-type: none"> <li>Current findings are preliminary and more testing is needed [69]</li> <li><i>In vivo</i> studies are needed to confirm efficacy and safety [70]</li> </ul>
<b>Antimicrobial Peptides Conjugated to Co-Polymer Brushes</b>	<ul style="list-style-type: none"> <li>Peptides are generally short, comprised on 10 to 50 residues of mainly lysine and arginine, making the peptide cationic [71, 72]</li> </ul>	<ul style="list-style-type: none"> <li>Antimicrobial peptides believed to disrupt bacterial cell wall and cell membrane, as well as many other bacterial processes (multiple targets) [72]</li> <li>Bacteria less likely to develop resistance due to the peptides' multiple targeting system [48]</li> <li>Effectiveness shown both <i>in vitro</i> and <i>in vivo</i> [72]</li> <li>Appear to possess wound-healing effects [48]</li> </ul>	<ul style="list-style-type: none"> <li>Potential pH sensitivity, sensitization and allergy after repeated exposures, susceptibility to proteolysis [73]</li> </ul>

Although many different types of antimicrobial coatings have been tested to date, it is important to note that, as described under the ‘Cons’ column of Table 3, most of the currently studied coatings have caveats. In particular, bacterial resistance, ineffective *in vivo* or clinical findings, and variable findings between different studies are some of the general problems associated with most of these coatings. One coating which isn’t complicated by these factors, however, is the antimicrobial peptide coating. Such coatings are less likely for bacteria to gain resistance to as a result of their multiple targeting system, have been shown to be effective both *in vitro* and *in vivo*, with separate studies suggesting them to be consistently effective [48]. As such, antimicrobial peptide coatings will be the main focus for this study.

### **1.3 Novel antimicrobial peptides as an alternative to conventional antibiotics**

#### **1.3.1 Antimicrobial peptides: What are they?**

Antimicrobial peptides (AMPs) are ancient defence molecules of the innate immune system, and has gained substantial attention over recent years [74]. Collectively, they show a broad range of anti-bacterial and anti-viral activities and modes of action [75]. They are present within a wide variety of species, including bacteria, fungi, insects, birds, amphibians, crustaceans, fish, mammals, and humans, and can be obtained from many different sources, such as neutrophils, macrophages, and epithelial cells [74, 76-78]. To my knowledge, nisin was the first AMP discovered in the late 1930s, with gramicidin soon to follow in 1942 [79, 80]. Fast-forward to over 7 decades later, at least 2,600 AMPs have now been identified from various cells and tissues, and it has been postulated that these peptides are key players of the host defense system in all living organisms [63]. An updated list of currently known AMPs are cataloged in

The Antimicrobial Peptide Database (<http://aps.unmc.edu/AP/main.php>), which has been established and maintained by researchers at the University of Nebraska Medical Centre in Omaha since 2003 [81].

Similar to many conventional antibiotics, AMPs have broad spectrum activity against a wide range of microorganisms, including both gram-positive and gram-negative bacteria, fungi, viruses, yeast, and protozoa [77, 82, 83]. However, unlike current antibiotics, these AMPs are known for their pleiotropic functions; while these peptides may disrupt the cell membrane of target organisms, they are also capable of translocating through the cell membrane and alter other essential cellular activities and promote immune responses, including but not limiting to, up-regulating or down-regulating DNA, RNA, and protein synthesis, altering gene expressions, enhancing neutrophil chemotaxis and function, promoting histamine release of mast cells, inhibiting tissue proteases, and stimulating wound healing [76, 77, 84-86]. The ability of these peptides to target multiple systems rather than single genes or proteins and the ability of them to modulate immune responses makes it highly unlikely for bacteria to gain multi-drug resistance against them, putting them at a great advantage compared to conventional antibiotics [46]. Because these AMPs can also work to promote immune responses rather than simply being “antimicrobial,” it has been recently suggested that these peptides should be named “host-defense peptides” rather than “antimicrobial peptides,” where the latter name was given simply based on their initially discovered characteristic [63, 84]. Other terms for the peptides have also been used in the past, including “alarmins” and “defensins” [63]. However, to appreciate the history of the discovery of these molecules, as well as their common unifying function to kill microbes, the term “AMPs” will be used for this thesis.

### 1.3.2 General properties of AMPs and their mechanisms of action for membrane disruption

Although AMPs lack any specific consensus amino-acid (AA) sequences associated with biological activity, in general, they are short in length, consisting of 10 to nearly 50 AA residues of mainly lysine and arginine, making the peptide cationic [72]. They are typically amphipathic, with a net positive charge of +2 to +9, and consist of a substantial portion ( $\geq 30\%$ ) of hydrophobic residues [74, 76, 84, 87]. Based on their size, AA composition, and conformational structures, these peptides can be divided into several categories. These categories include those with  $\alpha$ -helix structures, those with  $\beta$ -sheet structures which are stabilized by disulfide bonds, and those with extended or loop structures [63] (Fig. 2).

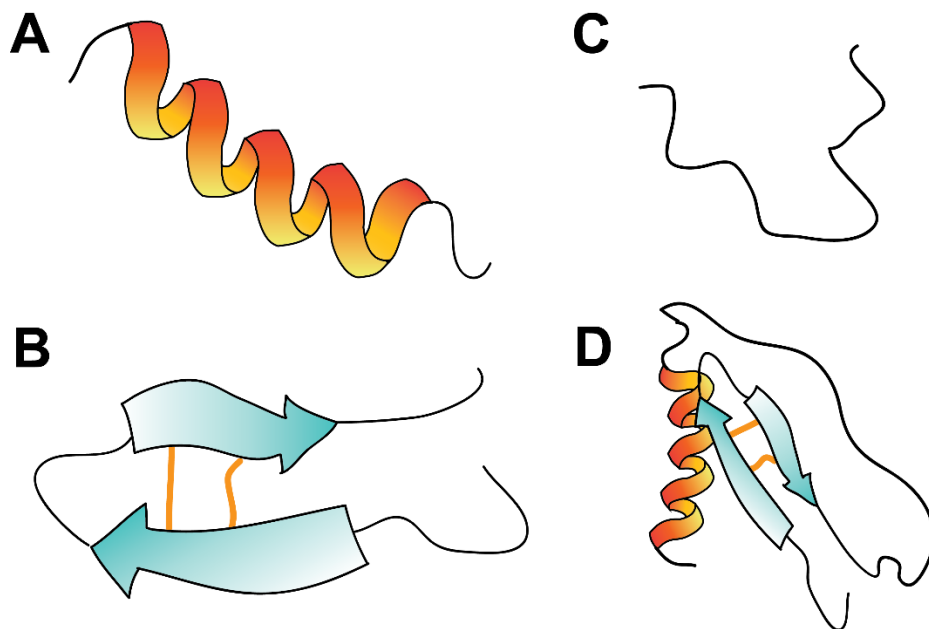


**Figure 2.** The main categories of AMPs based on their size, AA composition, and conformational structures; (A)  $\alpha$ -helix, (B)  $\beta$ -sheet, (C) Loop, (D) Mixed.



Although the mechanism of action is not well understood, it is believed that the amphipathic and positively-charged nature of AMPs allow them to associate with the bacterial cell wall and cell membrane by interacting with the negatively charged phospholipid head groups of microbial membranes via electrostatic bonding [63, 74]. Hydrophobic residues of the AMPs then allow them to be inserted into the lipid bilayer and permeabilise the membrane by interacting with the membrane's hydrophobic fatty acid chains, resulting in the release of cytosol components and potentially the translocation of peptides into the cell for further intracellular targeting [63, 74, 88-90].

At least three different models have been commonly discussed to explain the modes of action of free-floating AMPs on membrane perturbation and damage, with past experimental evidence made available [91]. Figure 3 outlines each of the three mechanisms of action. In the toroidal model, peptides form a pore which consists of peptides and lipids curving inwards in a continuous fashion (Fig. 3A).

In contrast, for the carpet model, peptides align parallel to the membrane to form a carpet, covering the cell membrane and disrupting the bilayer in a detergent-like manner, eventually leading to the formation of micelles (Fig. 3B) [92].

In the barrel-stave model, AMPs span the membrane and assemble into a helix bundle, forming a pore consisting only of peptides, where hydrophilic residues face the lumen of the pores, creating an aqueous channel in the microbial membrane (Fig. 3C).

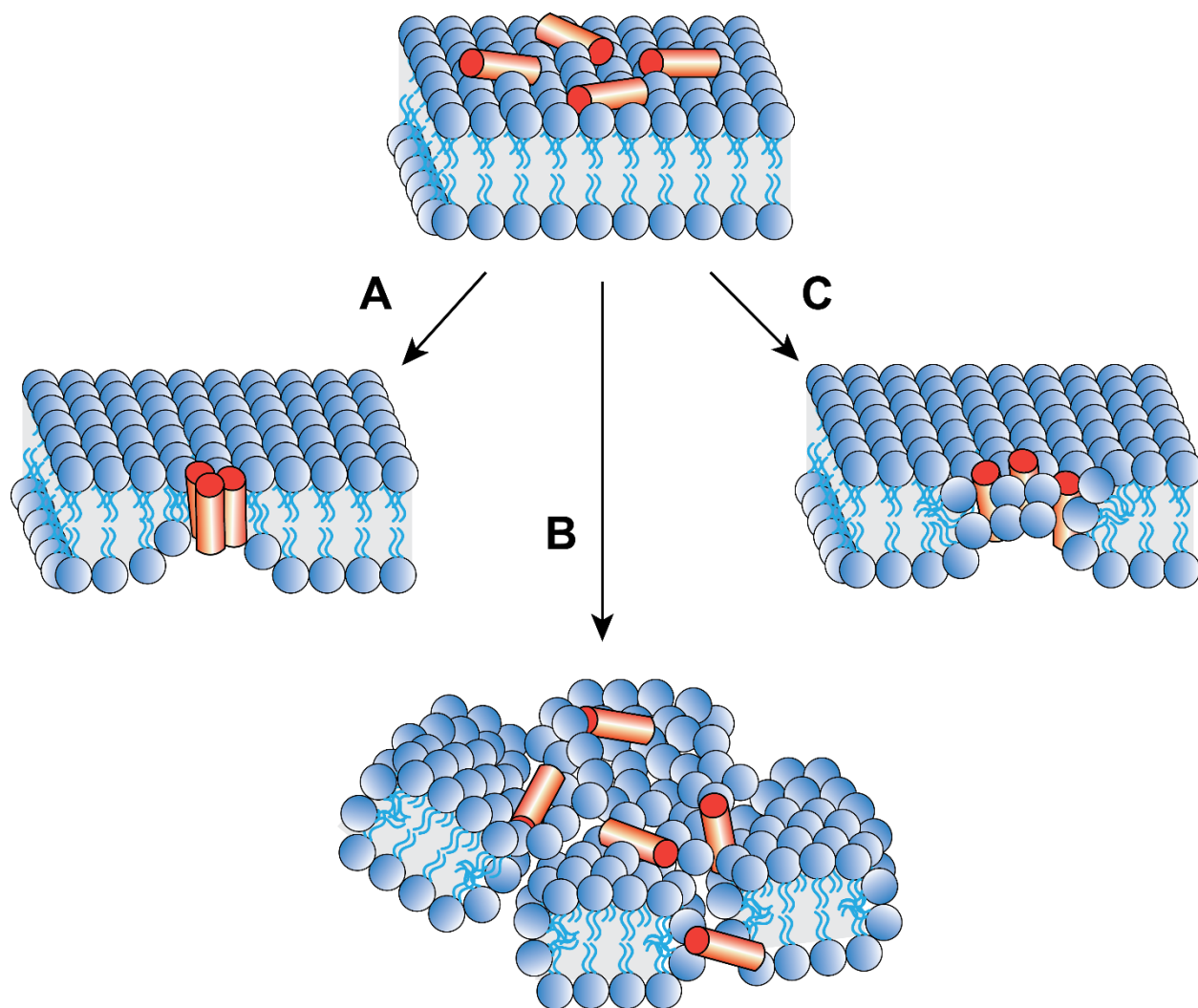


**Figure 3.** The three most commonly-discussed models of membrane disruption by AMPs; (A) Toroidal model, (B) Carpet model, (C) Barrel-stave model.

All of these mechanisms eventually lead to the insertion and translocation of AMPs into the microbial membrane, which disrupts the cell surface. This has been believed to be the main mode of action of free-floating AMPs in terms of their antimicrobial activity. However, recent studies suggest that membrane disruption may only be a transient rather than permanent effect, and that other mechanisms of action are involved in microbial death [93].

Although these modes of action have been described for free-floating AMPs, tethered AMPs (which are becoming increasingly popular for application to indwelling medical devices) may not disrupt bacterial membranes using these mechanisms; instead of inserting into the membranes, the mere contact between tethered AMPs and the bacterial membrane may cause the membrane to destabilise, leading to the formation of pores. This is supported by a past study, where results of scanning electron microscopy, adenosine triphosphate release, and depolarization assays indicate strongly that tethered peptides destabilize the cell envelope of the pathogens [94]. Hence, it is likely that the disturbance of surface electrostatics may trigger an autolytic and/or cell death mechanism [94].

### **1.3.3 Ability of AMPs to target intracellular components and processes**

Although membrane disruption is believed to be AMPs' main mechanism of action, it has been found that some of the peptides can cross the lipid bilayer without provoking any damage to the cell membrane. Once inside the microbial cell, they can target intracellular components by affecting DNA or RNA replication, inhibiting protein synthesis, preventing cell wall synthesis, blocking enzymatic activity and many other bacterial processes [72, 92]. For instance, buforin II, a partial  $\alpha$ -helix AMP, has been found to inhibit cellular activities by binding to nucleic acids after penetrating through the cell membrane [92].

Since AMPs are broad-spectrum and most likely target multiple processes at once, the likelihood of bacteria generating resistance against the peptides are relatively low, making them excellent antimicrobial agents [73].

### 1.3.4 Synthesis of AMPs with further modifications

Since the isolation and purification of AMPs from organisms can be a time-consuming and expensive process, a new challenge in the development of novel antibiotics in recent years has been to synthesise AMPs and develop with potentially higher antimicrobial activity [90]. Table 4 displays several recently synthesised AMPs.

**Table 4.** Recently synthesised AMPs based on past literature.

Peptide name	Sequence	Refs.
<b>A3-APO</b>	(H-Chex-Arg-Pro-Asp-Lys-Pro-Arg-Pro-Tyr-Leu-Pro-Arg-Pro-Arg-Pro-Pro-Arg-Pro-Val-Arg)2-Dab	[95]
<b>ABP-CM4</b>	RWKIFKKIEKVGQNIRDGIVKAG-PAVAVVGQAATI	[96]
<b>BP100</b>	H-KKLFFKKILKYL-NH <sub>2</sub>	[97]
<b>C<sup>15</sup>M<sup>19,30</sup></b>	C <sub>(ACM)</sub> YGTMIYQGRLWAFC <sub>(ACM)</sub> M	[98]
<b>DS1(1-29)-NH<sub>2</sub></b>	ALWKTMLKKLGTMLHAGKAALGAAADTI-NH <sub>2</sub>	[99, 100]
<b>G1</b>	LVRVRRGFGCPFDER	[100]
<b>L1</b>	DAACAAHCLWR-NH <sub>2</sub>	[101, 102]
<b>L-Bac7(1-35)</b>	RRIRPRPPRLPRPRPRPLPFPRPGPRPIP-RPLPFP	[103]
<b>P1</b>	GLGSVFGRLARILGRVIPKV-NH <sub>2</sub>	[104]
<b>Penetratin</b>	Fluo-RQIKIWFQNRRMKWKK-amide	[105]

### 1.3.5 Using AMPs to prevent CAUTI

Since fully-developed biofilms are more difficult to treat, coating urinary catheters with antimicrobial compounds prior to implantation has been of high interest to prevent the formation of biofilms [48]. To date, several different types of coatings have been tested, including antibiotics, silver, triclosan, gendine, and heparin [48]. However, these compounds are often

found to be cytotoxic, are associated with the development of antibiotic resistance, or are only effective *in vitro* and not *in vivo* [48, 106].

Recently, AMPs have been examined as a potential coating for urinary catheters and ureteral stents [48, 71, 106]. For instance, Tachyplesin III (KWCFRVCYRGICYRKCR-NH<sub>2</sub>) is an AMP isolated from horseshoe crabs, and has been shown to have broad spectrum activity [77]. Minardi *et al.* investigated the effect of coating Tachyplesin III on urinary implants in preventing biofilm formation *in vivo* using a rat subcutaneous pouch model, and found coated samples to inhibit bacterial growth by up to 1000 times [77]. No drug-related adverse effects were physically observed in any of the treated animals [77]. Similar findings were discovered by Rapsch *et al.*, where AMP BMAP-27 (GRFKRFRKKFKKLFKKLSPVIPLLHLG) displayed antimicrobial activity that reduced living bacteria by more than 4 orders of magnitude when immobilized to planar surfaces and introduced to *E. coli* [107]. Likewise, Yoshinari *et al.* evaluated coatings of histatin-5 (DSHAKRHHGYKRKFHEKHSHRGY) and lactoferricin (FQWQRNMRKVR) on titanium surfaces against *Porphyromonas gingivalis*, and found the coatings to strongly reduce biofilm formation by the bacterium [108]. Similar antimicrobial activity was observed by Lim *et al.* where the authors coated peptide CWR11 (CWFWKWRRRRR-NH<sub>2</sub>) onto commercial silicone-coated Foley catheters via polydopamine, a simple surface functionalization technique using dopamine molecules derived from mussels [109].

### 1.3.6 Challenges faced by AMPs

Although the use of AMPs has shown promising results in recent research, the commercial development of AMPs has been limited, with only several peptides having shown

outstanding *in vitro* activities against MDR pathogens and have entered Phase III clinical trials, such as pexiganan and omiganan [110, 111]. To date, no AMP has been approved or commercialised for clinical use. The only commercialized AMP that has been approved thus far is Nisin, a food additive in the United States and Europe [112].

One of the challenges of commercializing AMPs may be the high cost of chemical synthesis and low yields from natural sources [113]. Another challenge may be their limited serum half-life, which would mean that high dosages may be required to achieve desirable therapeutic effect. However, due to their hydrophobic property, high dosages may possibly correlate to higher haemolytic activity. The broad-spectrum activity of AMPs may also be a problem; although broad-spectrum activity is a desirable antimicrobial trait, it also carries the risk of disrupting the host's normal flora, providing a niche for opportunistic pathogens to take over. Hence, with all these challenges, many AMPs currently undergoing clinical trials are designed to be for topical rather than systemic use [111].

In the case of urinary catheter coatings, some of these complications may be overcome by attaching AMPs to the implant surface or by ensuring their slow release into the surrounding environment. By tethering AMPs onto surfaces, less quantities of peptides would be needed per application, and high local concentrations would be fixed to the device surface thus preventing systemic toxicity [91].

### **1.3.7 Optimizing the peptide coating: The use of polymer brushes**

To further optimize the AMP coating for catheters and other implants, polymer brushes have been used which help create low-fouling surfaces as well as act as branches to help increase the density peptides loaded on a given surface area on the catheter (Figure 4).

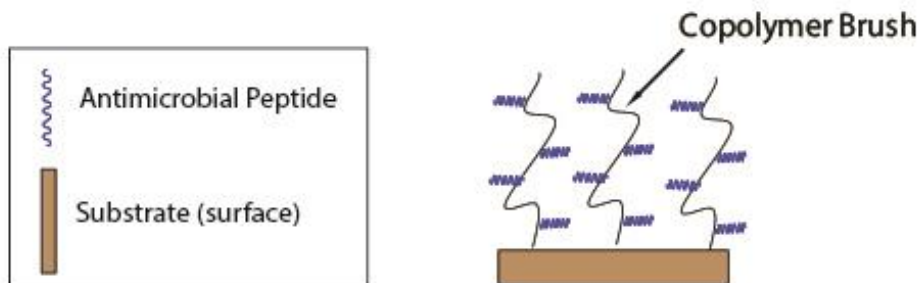


**Figure 4.** Increasing the density of peptides loaded onto implant surfaces using co-polymer brushes.

The use of these polymers helps prevent non-specific interactions between the implant surface and the indwelling biological environment, particularly the adsorption of proteins and other biomolecules. By having a low-fouling surface, it reduces the ability of planktonic microbes to adhere and hence prevents the earliest stages of biofilm formation [91]. Polymer coatings can also be easily applied to almost any substrate material, allowing the coating to be compatible with most biomaterials used to compose implant surfaces [91].

In general, two techniques have been used to apply polymers onto the implant surfaces to yield low-fouling, anti-adherence surfaces; one where polymers carrying the AMPs are synthesised in solution then tethered onto surfaces via reactions with complementary functional groups on the surface (the ‘grafting-to’ technique) (Fig. 5A), and the other where polymer chains are grown from surface-immobilized initiators or chain transfer agents with AMPs introduced along the graft polymer chain or at its terminal end (the ‘grafting-from’ technique) (Fig. 5B).

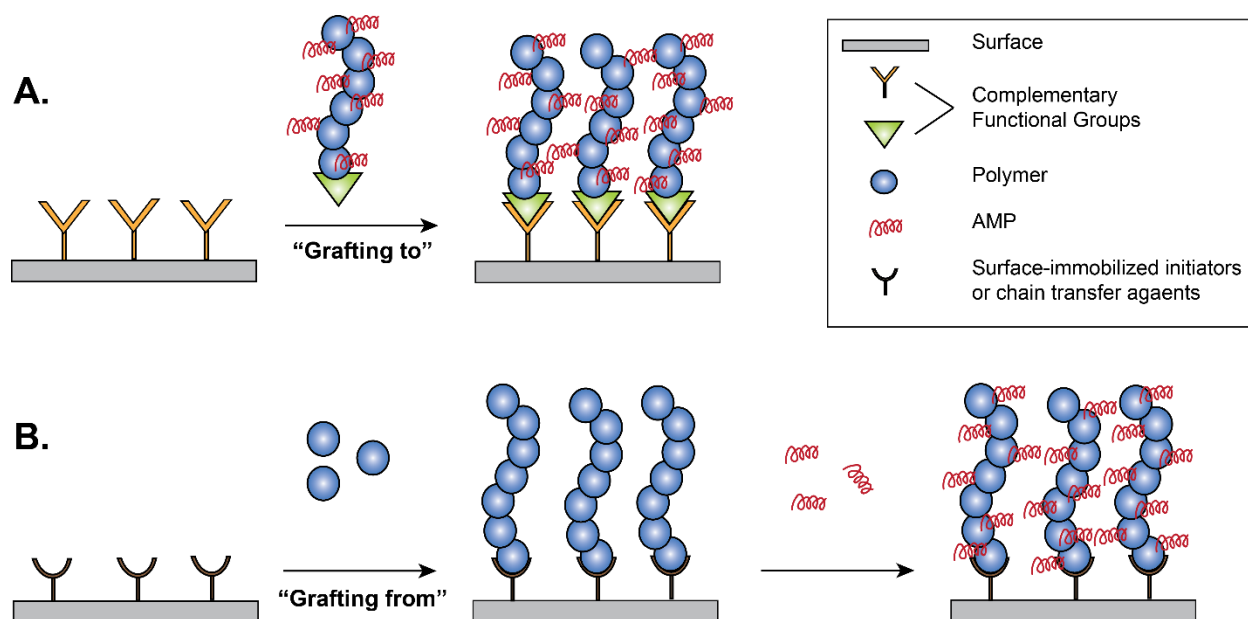


**Figure 5.** Two general techniques used to apply polymers (and AMPs) onto implant surfaces; (A) “Grafting to” method, (B) “Grafting from” method.

Some of the low-fouling polymers which have been demonstrated to be effective include polyacrylamide (PAM) [114], zwitterionic polymers such as poly(N-sulfobetaine methacrylamide (PSBMA) [115, 116], polyethylene glycol (PEG) [117], poly(N-hydroxypropyl methacrylamide (PHPMA) [118], and polysaccharides such as dextrane [119].

By impeding biomolecule adsorption, a broad range of processes which depend on the interaction of proteins or other biomolecules with the surface biomaterial becomes hindered. Such processes include cell attachment, platelet adhesion, blood clot formation, as well as foreign-body reaction and microbial colonization and biofilm formation [120, 121]. Hence, with the anti-fouling capability of polymers along with the antimicrobial activity of AMPs, polymer-AMP coatings have been of particular interest for the coating of implant surfaces and the prevention of implant-associated infections, particularly CAUTI.



### 1.3.8 Assessment of polymer-peptide coatings in past literature

To date, only several polymer-AMP coatings have been studied. Table 5 summarizes some of the recent low-fouling, AMP coatings that have been examined.

**Table 5.** Summary of AMPs used in combination with low-fouling surface coatings.

Peptide	Surface	Testing Stage	Bacteria tested	Refs.
LL37 (human cathelicidin) (LLGDFFRKSKKEKIGKEFKRIVQRIKDFLRNLPRTES)	Titanium (Ti)	<i>In vitro</i>	<i>E. coli</i>	[122]
Magainin I (GIGKFLHSAGKFGKAFVGEIMKS)	Ti	<i>In vitro</i>	<i>Listeria ivanovii</i>	[123]
	SiO <sub>2</sub> beads	<i>In vitro</i>	<i>L. ivanovii</i>	[124]
	Silicone (Si) wafers	<i>In vitro</i>	<i>L. ivanovii</i> , <i>Bacillus cereus</i>	[125]
	Si wafers	<i>In vitro</i>	<i>L. ivanovii</i> , <i>E. coli</i>	[126]
Cathelicidin library: Tet-20 (KRWRIRVRVIRKC); Tet-26 (WIVVIWRRKRRRC)	Ti and quartz slides	<i>In vitro</i> & <i>in vivo</i>	<i>P. aeruginosa</i> , <i>S. aureus</i>	[71]
	Ti	<i>In vitro</i> & <i>in vivo</i>	<i>P. aeruginosa</i>	[72]
RK1 (salt-tolerant) (RWKRWWRRKK); RK2 (salt-tolerant) (RKKRWRRKK)	polydimethylsiloxane and urinary catheter surfaces	<i>In vitro</i>	<i>E. coli</i> , <i>S. aureus</i> , and <i>Candida albicans</i>	[106]
CWR11 (engineered from Jelleine-I) (CWFWKWRRRRR-NH <sub>2</sub> )	PDMS <sup>a</sup>	<i>In vitro</i>	<i>E. coli</i> , <i>S. aureus</i> , <i>P. aeruginosa</i>	[127]
L5 (bovine lactoferrin 14-31) (PAWRKAFRWAWRMLKAA)	Si wafers	<i>In vitro</i>	<i>S. epidermidis</i>	[128]
Nisin <sup>b</sup> , tritrypticin (KKFPWWPFKK), lipopeptide 4K-C16 (KKKK-palmitoyl)	Stainless steel	<i>In vitro</i>	<i>E. coli</i> , <i>Bacillus subtilis</i>	[129]
AMP (ILPWRWPWWPWR-NH <sub>2</sub> ); RGD (Ac-GCGYGRGDSPG-NH <sub>2</sub> )	Si rubber	<i>In vitro</i>	<i>S. aureus</i> , <i>S. epidermidis</i> , <i>P. aeruginosa</i>	[130]

It is important to note that to my knowledge, only a few peptide-polymer implant coatings have been tested in animal models to date, and they were tested by Gao *et al.* [71, 72]. By covalently grafting hydrophilic co-polymer Poly (N,N-dimethylacrylamide) (PDMA) and Poly N-(3-aminopropyl) methacrylamide (PAPMA) chains onto a surface, and conjugating them to an optimized series of AMPs, Gao *et al.* was able to demonstrate the effective antimicrobial

activity of peptide-brush coatings [71]. Polymer brush structures served as a flexible linker between AMPs and the surface while maximizing the density of peptides per coating [71]. *In vitro*, when  $1\text{-}5 \times 10^5$  CFU/mL of gram-positive or gram-negative bacteria were introduced to titanium wires (Ti-wires) coated with peptide Tet-20, there was a 100,000-fold decrease in CFU for treated Ti-wires 4 hours post-incubation in comparison to uncoated controls [71]. The activity was also demonstrated *in vivo* using a rat infection model; when coated and uncoated Ti-wires were implanted into subcutaneous pockets of the rat and were challenged with  $10^8$  CFU of *S. aureus* under a 7-day implantation period, CFU was decreased by 85% for treated rats compared to controls [71]. During *in vivo* models, not only did the peptides show antibacterial effect, they also appeared to possess wound-healing effects (unpublished data). Moreover, using scanning electron microscopy, modified CH50 analysis, and MTT assays, the authors were able to demonstrate that peptides gave insignificant platelet activation and adhesion, no complement activation in human blood, and were non-toxic to osteoblast-like cells, respectively [71]. All these results suggest AMPs to be a promising alternative to catheter coatings.

Indeed, brush-peptide coatings may be golden promising coating for urinary catheters to help prevent biofilm formation and infection. However, because the only *in vivo* testing of polymer-peptide coats thus far was performed by implanting the coated samples into subcutaneous pockets of rats rather than implanting the samples within the urinary tract, more clinically-relevant *in vivo* models must be used to further test these coatings before they can be made available to the public.

### **1.3.9 The optimal polymer-peptide coating**

Although many different AMP coatings (with or without the use of polymers) have been tested, the search continues for the optimal AMP coating for urinary catheters. It is important that the coating combine several properties to help reduce the risk of bacterial adhesion and biofilm formation such that any adverse effects can be prevented. Since the initial attachment of microbes onto an indwelling implant surface is assisted by the attachment of biomolecules that initially populate the surface (i.e., the conditioning film), it is crucial that surfaces must have a low-fouling property. This is where the use of low-fouling polymers comes in [91].

However, with the persistence of microbes, this first line of defense may still be easily overcome; hence effective coatings must incorporate additional factors with long-lasting antimicrobial activity. In addition, it is important that any debris from microbes killed at the interface must be removed such that they do not build up, as they might serve as a conditioning film for renewed bacterial attachment and biofilm growth [91]. Hence, an optimal antimicrobial coating should be able to:

- i. Provide a surface topography that is unfavourable for microbial attachment.
- ii. Prevent the adsorption of biomolecules.
- iii. Kill all microbes that manage to overcome the anti-fouling barrier.
- iv. Remove dead microbes from the implant surface before they build up.

#### **1.4 Thesis objective: Investigating the use of novel antimicrobial peptide coating to prevent catheter-associated urinary tract infections**

The objective of this thesis is to carry on from the studies by Gao *et al.*, and to determine an optimal peptide-polymer coating to coat onto implants by conjugating different combinations of AMPs and polymers, followed by testing using various *in vitro* assays. Through the *in vitro* testing, we aim to uncover a coating which will fit the four criteria listed as characteristics of an optimal antimicrobial coating (see section 1.3.9). Once an effective combination of peptide and polymer has been found, the implant coating will be further tested *in vivo* using a clinically relevant CAUTI model.

## CHAPTER 2: METHODS

### 2.1 *In vitro* studies

#### 2.1.1 Large-scale activity screening of tethered AMPs using nanoparticles

All coated and uncoated nanoparticles were kindly made and provided by Dr. Kai Yu from the Kizhakkedathu Lab at the University of British Columbia.

##### 2.1.1.1 Synthesis of polymer-AMP coated nanoparticles

Primary amine-functionalized copolymer brushes were synthesized by surface-initiated atom transfer radical polymerization (SI-ATRP) onto the surface of polystyrene (PS) nanoparticles (NPs) of  $597 \pm 6.2$  nm in diameter. The functional brushes were subsequently modified by attaching cysteine-terminated peptides. The properties of the grafted polymer and peptide conjugated NPs were then characterized by water contact angle measurements, ellipsometry, ATR-FTIR, and atomic force microscopy analyses to confirm the presence and density of loaded polymer brushes and peptides.

Using this method, a total of three different polymers were synthesized onto NPs. These include poly(*N,N*-dimethylacrylamide)-co-*N*-(3-Aminopropyl)methacrylamide (PDMA-co-APMA), poly(2-methacryloyloxyethyl phosphorylcholine)-co-*N*-(3-Aminopropyl)methacrylamide (PMPC-co-APMA), and poly(3-methacryloylamido)propyl-*N,N*-dimethyl(3-sulfopropyl)ammonium hydroxide)-co-*N*-(3-Aminopropyl)methacrylamide (PMPDSAH-co-APMA). Figure 6 shows the chemical structure of each of these polymers (Fig. 6).

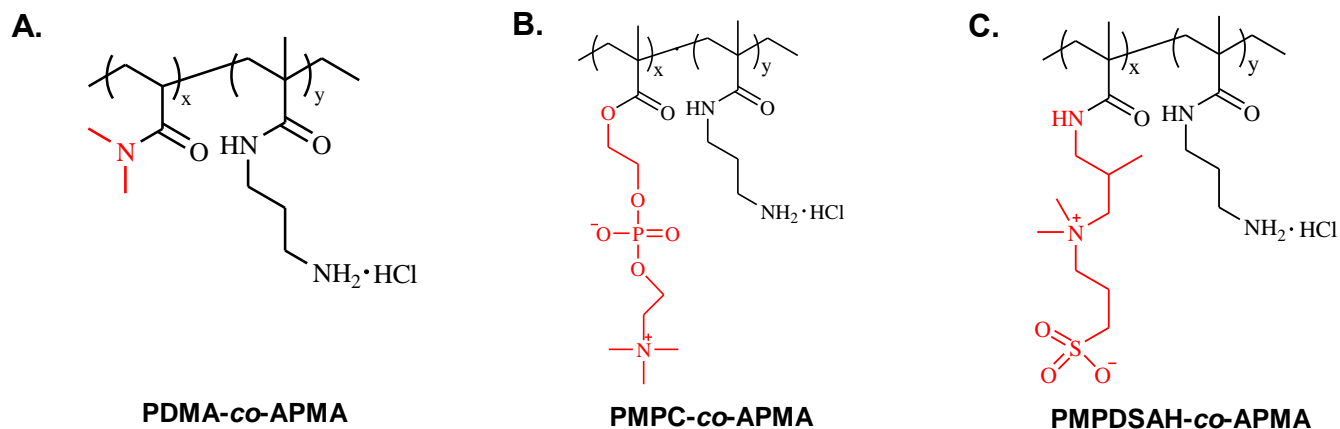


**Figure 6.** Co-polymer brushes tested *in vitro*; (A) PDMA-co-APMA, (B) PMPC-co-APMA, (C) PMPDSAH-co-APMA.

A total of 4 different AMPs were conjugated to these polymer brushes to produce various combinations of polymer-peptide coatings on NPs. These AMPs include E6, Tet20, Tet26, and Kai13. Tet20 and Tet26 were chosen based on the previously published paper by Gao *et al.*, where Tet26 significantly inhibited the formation of biofilm, while Tet20 showed good antimicrobial activity *in vivo* [71]. Peptides E6 (sub3) and Kai13 (w3) were chosen based on a recently published article by Yu *et al.*, where both peptides showed both good antimicrobial activity and biocompatibility [131]. Sequences of these peptides as well as densities tested can be found in Table 6.

**Table 6.** Name and amino acid sequence of peptides tested using NPs.

Peptide	Amino Acid Sequence	Peptide Densities (mg/10mg polymer)
E6	RRWRIVVIRVRRC	0.72, 1, 1.5, 1.8
Kai13	VRWRIRVAVIRAC	0.6
Tet20	KRWRIRVRVIRKC	0.75, 0.9, 1, 1.4, 0.2, 1,
Tet26	WIVVIWRRKRRRC	1

Figure 7 shows the general process of synthesizing polymer brushes on NPs followed by peptide conjugation.

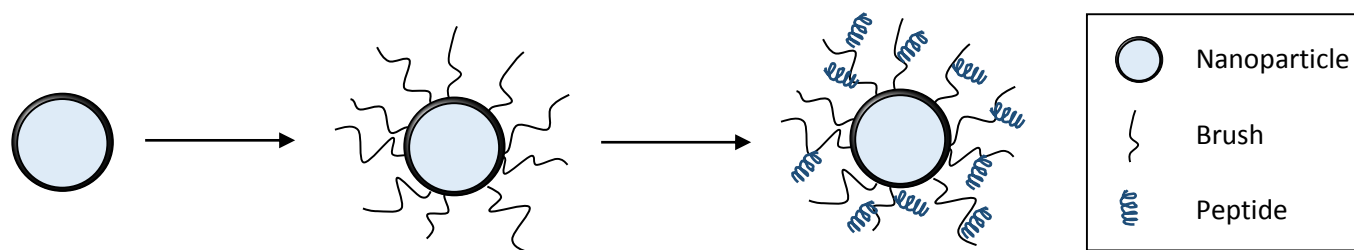


**Figure 7.** Synthesis of polymer brushes on NPs followed by conjugation of AMPs.

#### 2.1.1.2 Temporary storage of brush-peptide-coated nanoparticles

Once coated and uncoated NPs have been kindly prepared by Dr. Kai Yu at The University of British Columbia (UBC), all samples were transported to Jack Bell Research Centre (JBRC) where they were temporarily stored at 4°C prior to *in vitro* testing performed by Joey Lo.

### 2.1.1.3 *In vitro* testing of polymer-AMPs-coated, polymer-coated, and uncoated NPs

#### 2.1.1.3.1 Bacterial strains

Table 7 lists the bacterial strains used for *in vitro* testing of coated and uncoated NPs.

Luminescent strains of *P. aeruginosa*, *S. aureus*, and *E. coli* were kindly provided by the Hancock Lab at UBC. Freezer stocks were made by adding sterilised glycerol solution (50% w/w) to cultured bacteria for a final concentration of 10% glycerol. All freezer stocks were stored at -80°C until use.

To prepare fresh bacterial culture for *in vitro* testing, bacteria were grown in Lysogeny broth (LB; 10 g tryptone, 5 g yeast extract, and 10 g NaCl per litre) from freezer stocks at 37°C overnight (O/N), and was sub-cultured and used at approximately  $5 \times 10^5$  CFU/mL as determined by OD<sub>600</sub> readings using the approximate equation of  $0.1 \text{ OD}_{600} = 10^8 \text{ CFU/mL}$ .

**Table 7.** Bacterial strains used to test brush-peptide-coated nanoparticles.

Bacteria	Strain
<i>Escherichia coli</i> lux	DH-5 alpha, plasmid pUC 19
<i>Pseudomonas aeruginosa</i> lux	PAO1 Tn::Plac-lux
<i>Staphylococcus aureus</i> lux	Xen 36 lux

#### 2.1.1.4 Antimicrobial testing of AMPs tethered to NPs

The antimicrobial activity of NPs was assessed using a static microtitre plate assay. Briefly, 96-well plates (Corning® 96 well white flat bottom polystyrene not treated microplate, Product #3912) were sterilized for 30 min under UV light and were used for the NP testing. Peptide-conjugated brush-coated, unmodified brush-coated, and uncoated NPs were diluted to 512 µg/mL (AMP concentration) followed by serial doubling dilutions in minimal basal medium



2 g glucose medium (BM2; 62 mM potassium phosphate buffer, pH 7, 7mM (NH<sub>4</sub>)<sub>2</sub>SO<sub>4</sub>, 2 mM MgSO<sub>4</sub>, 10 µM FeSO<sub>4</sub>, and 0.4% (w/vol) glucose) across the sterile 96-well plate to obtain concentrations of 512, 256, 128, 64, 32, 16, 8, 4, 2, 1, and 0.5 µg/mL AMP equivalent in columns 1 to 11. BM2 medium containing uncoated NPs was added to the last column to serve as control. All concentrations were performed in triplicates per bacterium, and all wells should contain 100 µL of solution at this point. Bacteria (100 µL) of approximately 5 x 10<sup>5</sup> CFU/mL and re-suspended in BM2 medium was introduced to each well, making a total volume of 200 µL per well. Leftover bacterial solutions were serially diluted and spot plated for CFU counts to determine the actual starting concentration (See Fig. 8). All the wells were mixed gently and immediately scanned for luminescence using the Tecan Infinite 200 Pro for the 0 h timepoint reading. The plate was then incubated at 37°C.

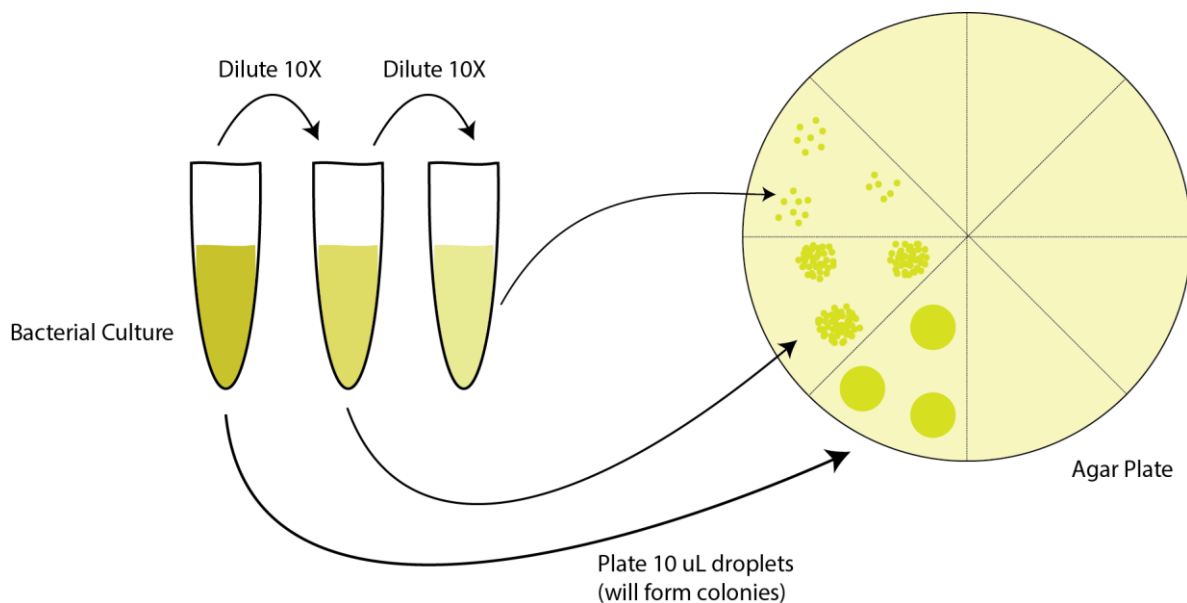


**Figure 8.** Spot plating method allowing for large-scale screening of antimicrobial activity.

#### **2.1.1.4.1 Determining bacterial concentration via luminescence**

At 1-, 2-, 3-, and 4-hours post-incubation, loaded 96-well plates were transferred to a luminescence reader (Tecan Infinite 200 Pro), and luminescence levels for each well were determined. All plates were transferred back to the incubator after each reading.

#### **2.1.1.4.2 Determining bacterial concentration via colony forming units (CFU) counts**

At 4-hours post-incubation and after the last luminescence reading was performed, all wells were serially diluted 10X in sterile phosphate buffered saline (PBS) buffer up to  $10^{-5}$  dilution, and spot plated onto LB agar plates for CFU measurements (Fig. 8). All plates were incubated at 37°C O/N or until visible colonies form. CFU counts were recorded for the dilutions at which between 3 to 30 colonies can be counted.

### **2.1.2 Testing tethered AMPs using polyurethane catheters**

#### **2.1.2.1 Preparing catheter pieces for coating**

Intravascular 18G polyurethane catheters (Terumo SurFlash® Polyurethane I.V. Catheter, Cat. #SS\*FF1832) were cut into 10mm-long pieces, and a longitudinal slit was made to better expose the inner surface area of the catheter for coating purposes (Figure 9).

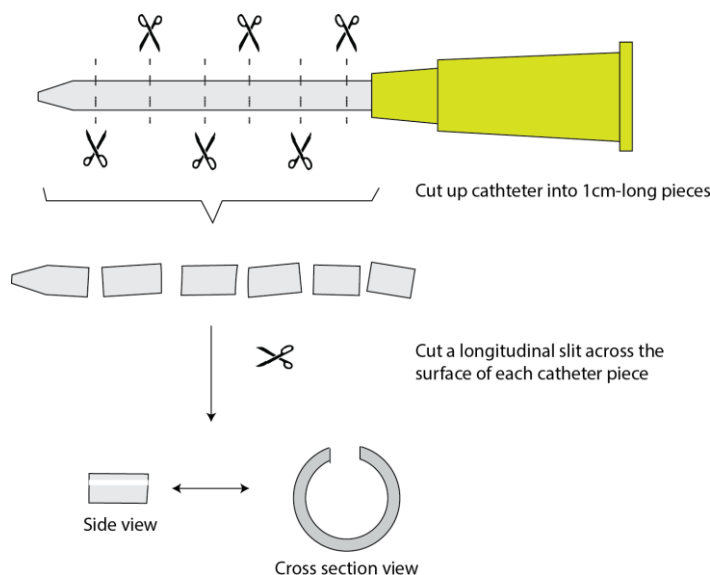


**Figure 9.** Preparing catheter pieces for coating.

#### 2.1.2.2 Synthesis of brush-AMP coating onto modified 18G PU catheter pieces

Once 18G PU catheters have been modified, as described in section 2.1.2.1, P(DMA-co-APMA) polymer brushes were then grafted onto the prepared catheter, and E6 peptides were conjugated to the polymer brushes at a density of approximately  $1.08 \mu\text{g}/\text{cm}^2$ . This was performed using similar methods as described in section 2.1.1.1. Coated samples were then stored at  $4^\circ\text{C}$  prior to testing.

#### 2.1.2.3 Bacteria and *in vitro* testing of coated 18G polyurethane catheters

Bacteria was inoculated into LB from freezer stocks and incubated at  $37^\circ\text{C}$  at 50 RPM O/N. Grown bacteria was then sub-cultured and used at a bacterial concentration of approximately  $5 \times 10^5 \text{ CFU}/\text{mL}$ , as determined by the  $\text{OD}_{600}$  readings based on the approximate equation of  $0.1 \text{ OD}_{600} = 1 \times 10^8 \text{ CFU}/\text{mL}$ .

#### **2.1.2.4 Antimicrobial testing of AMP tethered 18G PU catheters *in vitro***

Briefly, all coated and uncoated catheter pieces were disinfected by submerging each sample in 1 mL of 70% ethanol for 5 min. The ethanol was then removed, and samples were each rinsed in 1mL of sterile LB for a total of 3 times. Once LB from the last rinse was removed, one mL of the prepared  $\sim 5 \times 10^5$  CFU/mL bacterial culture was added to each sample in Eppendorf tubes, and all tubes were gently tapped on the lab bench to ensure all samples were fully submerged. Samples were incubated at 37°C at 50 RPM for a total of 6 h.

#### **2.1.2.5 Determining bacterial adherence on coated and uncoated polyurethane catheters**

At 6 h post-incubation, 100  $\mu$ L of bacterial culture from each sample tube was transferred to new, sterile tubes and set aside (see section 2.1.2.4). Each catheter piece was then rinsed in 1mL sterile PBS for a total of 3 times, using fresh PBS for each wash. The rinsed catheter pieces were transferred into Eppendorf tubes containing 500  $\mu$ L of sterile PBS and were sonicated in water bath (No. 21811-820, VWR®) for 10 min. After sonication, each sample was vortexed at high speed for 10 sec., then serially diluted and spot plated for CFUs (Fig. 8).

#### **2.1.2.6 Determining bacterial planktonic growth/survival when co-incubated with coated and uncoated polyurethane catheters**

With the 100  $\mu$ L of each culture set aside from section 2.1.2.5, all cultures were serially diluted and spot plated for CFUs (Fig. 8).

## **2.2 *In vivo* Studies**

A total of two *in vivo* models were studied. These included the Transurethral Catheterization Model and the Percutaneous Catheterization Model.

### **2.2.1 Transurethral catheterization model**

#### **2.2.1.1 Bacterial strain, culture medium and animals**

Freezer stock bacteria were cultured in LB (10 g/L tryptone, 5 g/L yeast extract, and 10 g/L NaCl) O/N at 37°C, sub-cultured and grown overnight. It was then re-suspended in PBS at approximately  $5 \times 10^5$  CFU/mL to be used for intravesical injection. All procedures were approved by The University of British Columbia animal care committee. A total of 10 female Sprague Dawley rats (Harlan®) at approximately 200g each were included in experiments.

#### **2.2.1.2 Modification of catheters**

Prior to animal procedures, 18 gauge angiocatheters (Terumo Surflash® Polyurethane I.V. Catheter 18G x 2 1/2", Cat. No. FF1864) were modified under strict aseptic conditions. Briefly, the needle portion of the catheter was removed, and a 10 mm section from the tip of the PU catheter was cut off using sterile blades. The 10 mm piece and the remaining 'pusher' PU catheter section was then assembled onto a guide wire prior to transurethral catheterization. Figure 10 depicts the catheter modification procedure

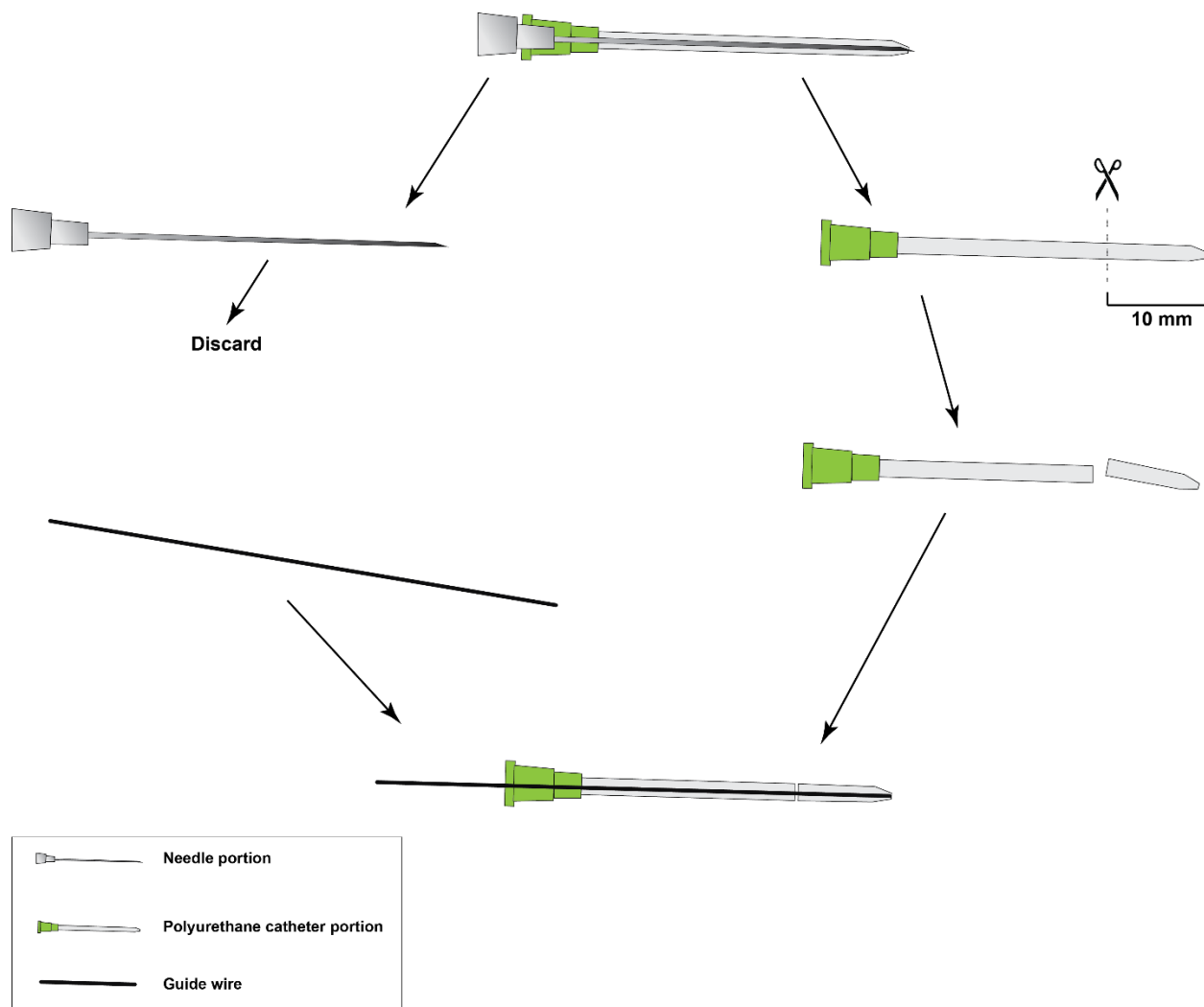


**Fig. 10.** Modification of 18G PU catheter. A 10mm-long section was cut off from the tip of the catheter, then assembled onto a guide wire along with the remaining portion of the PU catheter.

### 2.2.1.3 Day 0: Transurethral catheterization and bacterial instillation

All rats were administered inhalational anesthesia with 3% isoflurane for initial induction. Once anaesthetised, isoflurane was set to 2.5%, and animals were positioned dorsally on a heating pad set at 38°C. The modified catheter-guide wire assembly (Fig. 11A) was then carefully inserted toward the bladder (Fig. 11B). Once the 10 mm catheter segment was confirmed to be entirely inside the bladder based on a rat's average urethra length of 25 mm, as

determined previously through a urinary tract necropsy of the same strain of rat, the guide wire is removed while the 'pusher' is pushed slightly inward (Fig. 11C). This dislodges the short PU catheter segment into the lumen of the bladder, such that once the 'pusher' is removed, the only thing that remains inside the rat bladder is the implanted 10 mm catheter piece (Fig. 11D).

Using a separate unmodified 18G PU catheter, bacteria was introduced into the bladder lumen of the catheterized rat via transurethral instillation. Once successfully instilled, rats were kept asleep at 1% isoflurane for 1 h on a heating pad to allow for bacteria to adhere onto the implanted catheter. The starting amount of bacterial inoculum was confirmed by performing serial dilutions followed by CFU counts. Rats under the 'control' group did not receive bacterial instillation after bladder implantation.

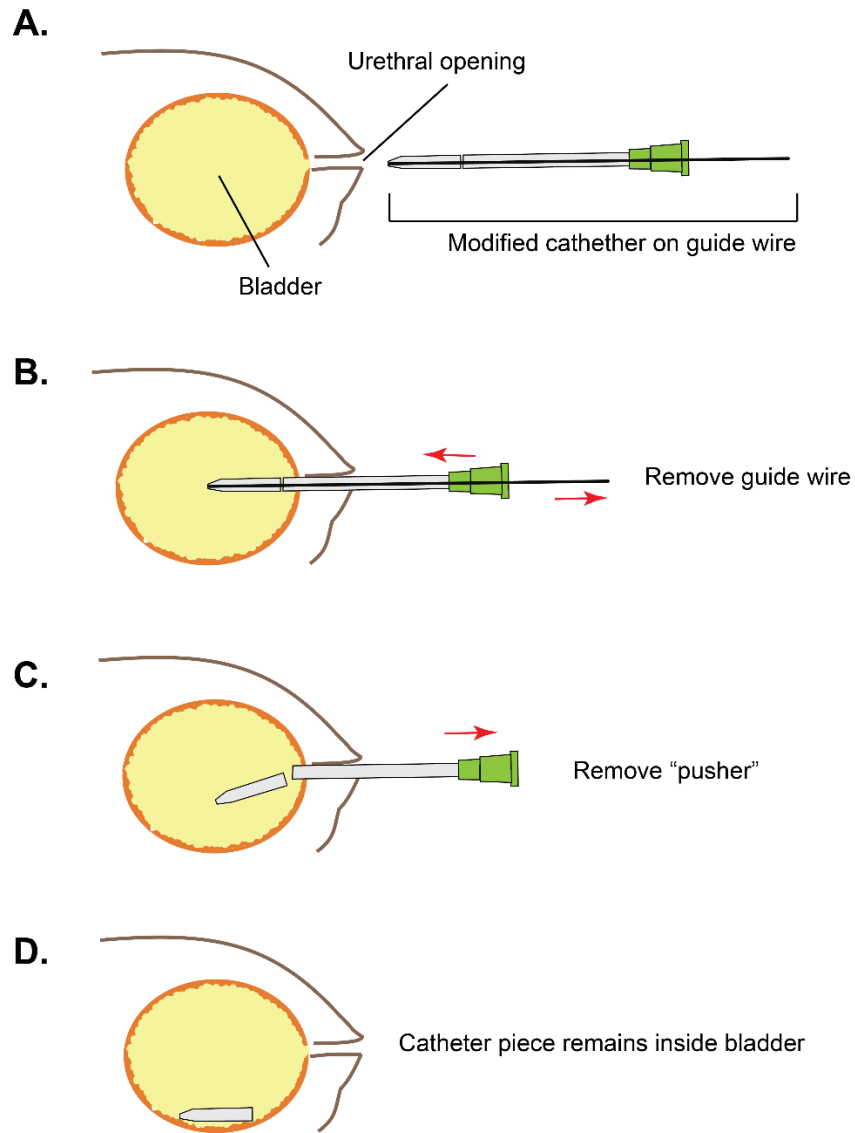


**Fig. 11.** Transurethral catheter implantation into rat bladder. (A) Close-up image of modified guide wire-mounted catheter entering the bladder. (B) Pusher was advanced over guide wire while the wire was slowly retracted to dislodge the 10mm implant piece into the bladder lumen. (C) The remaining pusher was withdrawn and implanted segment remained in situ (D).



#### **2.2.1.4 Daily monitoring**

All catheterized rats were monitored closely daily for physical health assessments as well as weight changes.

#### **2.2.1.5 Day 5: Assessment of urinary tract infection and bacterial adhesion and biofilm formation**

At 5 days post-instillation, all rats were sacrificed by CO<sub>2</sub> asphyxiation. Urine samples were collected from the bladder (if available), and the amount of bacteria in the urine was quantified via serial dilutions and CFU counts. Indwelling catheters were collected, rinsed in 200 µL of sterile PBS and transferred to 200 µL of fresh PBS prior to sonication at 50/60 Hz for 10 minutes in an ultrasonic water bath (No. 21811-820, VWR®) to aid biofilm dispersal. Samples were then vortexed at high speed for 10 sec, and bacterial numbers were determined by serial dilutions and CFU counts.

### **2.2.2 Percutaneous catheterization model**

#### **2.2.2.1 Bacterial strain, culture medium and animals**

Freezer stock bacteria were cultured in LB (10 g/L tryptone, 5 g/L yeast extract, and 10 g/L NaCl) O/N at 37°C, sub-cultured and grown overnight. It was then re-suspended in PBS at approximately  $5 \times 10^5$  CFU/mL to be used for intravesical injection. All procedures were approved by The University of British Columbia animal care committee. A total of 19 male C57BL/6 mice (Harlan®) at age 10 weeks were included in experiments.

### 2.2.2.2 Modification of catheter

Prior to animal procedures, 25 gauge angiocatheters (Terumo Surflash® Polyurethane I.V. Catheter 24G x 3/4", Cat. No. FF2419) were modified under strict aseptic conditions. Briefly, the needle portion of the catheter was temporarily removed, and a 4 mm section from the tip of the PU catheter was cut off using sterile blades. For uncoated samples, the 4 mm piece and the remaining catheter portion was re-assembled back onto the original needle (Fig. 12). For coated samples, the 4mm sections were coated with polymer-AMP coating (see section 2.2.2.3), rinsed in 70% ethanol for 5 min, and then rinsed in sterile PBS for 3 times prior to being assembled back onto the needle.

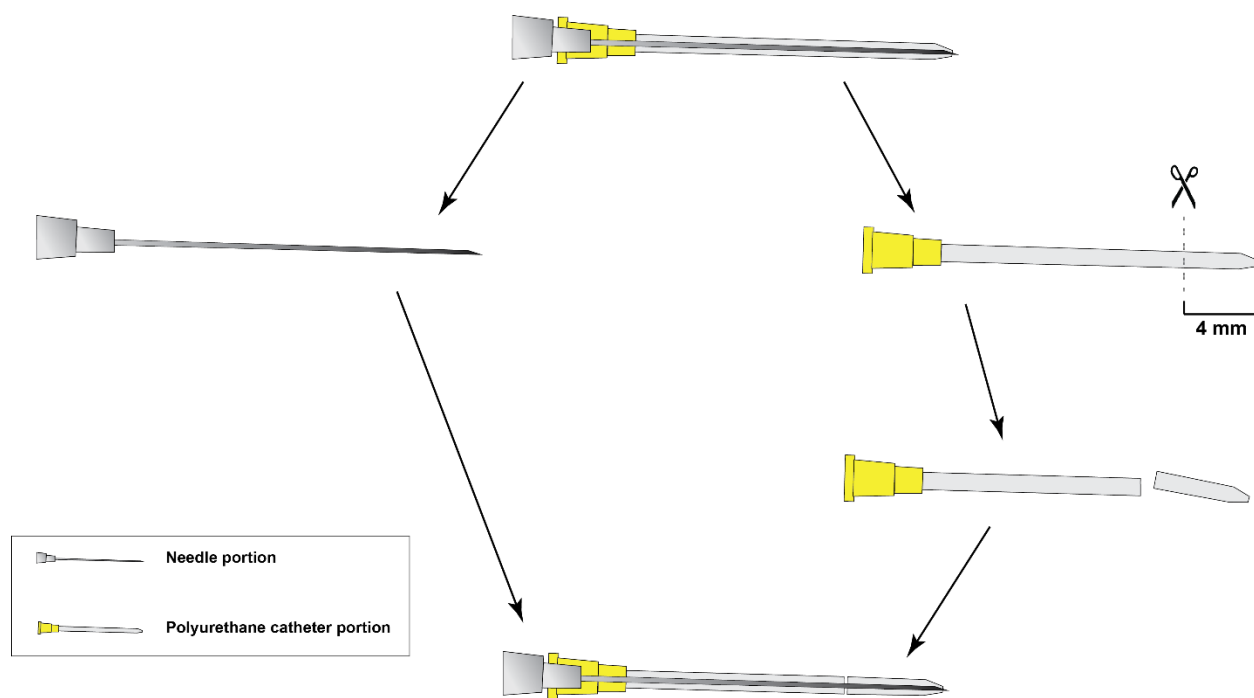


**Figure 12.** Modification of 24G I.V. PU catheter for *in vivo* testing

### 2.2.2.3 Coating 24G PU catheters for *in vivo* testing

Procedures for coating 24G PU catheters are similar to those used for coating 18G PU catheters. Please see section 2.1.2.2.

#### **2.2.2.4 Day 0: Percutaneous catheter implantation**

All mice were administered inhalational anesthesia with 3% isoflurane for initial induction. Once anaesthetised, isoflurane was set to 2.5%, and animals were positioned dorsally on a heating pad set at 38°C. The abdominal area was shaved, and mouse bladder was secured in place using a plastic belt. Sterile ultrasound gel was applied, and the Vevo 770® High-Resolution Imaging System was used to locate and visualize the rodent bladder. The modified 24 gauge polyurethane angiocatheter, mounted on the original needle, was positioned at a 30-degree angle just above the pubic bone with the bevel directed anterior (Fig. 13A). Once the needle has been properly aligned and can be visualized on the ultrasound machine, the needle was carefully inserted toward the bladder (Fig. 13B). Once the 4 mm catheter segment was confirmed to be entirely inside the bladder via ultrasound imaging, the needle is removed while the ‘pusher’ is pushed slightly inward (Fig. 13C). This dislodges the short PU catheter segment into the lumen of the bladder (Fig. 13D), such that once the ‘pusher’ is removed, the only thing that remains inside the mouse bladder is the implanted 4 mm catheter piece (Fig. 13E).

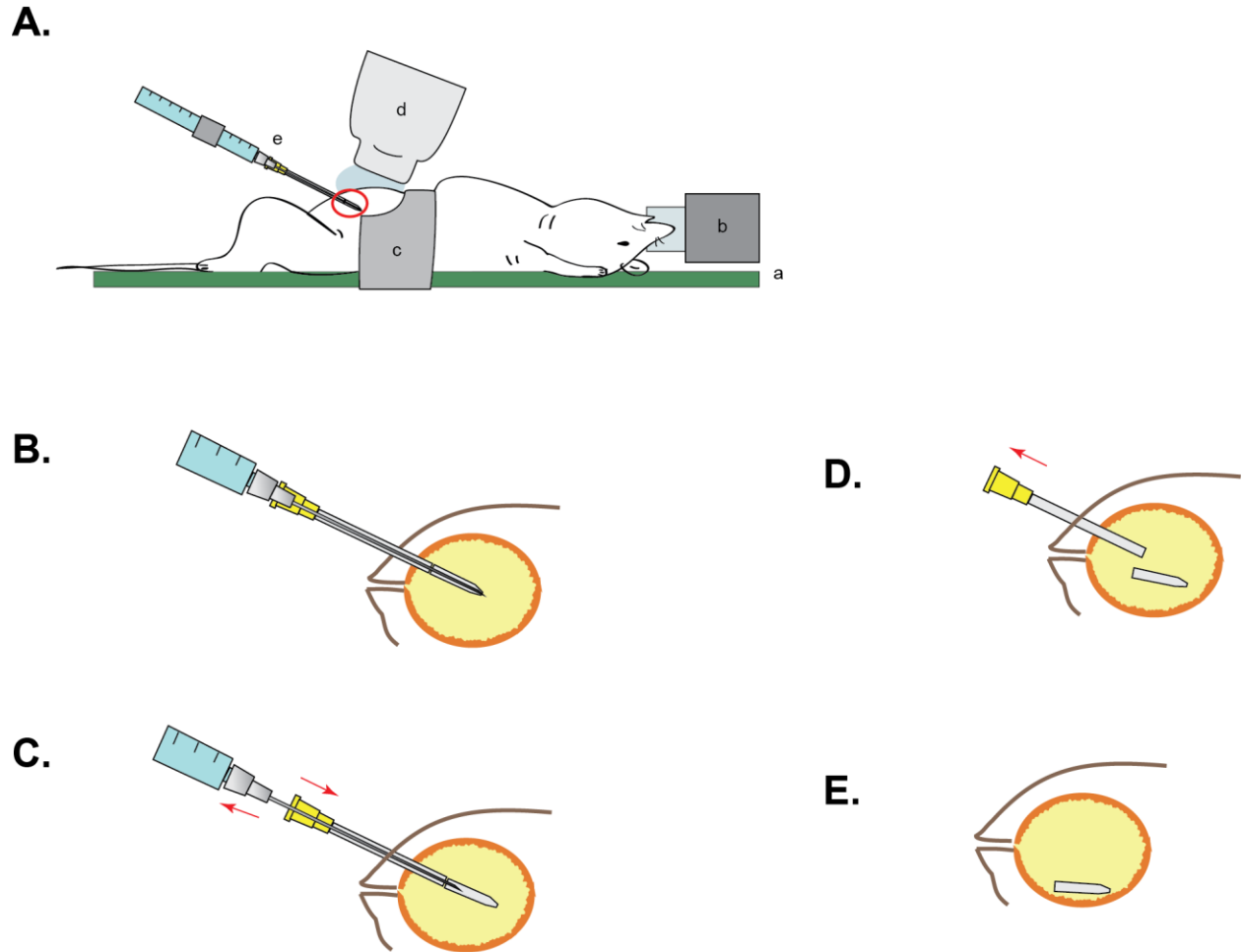


**Figure 13.** Ultrasound-guided percutaneous catheter implantation into mouse bladder. (A) Anaesthetised mouse was mounted onto a heated platform (a) while receiving isoflurane via nose cone (b). Plastic strap (c) was placed around the abdomen to secure the bladder position and prevent adjacent organ mobility. Ultrasound probe (d) was positioned over the lower abdomen with ultrasound gel in between. Once the bladder was visualized on screen, the modified needle-mounted angiocatheter (e) was brought in above the pubic bone and guided through the skin, abdominal wall muscles, and bladder wall (as visualized by ultrasound). (B) Close-up image of modified needle-mounted catheter entering the bladder. (C) Pusher was advanced over needle while needle was slowly retracted to dislodge the 4mm implant piece into the bladder lumen. (D) The remaining pusher was withdrawn and implanted segment remained in situ (E).

#### **2.2.2.5 Day 1: Bacterial instillation into rodent bladder**

One day after catheter implantation, all mice were anaesthetised. *P. aeruginosa* ( $5 \times 10^5$  CFU/mL in 50  $\mu$ L PBS) was percutaneously injected into the bladder lumen using a 30 gauge needle under ultrasound guidance, switching needles between each mouse. Once successfully injected, mice were kept asleep at 1% isoflurane for 1 h on a heating pad to allow for bacteria to adhere onto the implanted catheter. IVIS images were taken (see section 2.2.2.6), and the mice were then recovered from anesthesia. The starting amount of bacterial inoculum was confirmed by performing serial dilutions followed by CFU counts.

#### **2.2.2.6 Days 1 and 7: IVIS® Lumina imaging to confirm presence of bacteria**

Since the bacteria used in this study are of luminescent strains, the The Xenogen *in vivo* Imaging System (IVIS® Lumina, CA, USA) was used to image for the presence of bacteria by measuring luminescence levels detected within the mouse body immediately after mice were instilled with bacteria (Day1). Mice were then imaged for luminescence again at 7 days post-instillation (Day7). Bioluminescence from the region of interest (ROI) was defined manually, and data were expressed as total photon flux (photons/s). Background photon flux was defined from a ROI drawn over an area with no mouse.

#### **2.2.2.7 Daily monitoring**

All mice were monitored closely daily for physical health assessments as well as weight changes. The condition of the mice bladder and the implanted catheter piece was assessed every

2-3 days via ultrasound imaging. This was performed with mice under general anaesthesia using the Vevo 770 ultrasound device as described.

#### **2.2.2.8 Day 7: Assessment of urinary tract infection and bacterial adhesion and biofilm formation**

At 7 days post-instillation, all mice were sacrificed by CO<sub>2</sub> asphyxiation. Urine samples were collected from the bladder (if available), and the amount of bacteria in the urine was quantified via serial dilutions and CFU counts. Indwelling catheters were collected, rinsed in 100 µL of sterile PBS and transferred to 100 µL of fresh PBS prior to sonication at 50/60 Hz for 10 minutes in an ultrasonic water bath (No. 21811-820, VWR®) to aid biofilm dispersal. Samples were then vortexed at high speed for 10 sec, and bacterial numbers were determined by serial dilutions and CFU counts.

#### **2.2.2.9 Performing percutaneous catheterization on rats**

In addition to mice, a total of 3 Sprague Dawley rats were also used for percutaneous catheterization. The same steps were performed except 18G PU catheters were used instead of 24G, and a 10mm-long catheter piece was cut from the tip instead of a 4mm-long piece.

### **2.3 Statistical analysis**

Data are shown as the mean  $\pm$  SE. Statistical analysis was done using 2-sided ANOVA or T-Test as appropriate. Statistical significance was set at  $P < 0.05$ . A significance level of 0.05 indicates a 5% risk of concluding that an effect exists when there is no actual effect. For all graphs, \* indicates  $P \leq 0.05$ , \*\* indicates  $P \leq 0.01$ , and \*\*\* indicates  $P \leq 0.001$ .

## CHAPTER 3: RESULTS

### 3.1 Surface-tethered AMPs are less effective than free-floating counterparts

Various polymer-AMP combinations were tested *in vitro* to determine the combination which produces the most potent coating when tethered to implant surfaces. This large-scale screening of different antimicrobial coatings was conducted via the use of polystyrene NPs; since the activity of tethered peptides are often different compared to free-floating counterparts, it is important to test AMPs in tethered form. In addition, by using tiny particles with maximal surface area, polymer-AMPs are easily grafted from the surface of nanoparticles such that there is maximal exposure of the peptides at all directions when in solution. This allows us to conveniently test different combinations of polymer-AMPs *in vitro* using 96-well plates with agitation.

Using this method, unconjugated and conjugated AMPs were tested against three different luminescent bacteria (*E. coli*, *P. aeruginosa*, and *S. aureus*) by incubating the samples with each bacterium. Bacteria in each well were then quantified using two different methods: CFUs and luminescence detection. Luminescence was read at every hour, up to 4 hours post-incubation. Samples were then serially diluted and plated for CFUs.

Results indeed confirmed that based on the minimum peptide concentration required to kill all bacteria within the surrounding medium, tethered AMPs are at least 4-fold less bactericidal against free-floating counterparts, which is an important observation to keep in mind when designing tethered AMP coatings; the effectiveness of polymer-AMP coatings cannot be evaluated solely based on the effectiveness of free-floating AMPs (Fig. 14-15).

### **3.2 PDMA results in better antimicrobial activity than PMPC and PMPDSAH when conjugated to selected peptides**

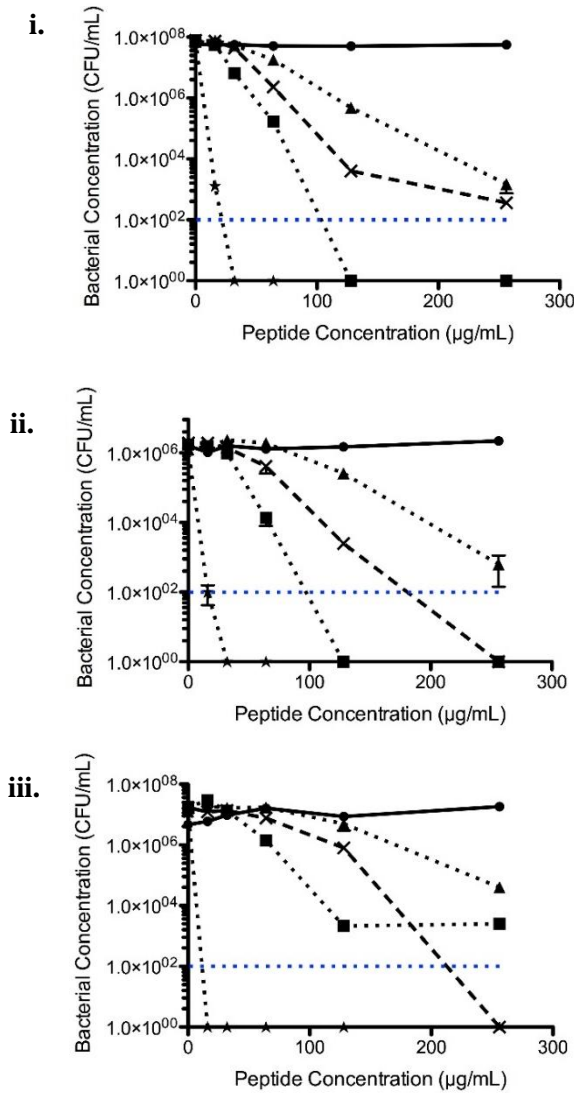
Using the NPs method, we tested different combinations of polymer and AMP by conjugating polymers (PDMA, PMPC, or PMPDSAH) to unique AMPs (E6, Tet20, Tet26, or Kai13).

Unfortunately, Tet26 and Kai13 coatings were not effective and are not presented in the results here for better clarity. For each of the peptides E6 and Tet20 which were effective, those conjugated to PDMA consistently resulted in higher antimicrobial activity against *E. coli* than those conjugated to either PMPC or PMPDSAH (Fig. 14A.i. and 14B.i.). When comparing between PMPC and PMPDSAH, peptides conjugated to the former polymer showed better antimicrobial activity than those conjugated to the latter, hence suggesting the order of conjugated brushes, from strongest associated antimicrobial activity to weakest, to be: PDMA > PMPC > PMPDSAH. For instance, at 128 µg/mL of peptide concentration, PDMA-E6 reduced the concentration of *E. coli* by 6 logs, while PMPC-E6 reduced it by ~2.5 log, and PMPDSAH-E6 by less than 1 log. This trend was observed as well when the samples were tested against *S. aureus* (Fig. 14A.ii.), and *P. aeruginosa* (Fig. 14A.iii.). This trend was also observed when the same polymers were conjugated to Tet20, albeit the antimicrobial activities observed were much lower than those observed when the polymers were tethered to E6 (Fig. 14B). Similar findings were also observed via luminescence measurements, thus further confirming the results (Fig. 15). For both Figures 14 and 15, polymer-only coatings were also tested, and showed very similar results as the uncoated controls. However, data from those results were excluded from the graphs above for clarity purposes.



—●— Uncoated Control    —■— PDMA-Peptide Coating    —×— PMPC-Peptide Coating  
 —▲— PMPDSA-Peptide Coating    —★— Free-floating Peptide    --- Detection Limit

### A. E6 Peptide



### B. Tet20 Peptide

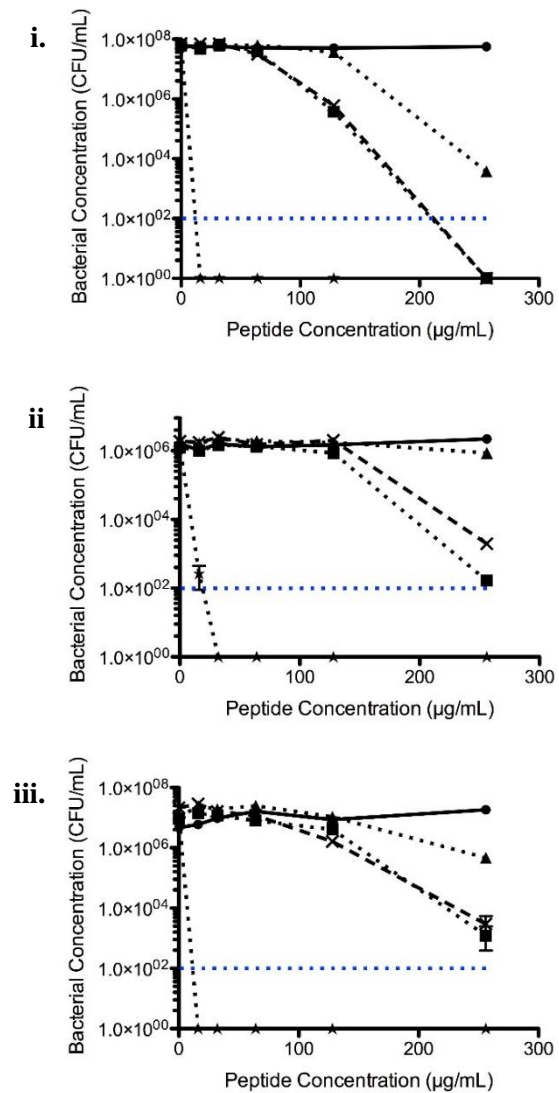
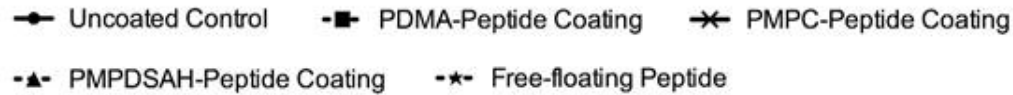
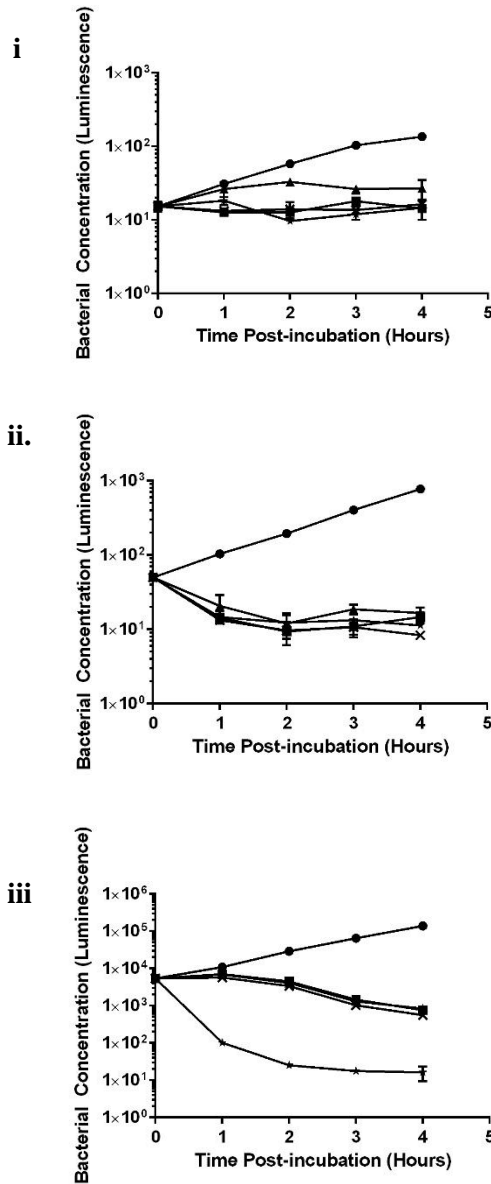


**Figure 14.** CFU counts of different brush-peptide samples with either (A) E6 peptide or (B) Tet20 peptide at 4 h post-co-incubation with either (i) *E. coli* lux, (ii) *S. aureus* lux, or (iii) *P. aeruginosa* lux. All results were gathered from a total of 3 replicates per condition. Standard errors range from 0 - 30% of the mean.



### A. E6 Peptide



### B. Tet20 Peptide

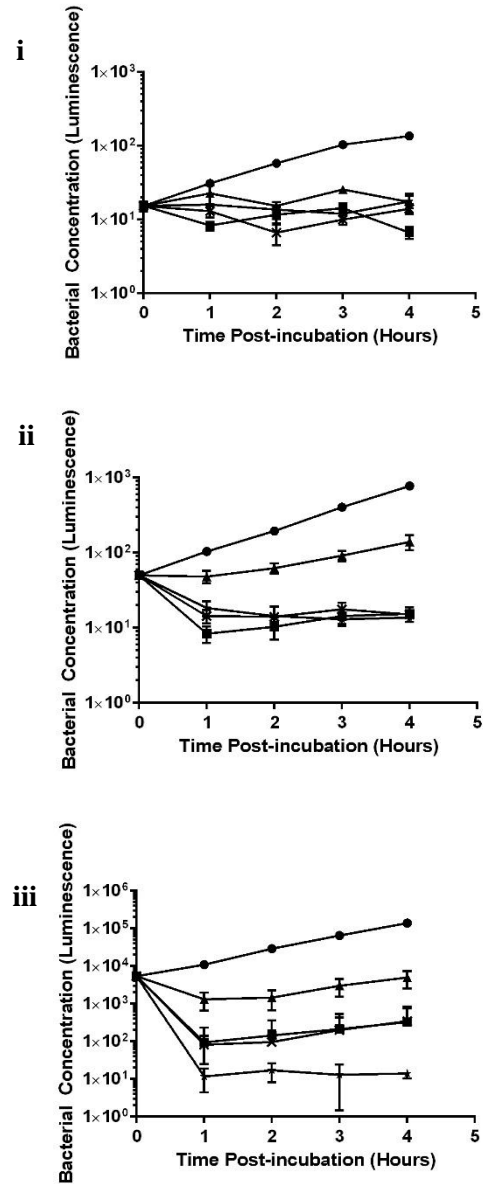


**Figure 15.** Relative luminescence readings of different brush-peptide combinations with either (A) E6 peptide or (B) Tet20 peptide at 256  $\mu\text{g/mL}$  over the period of 4 hours of co-incubation with either (i) *E. coli* lux, (ii) *S. aureus* lux, or (iii) *P. aeruginosa* lux. All results were gathered from a total of 3 replicates per condition. Standard errors range from 0.5 – 50% of the mean.

### **3.3 Tethered E6 is more potent than tethered Tet20**

When comparing the antimicrobial activity between tethered E6 and tethered Tet20, it was evident that the former peptide was more potent than the latter one (Fig. 16). This was interesting, as Tet20 was actually more potent than E6 when comparing their activity as non-tethered, free-floating peptides.

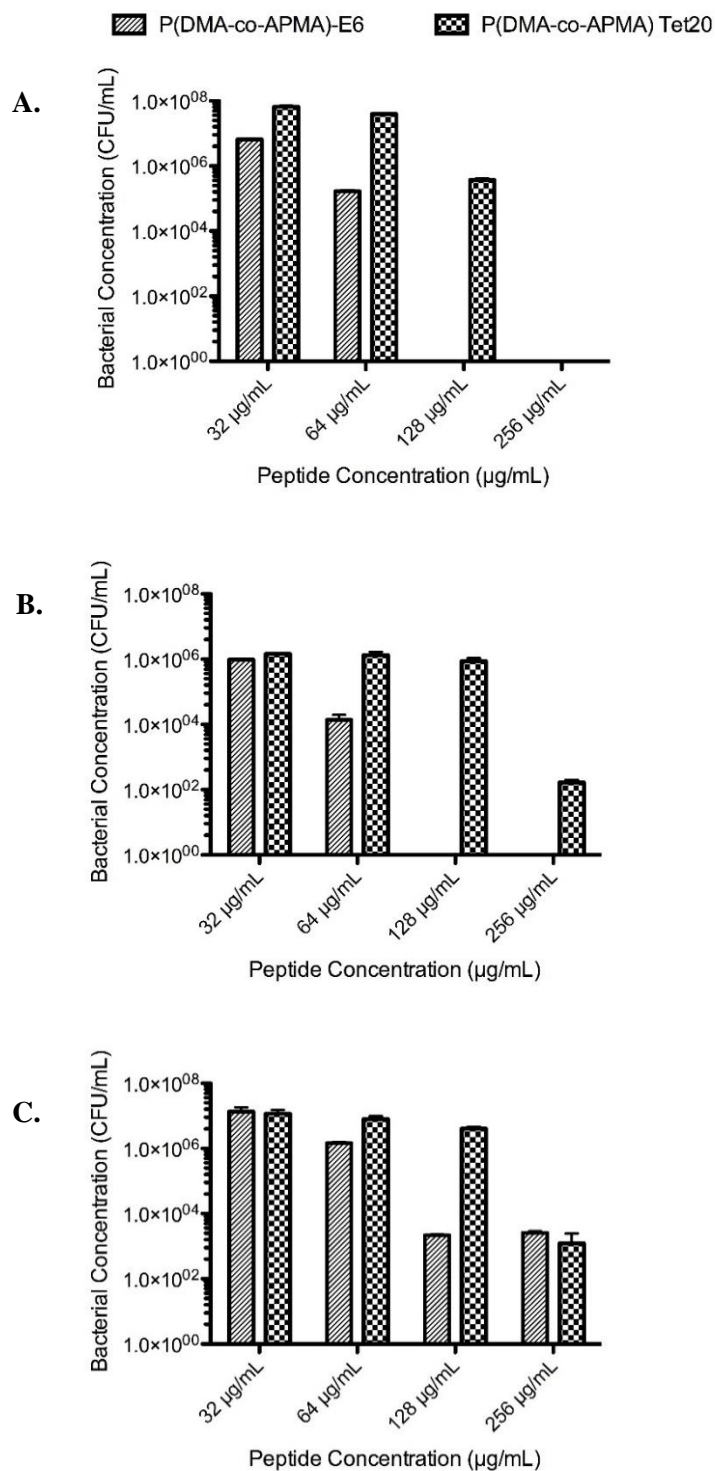


**Figure 16.** Comparison in bactericidal properties between PDMA-E6 and PDMA-Tet20 against (A) *E. coli*, (B) *S. aureus*, and (C) *P. aeruginosa*. Data presented here are the same as those from Fig. 14. Standard errors range from 6 – 50% of the mean.

### **3.4 PDMA-E6 coated PU catheters significantly reduce both bacterial adhesion and planktonic bacterial growth *in vitro***

With PDMA-E6 coating giving the most potent antimicrobial activity when tethered to NPs, the same coating was tested on polyurethane angiocatheters *in vitro*. When coated and uncoated samples were co-incubated with *P. aeruginosa* for 6h, the amount of bacteria adhered to polymer-peptide-coated samples was significantly less than the amount tethered to uncoated controls. PDMA-coated catheters without E6 was also able to reduce bacterial adhesion, albeit to a lesser degree than PDMA-E6 coated surfaces (Fig. 17A). The PDMA- and PDMA-E6-coated catheters were also able to reduce the planktonic growth of *P. aeruginosa* by approximately 40% when compared to uncoated controls (Fig. 17B). However, no difference in activity on planktonic growth was observed between PDMA- and PDMA-E6 coatings (Fig. 17B).

Similar findings were observed by co-incubating uncoated and uncoated catheters with *S. saprophyticus* (Fig. 18).

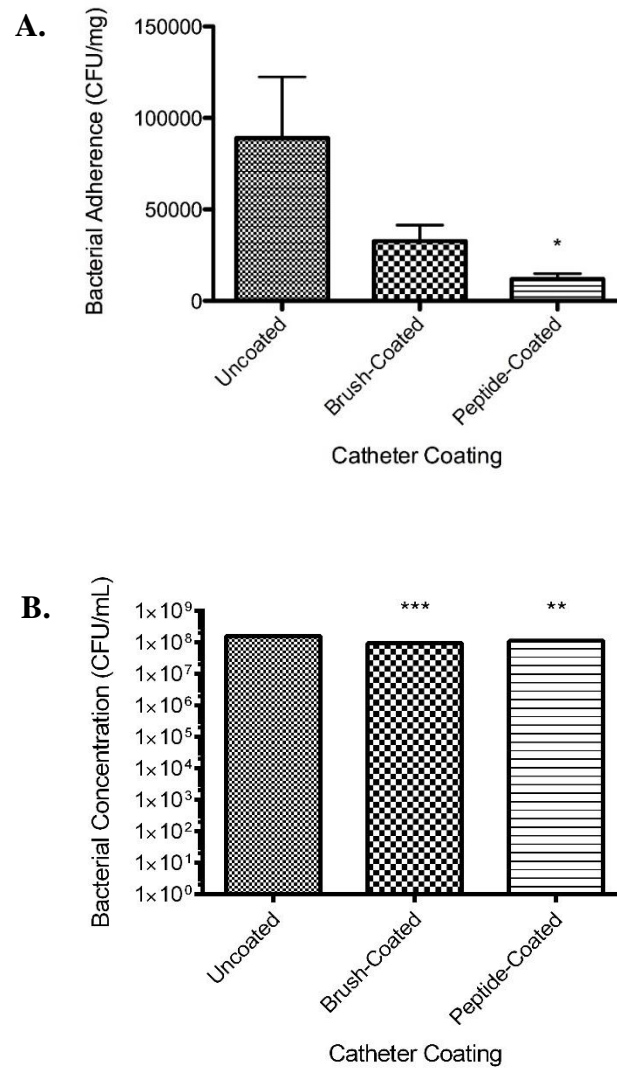


**Figure 17.** Effect of PDMA- and PDMA-E6-coated polyurethane catheters on the (A) bacterial adherence and (B) planktonic growth of *P. aeruginosa* 6h post-co-incubation. \* indicates  $P \leq 0.05$ , \*\* indicates  $P \leq 0.01$ , and \*\*\* indicates  $P \leq 0.001$ . All data are based on a total of 3 replicates per condition. Standard errors range from 25 – 38% of the mean.

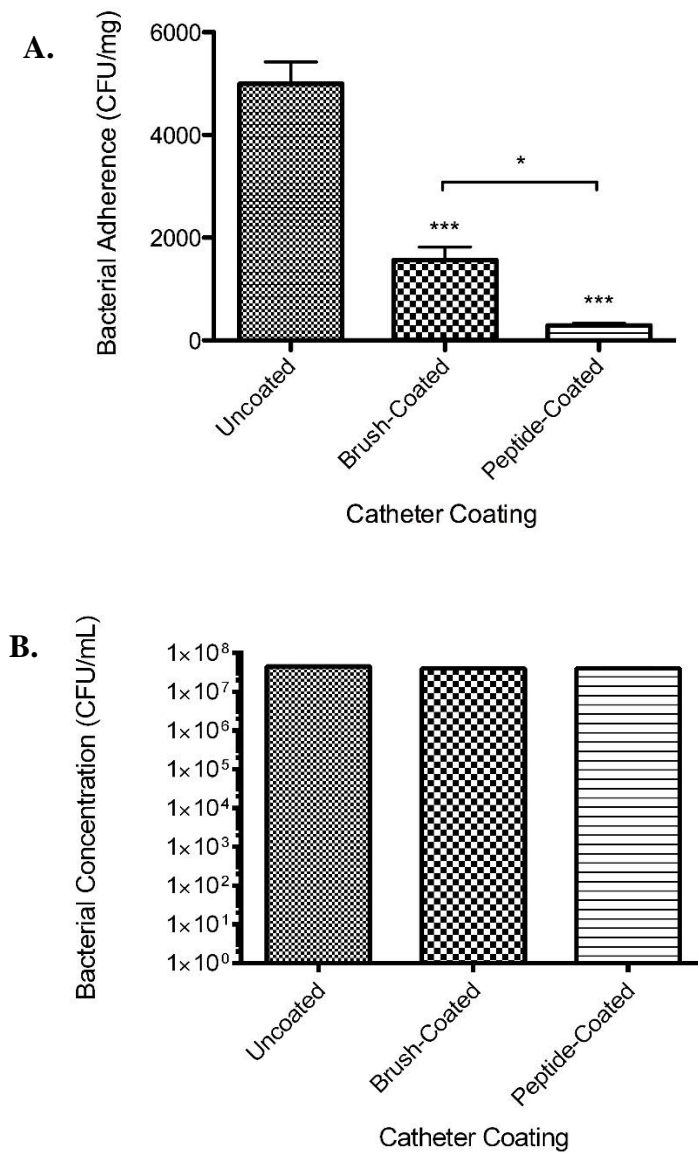


**Figure 18.** Effect of PDMA- and PDMA-E6-coated polyurethane catheters on the (A) bacterial adherence and (B) planktonic growth of *S. saprophyticus* 6h post-co-incubation. \* indicates  $P \leq 0.05$ , \*\* indicates  $P \leq 0.01$ , and \*\*\* indicates  $P \leq 0.001$ . All data are based on a total of 3 replicates per condition. Standard errors range from 8 – 16% of the mean.

### **3.5 Ultrasound-guided percutaneous catheterization model is a more reliable CAUTI model than the transurethral catheterization model.**

Female rodents have been preferred in previously published papers where authors tried to transurethrally catheterize the animals' bladder [132]. This is mainly due to differences in the characteristics of the urethra between the two genders; a female's urethra tends to be short and straight, whereas a male's urethra tends to be much longer and spirally-shaped. In addition, the presence of the prostate gland in male rodents blocks the accessibility of the urethra towards the urinary bladder.

A total of two different *in vivo* CAUTI models were tested in this study: the transurethral catheterization model and the percutaneous catheterization model. Based on our experiments, the latter model is preferred as it is more reliable and feasible, particularly when it comes to the use of using smaller animals. This is due to female rats being much harder to transurethrally catheterize than female mice. Through multiple attempts to transurethrally catheterize female rats, we repeatedly discovered that the female rats' urethra anatomy is more complicated than that of female mice; it appears that unlike mice, a rat's urethral opening (meatus) does not lead directly to the urethra of the rodent. Rather, it leads to a split route, where one end is a dead-end groove, while the other end is the urethra (Fig. 19). Hence, when inserting a modified catheter through the urethral opening, there is a high chance that the catheter ends up in the dead-end groove, leading to unsuccessful catheterization of the rat. On the other hand, such groove appears to be absent in female mice.



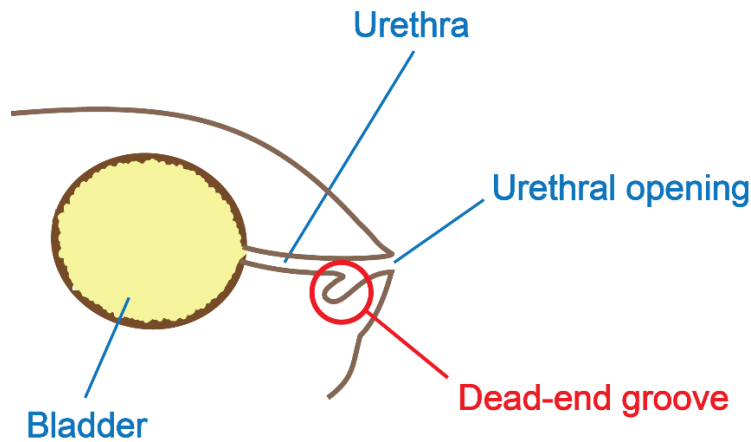


**Fig. 19.** The Sprague Dawley rat's urethral opening (meatus) appears to lead to both the urethra and a dead-end groove.

In addition to the presence of the dead-end groove, once rodents are transurethral catheterized successfully, they are also capable of peeing out the implant regularly, causing the implant piece to be lost. This was observed in 4 out of 6 successfully catheterized rats. The implanted pieces were typically lost within 2 days post-implantation.

However, of the rats catheterized transurethral, two rats infected with *S. aureus* and one untreated control rat did manage to hold on to the indwelling implants for up to 5 days post-catheterization. Urine and indwelling implants were collected from these rats for CFU analyses, with results shown in Figure 20.

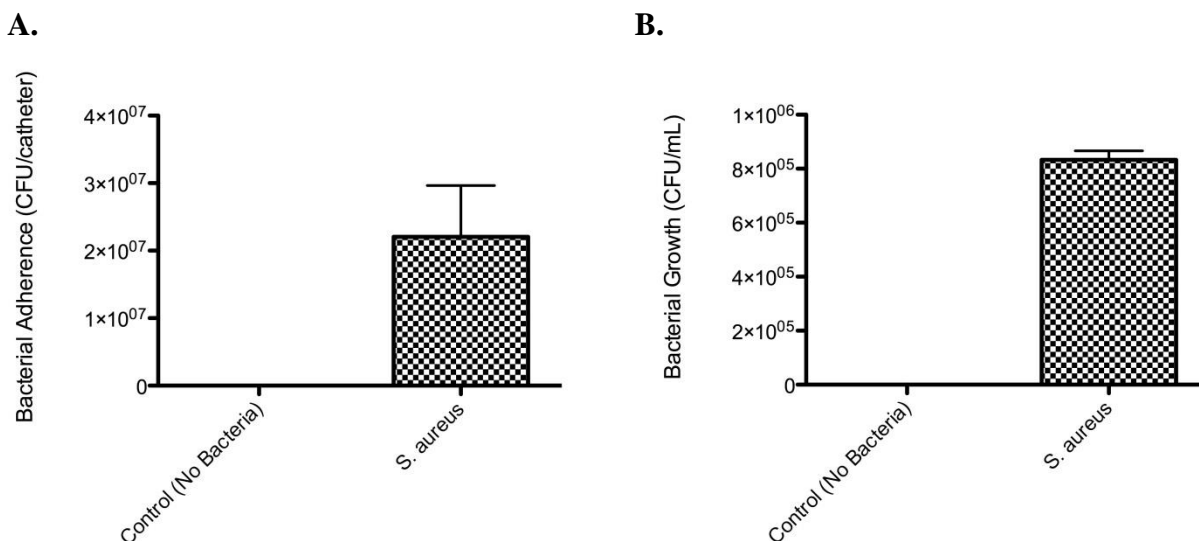


**Fig. 20.** Amount of bacteria recovered via CFU counts from (A) implanted catheters, and (B) rodent urine from *S. aureus*-infected and uninfected control rats. Data shown was gathered from 2 infected rats and 1 control rat. Standard errors range from 0 – 48% of the mean.

Since the transurethral catheterization model was inefficient and not reliable, the ultrasound-guided percutaneous catheterization mouse model, which was recently developed by the Lange Lab, was adopted for the testing of implant coatings. The procedure was attempted on both mice and rats. However, coated peptide implants were tested in mice only, as multiple attempts using rats suggested the larger rodent to have a much thicker, tougher bladder wall, preventing successful percutaneous bladder penetration and implantation.

### **3.6 Coated and uncoated 4mm-long, 24 gauge polyurethane catheters successfully implanted percutaneously into mice bladder**

Polyurethane implants of 24G and 4mm in length were successfully catheterized via ultrasound-guided percutaneous implantation for a total of 19 mice (11 with PDMA-E6 coated, 8 with uncoated controls).

Upon instillation of bacteria into the implanted mice bladder on Day 1, IVIS® imaging confirmed the presence of luminescent *P. aeruginosa* culture within the bladder of all infected mice (Fig. 21A). Average total photon flux measured for untreated mice was  $1.43 \times 10^5$  photons/s, whereas for mice bearing coated implants, it was  $1.51 \times 10^5$  photons/s, confirming that initial bacterial load instilled into mice bladder was similar between control and treated animals (Fig. 22)

Based on ultrasound imaging, most bladders become swollen within 24 hours after being instilled with bacteria (Fig. 23). However, by 4 days post-instillation, the majority of the mice bladders start to heal physically (Fig. 24). This trend of healing bladder continues at 7 days post-instillation (Fig. 25). Interestingly, not much difference was observed between the physical bladder conditions of mice bearing uncoated versus coated implants based on ultrasound images. However, the surface of indwelling, uncoated catheters look slightly more uneven than that of indwelling, coated catheters at 4 days post-instillation; the outline of the catheters for uncoated samples appear to be generally more uneven than that of coated catheters (Fig. 24).

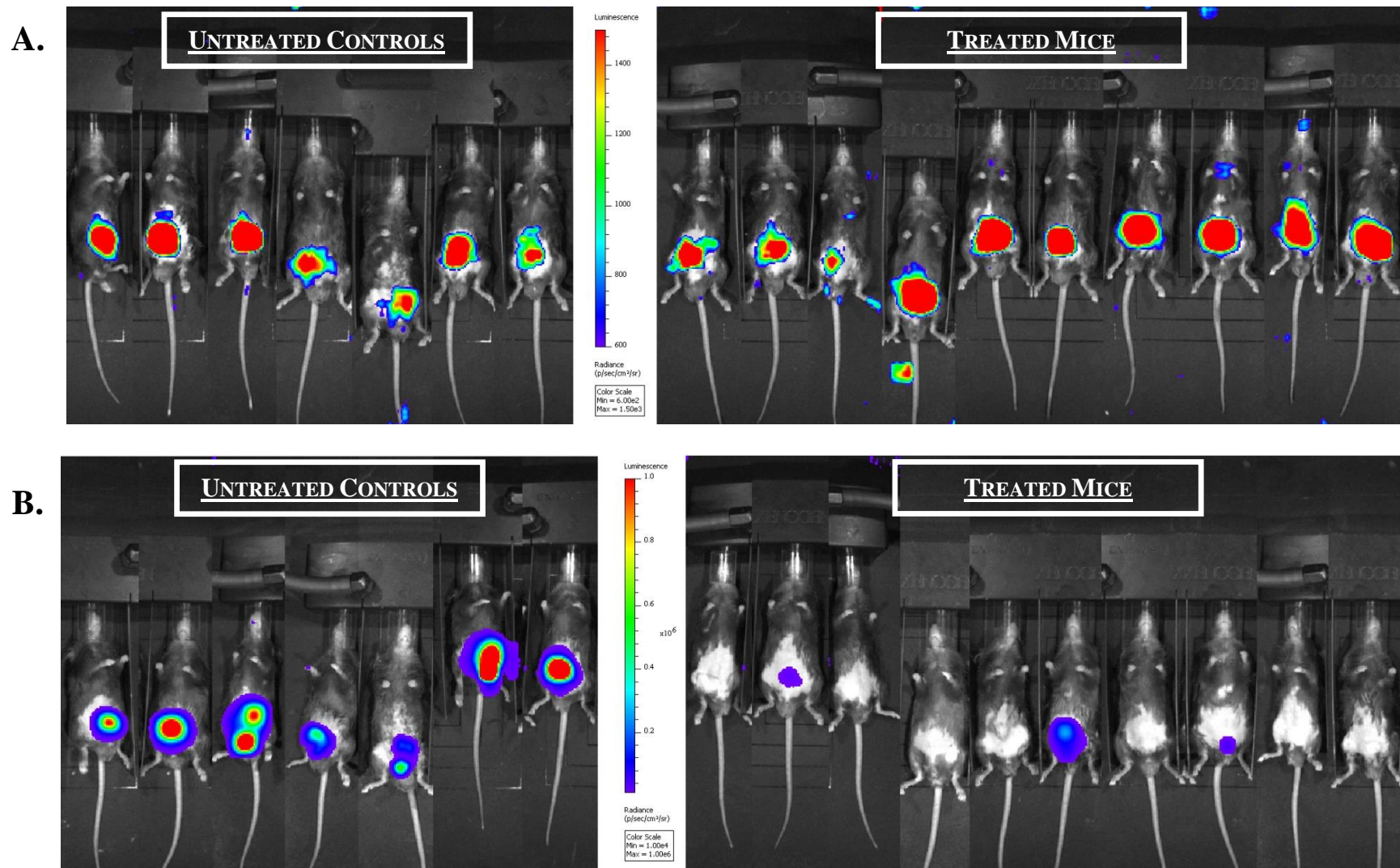


**Figure 21.** IVIS images of mice bearing either uncoated (untreated) or PDMA-E6-coated (treated) catheter at (A) 1 h and (B) 7 days post-institution with *P. aeruginosa* lux into bladder.

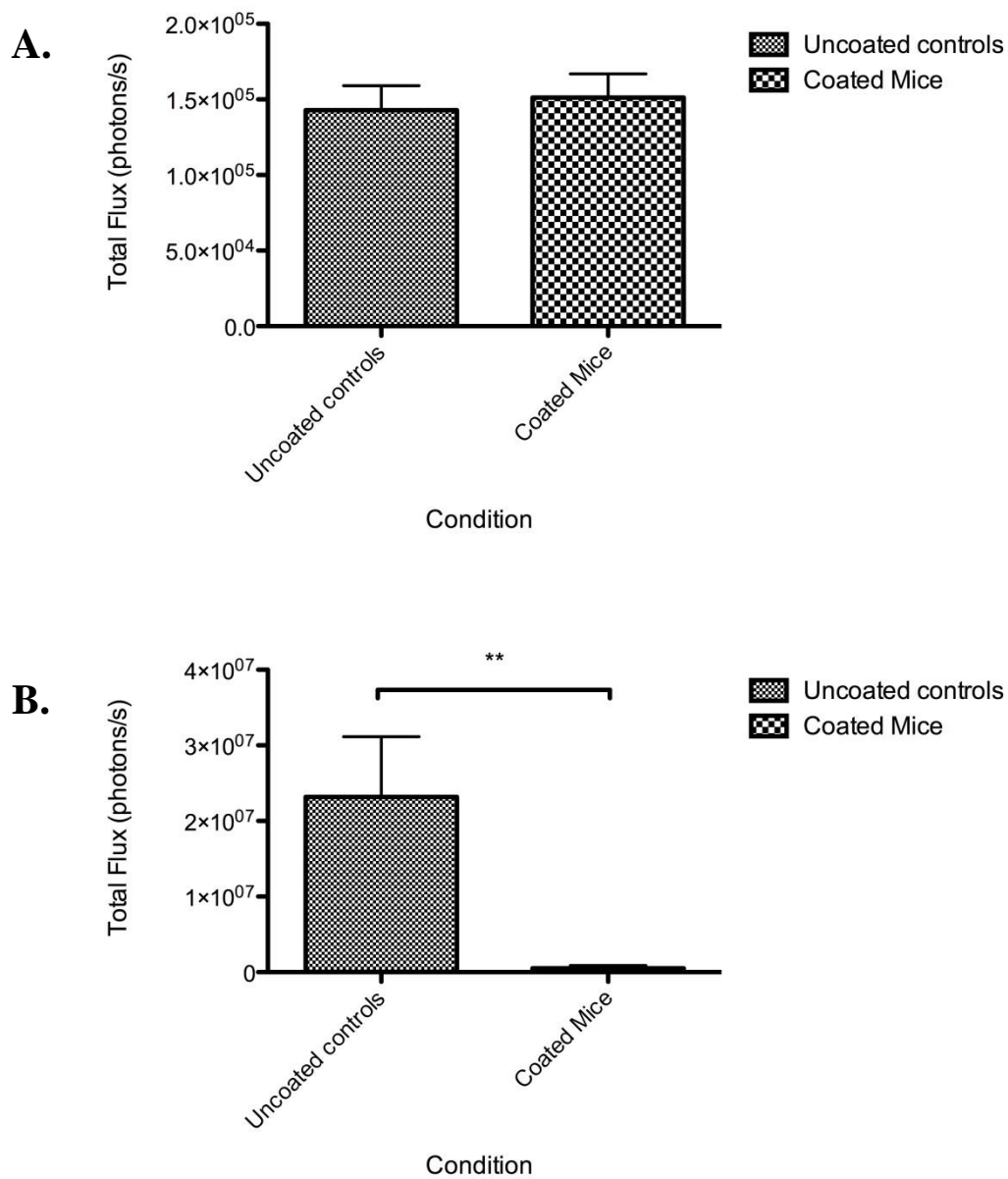


**Figure 22.** Bioluminescence readings measured for untreated and treated mice using the IVIS® Lumina. Bioluminescence from the region of interest (ROI) was defined manually, and the data were expressed as total photon flux (photons/s). All bioluminescent data were collected and analyzed using IVIS at (A) 1h and (B) 7 days post-bacterial-instillation into mice bladder. \* indicates  $P \leq 0.05$ , \*\* indicates  $P \leq 0.01$ , and \*\*\* indicates  $P \leq 0.001$ . Standard errors range from 34 – 40% of the mean.

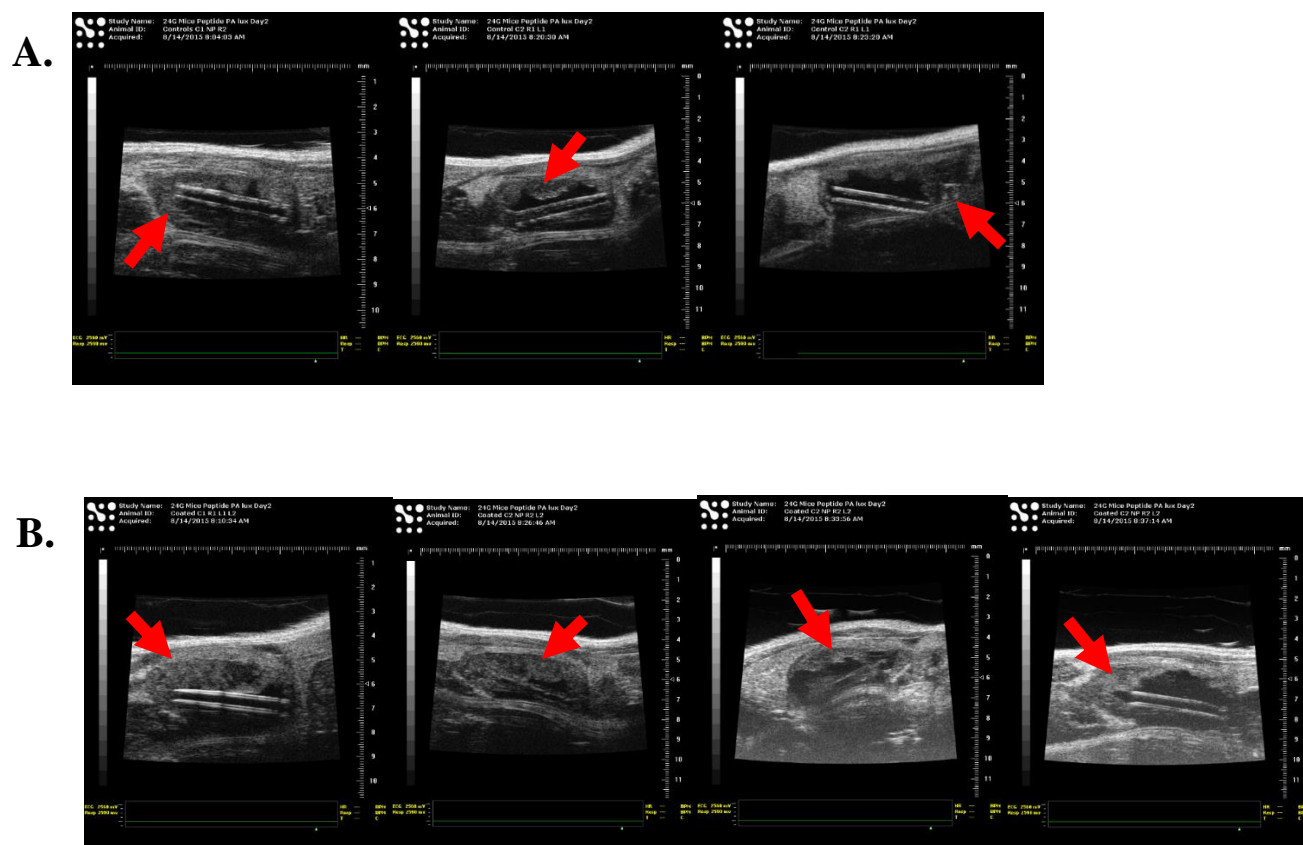
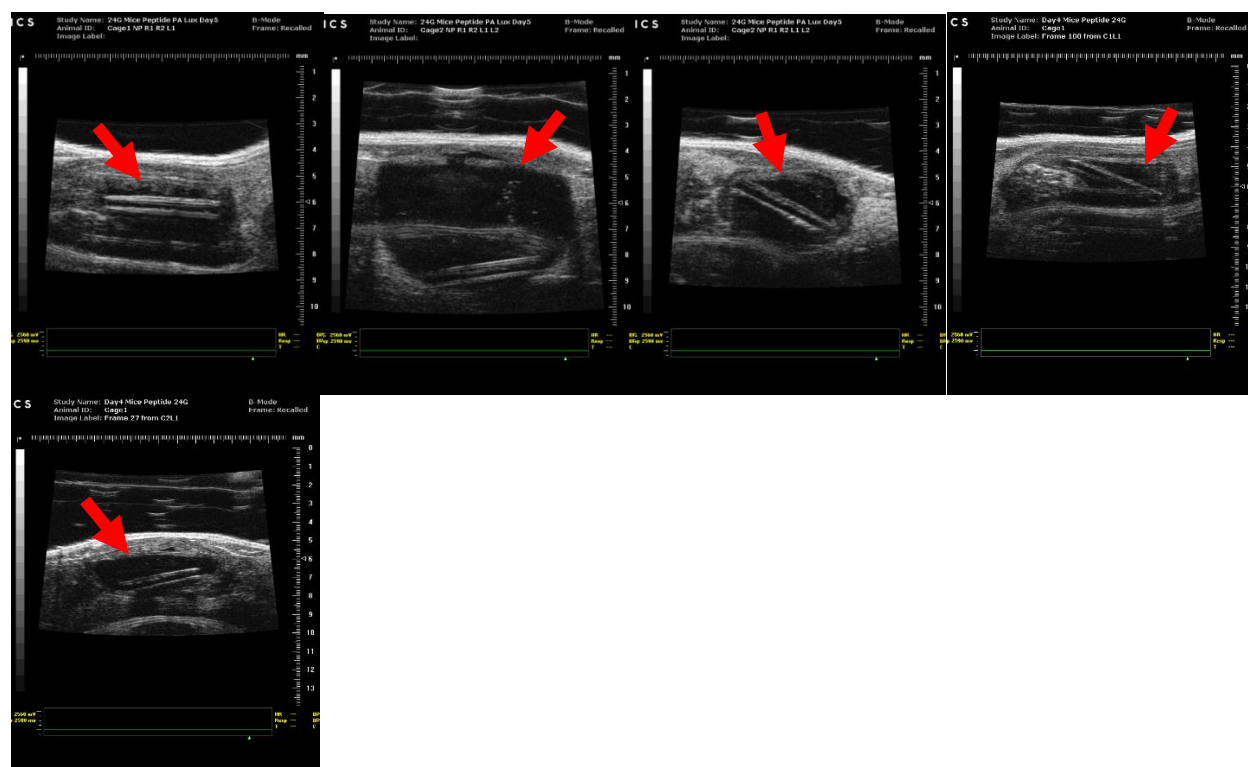


**Figure 23.** Ultrasound images of bladders of mice with (A) uncoated implant pieces and (B) PDMA-E6-coated implant pieces at 24h post-bacterial instillation. Red arrows indicate bladder areas that appeared to be swollen.



A.



B.

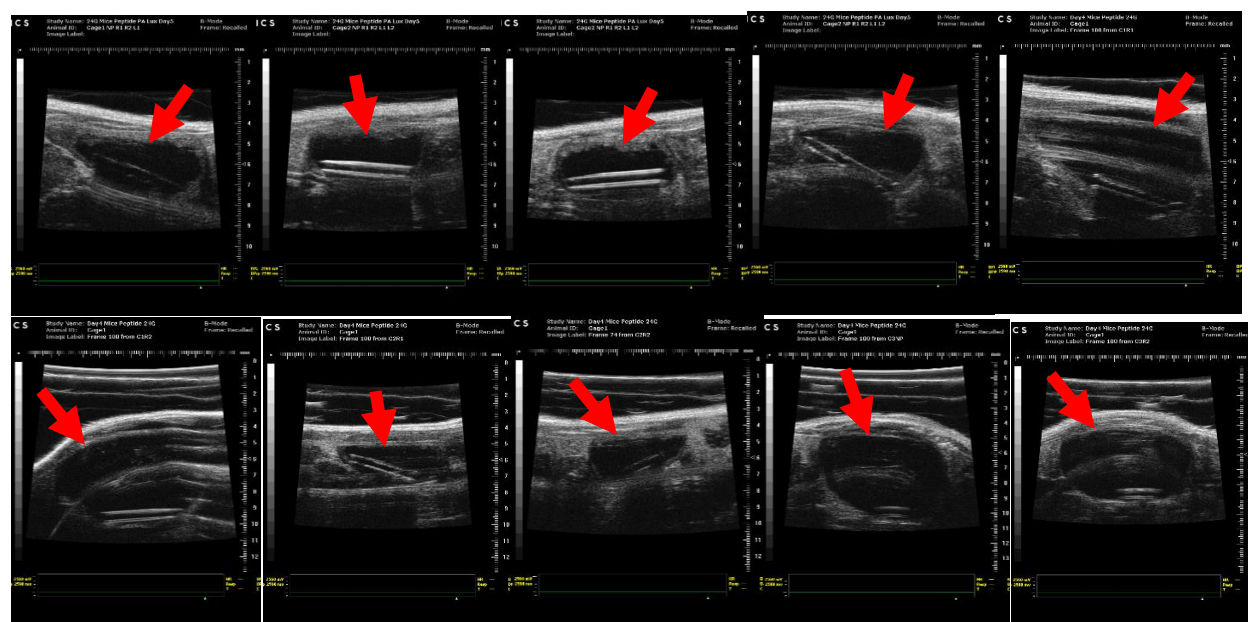
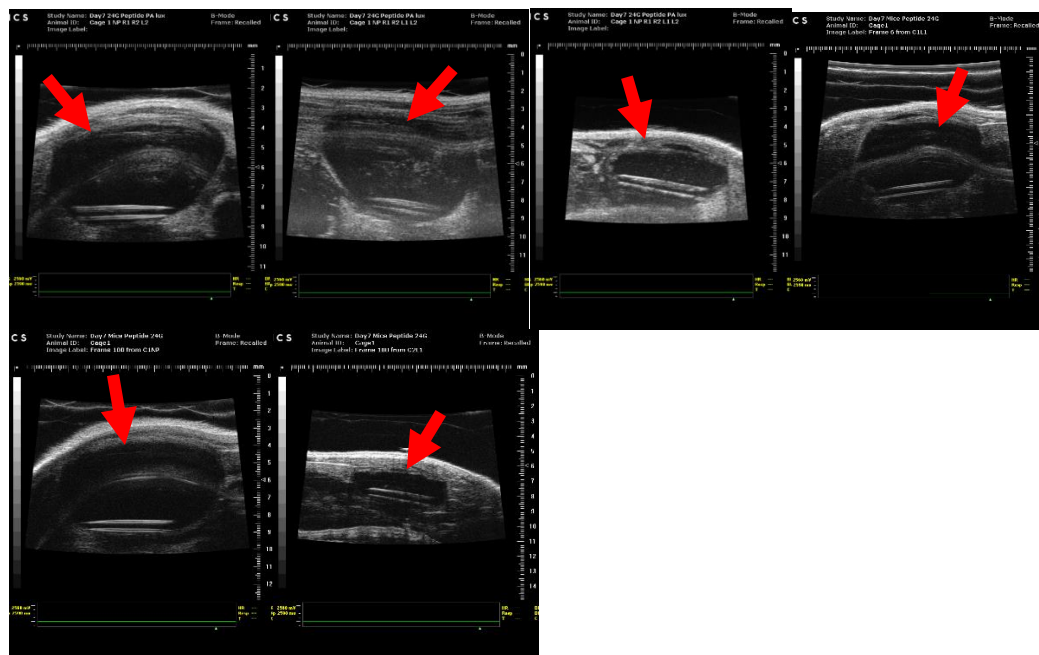


**Figure 24.** Ultrasound images of bladders of mice with (A) uncoated implant pieces and (B) PDMA-E6-coated implant pieces at 4 days post-bacterial instillation. Bladder walls (indicated by red arrows) are overall less swollen compared to 24h post-bacterial instillation (see Fig. 23).

A.



B.

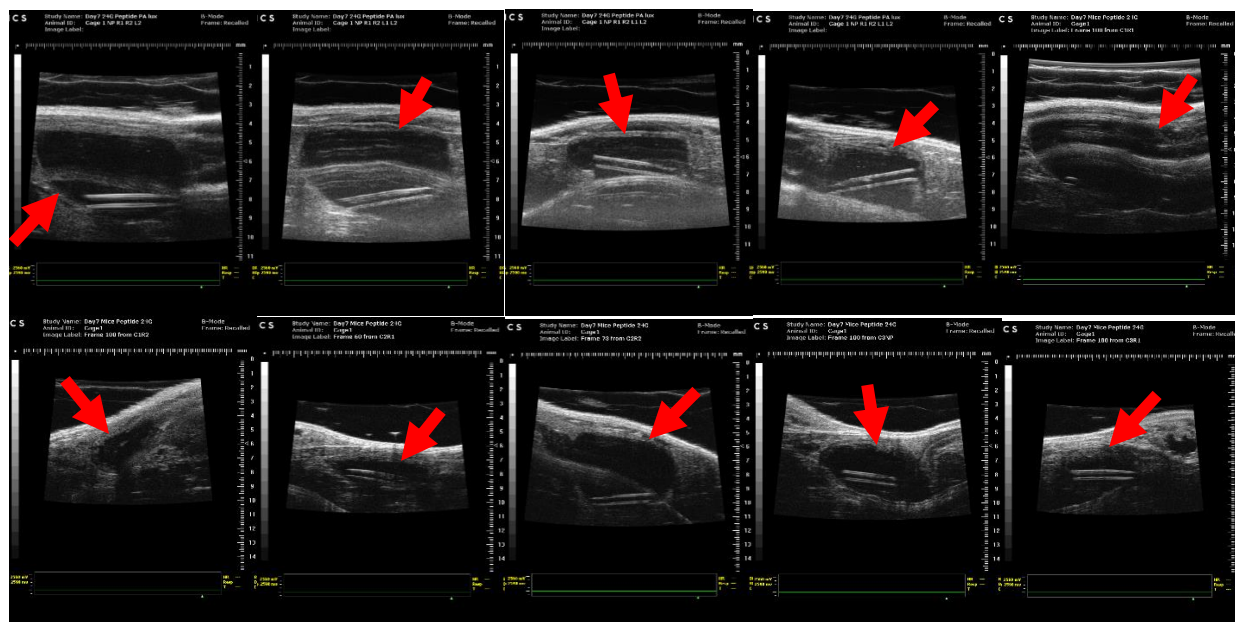


**Figure 25.** Ultrasound images of bladders of mice with (A) uncoated implant pieces and (B) PDMA-E6-coated implant pieces at 7 days post-bacterial instillation. Red arrows indicate where bladder wall is located.



### **3.7 Antimicrobial activity of PDMA-E6-coated implants is observed *in vivo* 7 days post-instillation**

At 7 days post-instillation, IVIS imaging showed the amount of bacterial luminescence detected is significantly less in mice bearing a peptide-coated bladder implant than those with uncoated control implants (Fig. 21B). The average total photon flux reading for mice bearing uncoated catheters was  $2.32 \times 10^7$  photons/s, while for those bearing coated catheters, it was  $5.25 \times 10^5$  photons/s. Hence, the average photon flux was reduced by 97.7% for treated mice compared to untreated controls (Fig. 22B).

These findings were also confirmed by CFU counts (Fig. 26). At 7 days post-instillation, the average amount of *P. aeruginosa* adhered onto uncoated control implants were  $1.20 \times 10^6$  CFU, whereas for PDMA-E6-coated samples, it was  $5.00 \times 10^1$  CFU, giving a 99.9958% reduction in bacterial adherence.

Similarly, for planktonic growth/survival of *P. aeruginosa* within the urine of mice, untreated control mice had an average of  $1.10 \times 10^7$  CFU/mL while treated mice had an average of only  $1.47 \times 10^4$  CFU/mL, a 99.8660% reduction in presence of bacteria within the mouse urine.

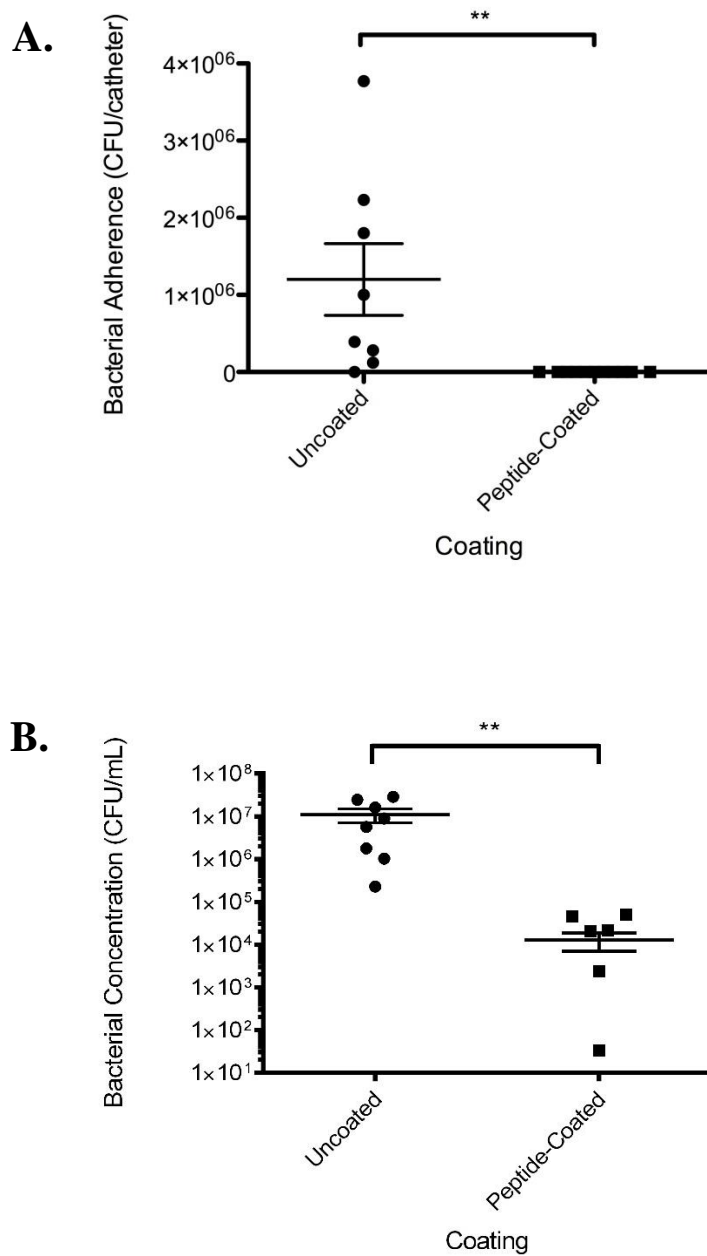


**Figure 26.** Antimicrobial activity of PDMA-E6-coated catheters *in vivo* on (A) bacterial adhesion, and (B) bacterial planktonic growth/survival as determined by CFUs. Each dot represents data from one animal. \* indicates  $P \leq 0.05$ , \*\* indicates  $P \leq 0.01$ , and \*\*\* indicates  $P \leq 0.001$ . Standard errors range from 39 – 48% of the mean.

## CHAPTER 4: DISCUSSION

Antimicrobial peptides (AMPs) have gained increasing interest over recent years, with their broad-spectrum, multi-target activity making them potential alternative treatments for MDR bacteria. In particular, coating medical implants which are often prone to bacterial adhesion and infection with AMPs have shown promising results in recent studies.

In terms of coating medical devices with peptides, tethering the peptides to polymer brushes have become an attractive approach for creating highly effective antimicrobial coatings. By creating a low-fouling surface to prevent non-specific interactions between the implant surface and the indwelling biological environment, and by acting as branches to help increase the density of peptides loaded onto a given surface area, these polymers greatly increased the activity of AMPs as coatings. In addition, polymer brushes are highly stable both chemically and mechanically, and they have excellent biocompatibility, making them suitable for coating a vast variety of surface materials.

In this study, we examined the antimicrobial activity of different polymer brushes (PDMA, PMPC, and PMPDSA) conjugated to various AMPs (Table 6). Polymer brushes and peptides for testing were chosen based on recently published studies of AMPs and polymer brushes [71, 131]. To screen for the most potent peptide-brush combination, we covalently attached the brushes onto PS NPs and determined for antimicrobial activity by introducing them to several luminescent strains of common uropathogens. By using luminescent bacteria, it allows us to perform high throughput screen by not only plating for CFUs 4h post-incubation, but also detecting for luminescent levels at every hour post-incubation prior to the 4h time point; by genetically engineering bacteria by placing a *lux* gene construct under the control of an inducible

promoter of housekeeping genes, only live bacteria would be transcribing the gene to confer a bioluminescent phenotype detectable by luminometers [133].

Results of CFU counts as well as luminescence both suggest that of the peptides tested, only E6 and Tet20 showed decent antimicrobial activity (Fig. 14, data for ineffective peptides not included). This is most likely due to the fact that when free-floating peptides are tethered to polymer brushes, one of the peptide (usually the carboxyl end) becomes immobilized. This could change the mobility and the mechanism of action of the peptide; AMPs are usually able to penetrate through the bacterial wall and possibly into the bacterial cell, further altering cellular activities. By tethering the peptide on one end, the peptide would only be able to interact with the wall but not penetrate through or travel into the cell. In addition, the original activity of the peptide may also be influenced, especially if the active site of the peptide is close to the tethered end. This also explains our observation of tethered AMPs being significantly less effective than their free-floating counterparts;

Of the polymer brushes tested, peptide combinations with PDMA generally resulted in greater antimicrobial activity, followed by PMPC, then PMPDSA. For instance, for E6-conjugated NPs against *E. coli*, E6-PDMA coating decreased bacterial load by approximately 8 logs at 256  $\mu\text{g/mL}$  peptide concentration and 4 h post-incubation compared to untreated control, while E6-PMPC and E6-PMPDSA decreased the load by approximately 8 logs and 4.5 logs, respectively (Fig. 14A.i.). Similar trends can be observed when the same polymers are conjugated to peptide Tet20 (Fig. 14B). While it has been known that the characteristics of AMPs can greatly influence a peptide coating's antimicrobial activity, we believe that the present work suggests for the first time that the chemistry of polymer brushes can also greatly influence

the activity of the overall coating. Hence, the choice of polymer to conjugate peptides to is an important factor when designing a tethered AMP coating.

Of the two peptides that show antimicrobial activity, peptide E6 resulted in more potent activity than peptide Tet20 (Fig. 16). When testing peptide concentrations between 32  $\mu\text{g/mL}$  to 256  $\mu\text{g/mL}$ , PDMA-E6 consistently showed better antimicrobial activity against all of *E. coli*, *S. aureus*, and *P. aeruginosa* than PDMA-Tet20. At 128  $\mu\text{g/mL}$  peptide, conjugation with E6 killed both *E. coli* and *S. aureus* 6 logs better than conjugated to the same concentration of Tet20 (Fig. 16A-C), despite the fact that Tet20 was more potent than E6 when tested in their free-floating forms. This may be a result of differences in the peptide sequence, peptide density, and surface hydrophobicity. When comparing E6 to Tet20, the former peptide has more hydrophobic residues located in the centre of the peptide chain, away from the fixed conjugation site and thus allowing for optimal interaction with the bacterial membrane upon contact. Figure 27 highlights the hydrophobic residues in both E6 and Tet20.



**Figure 27.** Amino acid sequence of peptides E6 and Tet20. Red, underlined residues indicate those of high hydrophobicity characteristic.

With PDMA-E6 giving us the best antimicrobial activity based on coated NPs, we proceeded to testing the coating on 18G PU catheters *in vitro*, which gives us a more realistic understanding of the coating since catheters do not have as high of a surface-area-to-volume ratio than NPs. Moreover, PU is a common biomaterial in which human urinary catheters are

comprised of, allowing the results to relate more to the ultimate goal of the study: to develop an AMP coating for urinary catheters to help prevent and lower the occurrences of CAUTI.

*In vitro* testing of PDMA-E6 coated PU catheters showed promising results; when testing the samples against *P. aeruginosa*, coated catheters reduced bacterial adhesion by 87.4% compared to uncoated samples. Interestingly, brush-only coated catheters also reduced bacterial adhesion compared to uncoated samples, albeit to a slightly lower extent (65.6%) (Fig.17A). Activity against the growth or survival of planktonic bacteria were similar for peptide-brush and brush-only coatings, with 63.8% and 69.8% reduction in bacterial load compared to untreated controls, respectively. This was an interesting finding, as little/no effect was seen for polymer brush coatings without peptides when tested using NPs. Possible explanations may be that bacteria tend to grow faster when there is a surface for them to adhere onto. Since a 10 mm-long 18G catheter piece provides a much larger, continuous surface area than NPs which are only a few nm in diameter, bacteria, which tends to be a few  $\mu\text{m}$  in diameter, will be more capable of adhering onto the catheters than NPs (Fig. 28). Once adhered, bacteria will grow faster especially as a biofilm forms. Once a mature biofilm forms, individual bacterial cells from the film can detach, becoming a planktonic cell which may later re-adhere onto a nearby area of the surface to form more biofilms. Given that polymer brushes themselves are anti-fouling, by preventing the adsorption of biomolecules within the surrounding medium, less bacteria may readily adhere onto the implant surface, thus preventing the subsequent formation of a biofilm. With less adhesion, which allows for rapid bacterial growth, less bacteria will be present both on the implant and within the surrounding medium compared to cultures incubated with uncoated control catheters. Hence, this brush-only anti-adhesion effect was only observed with catheters but not NPs.

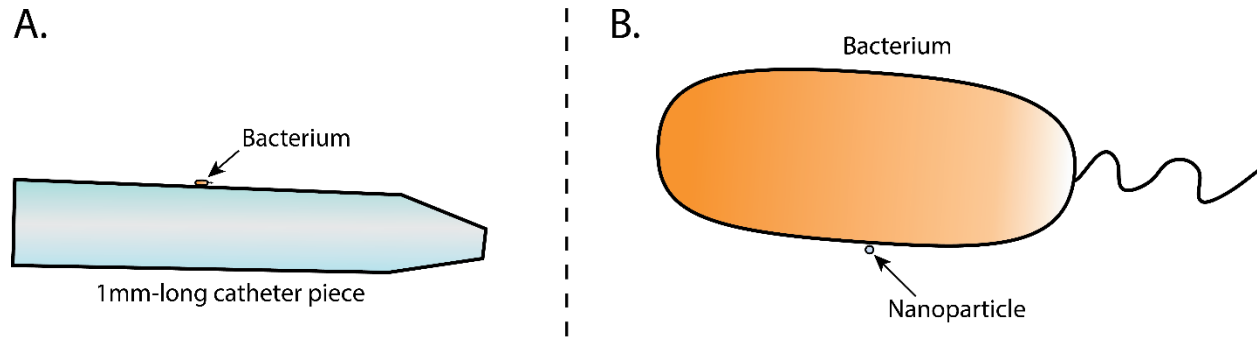


**Figure 28.** Illustration of the relative size of bacteria in comparison to: (A) 1 mm-long catheter pieces and (B) NPs. Note: This drawing for illustration purposes only, and do not represent exact size ratios.

Since not much difference was observed between peptide-brush and brush-only coatings against planktonic bacterial growth (presence of tethered peptides only further reduced bacterial growth by 6% compared to brush-only), it suggests that the tethered peptides only act on bacteria directly contacting the surface of the samples (adhesion) but have little/no effect in terms of killing the bacteria growing within the surrounding medium (Fig. 17B).

Similar findings were observed when coated and uncoated catheter pieces were tested *in vitro* against *S. saprophyticus*. Although *S. aureus* was used when testing with NPs, due to the naturally poor capability of the bacterium to adhere onto uncoated PU surfaces, *S. saprophyticus*, which is another common uropathogen, was tested against coated catheter pieces in place of *S. aureus*. Results are promising; after 6h post-incubation, a 94.1% reduction in bacterial adhesion was observed for peptide-brush-coated samples in comparison to uncoated controls. Brush-coated samples was also able to reduce bacterial adhesion by 68.8% compared to controls.

However, a much lesser degree of effect on planktonic bacterial growth was observed for *S. saprophyticus* in comparison to *P. aeruginosa*; peptide-brush coated and brush-coated catheters reduced planktonic growth of *S. saprophyticus* by 10.4% and 11.5%, respectively, in comparison to uncoated controls. Similar to results with *P. aeruginosa*, the presence of tethered peptides did not further reduce the amount of planktonic growth, suggesting the peptides to have no effect against free-floating bacteria, and that the decrease in planktonic growth observed for both peptide-brush and brush-only coatings may simply reflect the decreased in adhesion of bacteria.

Hence, although both peptide-brush and brush-only coatings have better anti-adherence activity against *S. saprophyticus* than against *P. aeruginosa*, the same observation was not observed in terms of the coatings' activity against their planktonic growth. This is possibly due to the nature of their outer membrane; being a gram-positive bacterium, *S. saprophyticus* possesses a much thicker peptidoglycan (PG) layer than the gram-negative *P. aeruginosa*; 20-80 nm thick in gram-positive bacteria, versus only 7-8 nm thick in gram-negative bacteria [134]. In addition, instead of having lipopolysaccharides (LPS) with porins like gram-negative bacteria, gram-positive bacteria have lipoteichoic acids (LTA) on its surface, which get released spontaneously into the culture medium along with PG during the growth of gram positive bacteria [135]. In order to target the outer membranes of each type of bacteria, positively-charged AMPs must bind to and neutralise the negatively-charged molecules on the bacterial membrane (LTA for gram positive bacteria, LPS for gram-negative bacteria) before binding and possibly inserting into the lipid bilayers for disruption, aided by their hydrophobic properties.

Since gram-positive bacteria do shed their LTA upon cellular division, it is possible that AMPs coated on our catheter pieces may be attracted to LTA released by growing bacterial cells,



which could subsequently block the active AMPs from attracting to and killing live bacterial cells within the surrounding culture [136, 137]. If cationic AMPs attract negatively-charged LTA on gram positive bacteria, hydrophobic residues of the peptide may allow for the insertion and disruption of the bacterial membrane, leading to bacterial cell death. The still-active AMPs could then theoretically repel the dead cellular debris away as hydrophilic, anti-fouling polymer brushes come in contact with the cellular debris. Thus, a highly effective AMP-brush coating would attract bacteria, kill them, and then repel off the cellular debris to free up the active peptides which can then act on other bacterial cells. However, if the AMPs get attracted to LTA shed off by growing cells, the LTA may simply bind to the peptides without getting repelled off, limiting the coating's ability to act on surrounding live bacterial cells (Fig. 29). This could be a possible explanation as to why we see a significant effect of our peptide-brush coating against the planktonic growth of *P. aeruginosa* which is not present for the planktonic growth of *S. saprophyticus*.

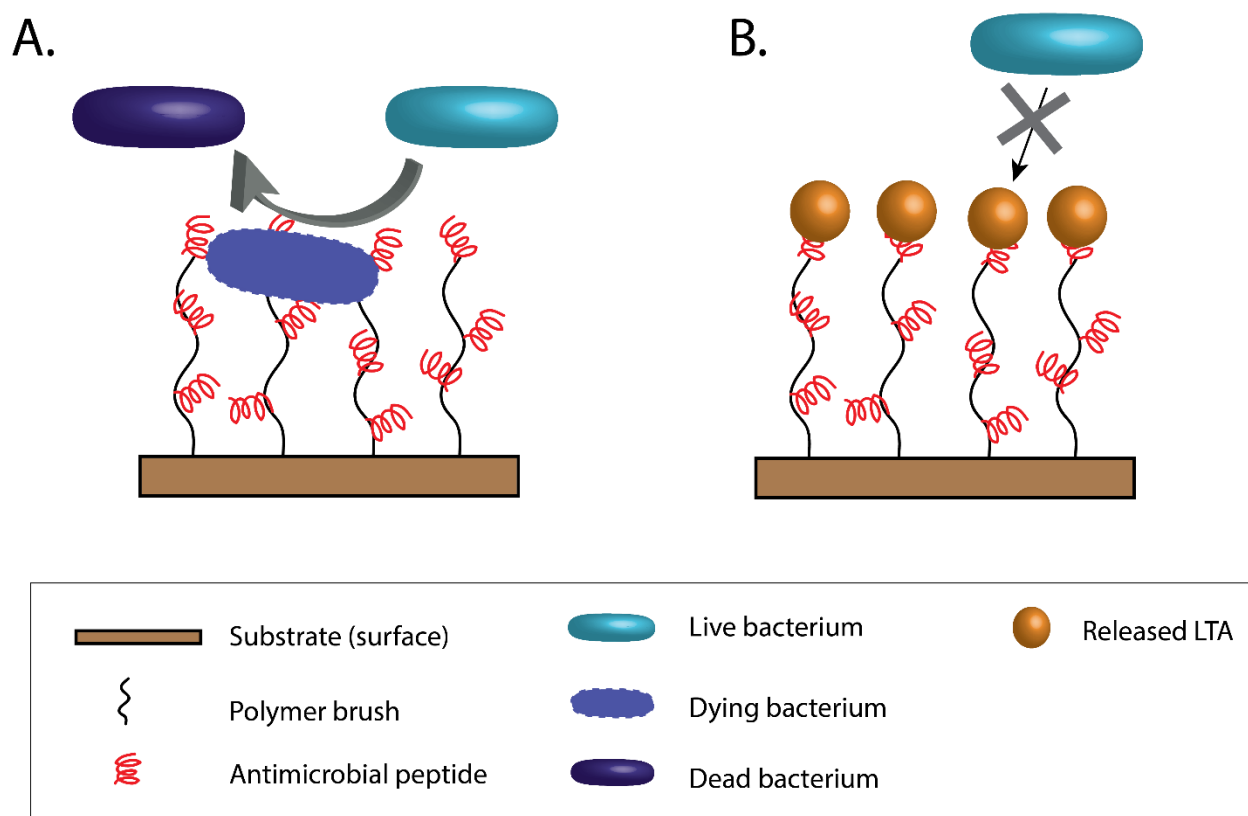


**Figure 29.** Possible outcome of when AMPs of peptide-brush coatings come in contact with (A) live bacteria and (B) LTA released by gram positive bacteria upon growth; the peptides may be able to repel off bacterial debris after killing the live bacterium, while released LTA may bind to AMPs without getting released, thereby preventing the peptides from acting on surrounding live bacteria.

With PDMA-E6-coated catheter pieces showing significant anti-adhesion and antimicrobial activity against *P. aeruginosa*, we tested the effectiveness of our coating further using a clinically relevant *in vivo* model.

The transurethral catheterization model (Fig. 11) was first tested using uncoated catheters as a means of ensuring that the model works. However, based on our multiple tries, out of 8 mice, only 3 of them managed to be successfully bladder catheterized and hold on to the

implants for a total of 5 days. The rest of the rats were either unsuccessfully catheterized, or they lost their implanted catheter within 2 days post-catheterization. After a urinary tract necropsy of several rats, we discovered that the anatomy of the Sprague Dawley rat was unique in that their urethral opening leads to a split route, one towards a dead-end groove, the other end towards the urethra (Fig. 19).

With high rate of rats urinating out implanted catheters and the difficulty involved in catheterizing them due to the presence of the groove, another *in vivo* model, the percutaneous catheterization model, was adopted, which involved percutaneously catheterizing mice via ultrasound guidance (Fig. 13). This *in vivo* CAUTI model was recently developed in our laboratory and published by Janssen *et al.*, which is applicable to both female and male mice; previously reported CAUTI mouse models introduce the implant piece into the rodent bladder either transurethrally via blind insertion or through tedious surgical procedures where there is a high risk for post-procedural complications, including surgical contamination or even sepsis. By percutaneously catheterizing mice with the visual aid of ultrasound, one can be confident in successfully catheterizing the mouse bladder (can see successfully implanted catheter on screen) using a procedure that is minimally invasive while minimizing the duration of the procedure (only takes minutes to catheterize mice this way when performed by a skilled technician). This is significant, as by being able to percutaneously catheterize both male and female mice, CAUTI, which is normally present in both men and women, can be properly studied in both genders, allowing for findings that are more applicable to humans. Unfortunately, this model can only be applied to mice but not rats, as several attempts to percutaneously catheterize rats suggested the rat bladder wall to be too tough and thick to be successfully penetrated to implant the catheter piece.

Using the described *in vivo* model, uncoated and PDMA-E6-coated 4 mm-long 24G PU catheter pieces were introduced to mice bladder, and *P. aeruginosa* was instilled into the bladder one day post-implantation. IVIS imaging showed the presence of luminescent bacteria at similar levels in all mice immediately after bacterial instillation. However, by 7 days post-instillation, the amount of detected luminescence was 97.7% in mice implanted with a coated catheter piece compared to those bearing an uncoated catheter (untreated controls), suggesting the peptide-brush coating to be highly effective under *in vivo* settings (Fig. 21-22). This was confirmed via CFU counts of both bacteria adhered only the implant pieces at 7 days post-instillation and bacteria found within the urine of treated and untreated mice. There was a 99.9958% reduction in bacterial adhesion on coated catheters when compared to that of uncoated samples. CFU counts from collected urine also looked promising; a 99.8660% reduction in bacteria was observed in urine collected from treated mice in comparison to urine collected from untreated control mice (Fig. 26). These results were significantly positive in terms of demonstrating the anti-adhesion and antimicrobial properties of our PDMA-E6 coating, as *in vivo* results look even more promising than our *in vitro* results with coated and uncoated PU catheters.

To understand why *in vivo* testing resulted in better anti-adhesion and antimicrobial activity of our AMP-brush coating than our *in vitro* experiments, it is important to keep in mind that urine inside the mouse bladder is constantly being expelled while fresh urine is flowing in as the mouse drinks water as part of its daily needs. However, when coatings were tested *in vitro*, the catheters were incubated inside 1 mL of LB containing bacteria for a total of 6 h with minimal agitation and static flow.

As bacteria within the urine come in contact with the indwelling catheter surface, tethered peptides from the coated samples would kill any incoming bacteria, as suggested by the decrease

in adhesion levels observed in Fig. 26A. Once those bacteria are killed, they are believed to leave behind bacterial debris, which gets distributed around the surrounding urine inside the mouse bladder. When these debris come in contact with the mouse bladder epithelial cells, they can act as inactivated vaccines, where the bacterial particles will evoke an immune response without leading to infection. Once these particles are recognized by the mouse immune system, immune reactions towards any live bacteria may be improved as a result of the mouse adaptive immune system responding, such as the presence of specific T cells and B cells. This immunomodulatory effect may explain for the decrease in bacteria within the urine for treated mice; the tethered peptides produce bacterial debris picked up by the host cells, leading to increased immune responses that help fight off the infection.

Additionally, it has been known that free-floating peptides are able to travel into the host cells and lead to immunomodulatory effects. However, it is possible that the mere interaction of tethered peptides to the surface of host cells may also elicit some immunomodulatory responses. However, more studies would be needed to support this hypothesis.

Overall, both *in vitro* and *in vivo* results look very promising with regards to the anti-bacterial adhesion capability of our E6-PDMA implant coating. Since the development of CAUTI does start off with the adhesion of bacteria onto the implant surface followed by subsequent biofilm formation and infection, it is important to note that the current E6-PDMA coating does show significant anti-bacterial adhesion properties against both gram-positive and gram-negative bacteria. Although *in vitro* testing of coated catheters against *S. saprophyticus* showed minimal effect on the planktonic growth of the bacterium, it will be interesting to see how well the coating will work against the bacterium when tested using the current CAUTI animal model. Since bladder contents will be constantly refreshed overtime, it is possible that

any released LTA from growing bacterial cells will be expelled out of the mouse bladder upon urination. If this is the case, then perhaps E6-PDMA-coated catheters will show better activity against planktonic bacteria *in vivo* than *in vitro*, similar to the *in vivo* *P. aeruginosa* results observed.

## CHAPTER 5: CONCLUSION AND FUTURE DIRECTIONS

In this study, we have established the efficacy of peptide-brush coating, E6-PDMA, both *in vitro* and *in vivo*. This brings us a step closer to preventing and limiting the occurrence of CAUTI; by designing effective antimicrobial coatings to prevent the adhesion of bacterial onto the implant surface, the chances of a biofilm formation is significantly decreased. This is important, as biofilms are the key culprit leading to bacterial infections.

Once an effective anti-adhesion and antimicrobial coating has been developed, due to the biocompatible nature of polymer brushes, the coating can be applied to various types of biomaterial, expanding the application of these coatings not only to urinary catheters, but also to any medical devices that may be susceptible to bacterial adhesion and infection.

Indeed, more experiments must be performed to fully assess both the efficacy and safety of the currently studied AMP-brush coating. These may include further *in vivo* testing of the coating against various gram-positive and gram-negative bacteria. Examination of the bladders of treated and untreated mice may also provide valuable data on how coated and uncoated implants affect the mice. Further experiments can also look into the cytokines released by the mice into the bladder in response to coated versus uncoated implants, which will allow for a better understanding in terms of what types of immune responses are elicited upon infection and treatment. This technology has the ability to significantly reduce the major problem in healthcare of urinary device-related urinary tract infection.

## REFERENCES

1. Nowatzki, P.J., et al., *Salicylic acid-releasing polyurethane acrylate polymers as anti-biofilm urological catheter coatings*. Acta Biomater, 2012. **8**(5): p. 1869-80.
2. Nicolle, L.E., *Catheter associated urinary tract infections*. Critical Care, 2014. **1**: p. 4.1.
3. Saint, S., et al., *Catheter-associated urinary tract infection and the Medicare rule changes*. Ann Intern Med, 2009. **150**(12): p. 877-84.
4. Cardenas, D.D. and T.M. Hooton, *Urinary tract infection in persons with spinal cord injury*. Arch Phys Med Rehabil, 1995. **76**(3): p. 272-80.
5. Warren, J.W., *Catheter-associated urinary tract infections*. Int J Antimicrob Agents, 2001. **17**(4): p. 299-303.
6. Warren, J.W., *Catheter-associated urinary tract infections*. Infect Dis Clin North Am, 1997. **11**(3): p. 609-22.
7. Robinson, J., *Deflation of a Foley catheter balloon*. Nurs Stand, 2003. **17**(27): p. 33-8.
8. Macias Nuñez, J.F., et al., *The aging kidney in health and disease*, 2008, Springer,: New York. p. 1 online resource.
9. Zimmerli, W. and A. Trampuz, *Implant-associated infection*, in *Biofilm Infections*. 2011, Springer. p. 69-90.
10. Dave, R.N., H.M. Joshi, and V.P. Venugopalan, *Novel biocatalytic polymer-based antimicrobial coatings as potential ureteral biomaterial: preparation and in vitro performance evaluation*. Antimicrob Agents Chemother, 2011. **55**(2): p. 845-53.
11. Gristina, A.G., et al., *Cell biology and molecular mechanisms in artificial device infections*. Int J Artif Organs, 1993. **16**(11): p. 755-63.
12. Stickler, D., et al., *Proteus mirabilis biofilms and the encrustation of urethral catheters*. Urol Res, 1993. **21**(6): p. 407-11.
13. Chatterjee, S., et al., *Biofilms on indwelling urologic devices: microbes and antimicrobial management prospect*. Ann Med Health Sci Res, 2014. **4**(1): p. 100-4.
14. Tenke, P., et al., *Update on biofilm infections in the urinary tract*. World J Urol, 2012. **30**(1): p. 51-7.
15. Reid, G., *Biofilms in infectious disease and on medical devices*. Int J Antimicrob Agents, 1999. **11**(3-4): p. 223-6; discussion 237-9.
16. Winson, L., *Catheterization: a need for improved patient management*. Br J Nurs, 1997. **6**(21): p. 1229-32, 1234, 1251-2.
17. Hoiby, N., et al., *The clinical impact of bacterial biofilms*. Int J Oral Sci, 2011. **3**(2): p. 55-65.
18. Tenke, P., et al., *The role of biofilm infection in urology*. World J Urol, 2006. **24**(1): p. 13-20.
19. Stewart, P.S. and J.W. Costerton, *Antibiotic resistance of bacteria in biofilms*. Lancet, 2001. **358**(9276): p. 135-8.
20. Keane, P.F., et al., *Characterization of biofilm and encrustation on ureteric stents in vivo*. Br J Urol, 1994. **73**(6): p. 687-91.
21. Malic, S., et al., *Development of an "early warning" sensor for encrustation of urinary catheters following Proteus infection*. Journal of Biomedical Materials Research Part B: Applied Biomaterials, 2012. **100B**(1): p. 133-137.



22. Arciola, C.R., et al., *Biofilm formation in Staphylococcus implant infections. A review of molecular mechanisms and implications for biofilm-resistant materials*. Biomaterials, 2012. **33**(26): p. 5967-82.
23. Rudrappa, T., et al., *A degradation product of the salicylic acid pathway triggers oxidative stress resulting in down-regulation of Bacillus subtilis biofilm formation on Arabidopsis thaliana roots*. Planta, 2007. **226**(2): p. 283-97.
24. Prithiviraj, B., et al., *Staphylococcus aureus pathogenicity on Arabidopsis thaliana is mediated either by a direct effect of salicylic acid on the pathogen or by SA-dependent, NPR1-independent host responses*. Plant J, 2005. **42**(3): p. 417-32.
25. Alem, M.A. and L.J. Douglas, *Effects of aspirin and other nonsteroidal anti-inflammatory drugs on biofilms and planktonic cells of Candida albicans*. Antimicrob Agents Chemother, 2004. **48**(1): p. 41-7.
26. Stepanovic, S., et al., *Influence of acetylsalicylic acid (aspirin) on biofilm production by Candida species*. J Chemother, 2004. **16**(2): p. 134-8.
27. Hola, V., F. Ruzicka, and M. Horka, *Microbial diversity in biofilm infections of the urinary tract with the use of sonication techniques*. FEMS Immunol Med Microbiol, 2010. **59**(3): p. 525-8.
28. Morris, N.S., D.J. Stickler, and R.J. McLean, *The development of bacterial biofilms on indwelling urethral catheters*. World J Urol, 1999. **17**(6): p. 345-50.
29. Minardi, D., et al., *Urinary Catheters and Biofilm Formation*. Recent Patents on Biomarkers, 2013. **3**(3): p. 196-203.
30. Chew, B.H. and D. Lange, *Ureteral stent symptoms and associated infections: a biomaterials perspective*. Nat Rev Urol, 2009. **6**(8): p. 440-8.
31. Allison, D.G. and I.W. Sutherland, *The role of exopolysaccharides in adhesion of freshwater bacteria*. Journal of General Microbiology, 1987. **133**(5): p. 1319-1327.
32. Wagenlehner, F.M., W. Weidner, and K.G. Naber, *Optimal management of urosepsis from the urological perspective*. Int J Antimicrob Agents, 2007. **30**(5): p. 390-7.
33. Meddings, J., et al., *Reducing unnecessary urinary catheter use and other strategies to prevent catheter-associated urinary tract infection: an integrative review*. BMJ Qual Saf, 2014. **23**(4): p. 277-89.
34. Chenoweth, C.E., C.V. Gould, and S. Saint, *Diagnosis, management, and prevention of catheter-associated urinary tract infections*. Infect Dis Clin North Am, 2014. **28**(1): p. 105-19.
35. Lo, E., et al., *Strategies to prevent catheter-associated urinary tract infections in acute care hospitals*. Infect Control Hosp Epidemiol, 2008. **29 Suppl 1**: p. S41-50.
36. Gould, C.V., et al., *Guideline for prevention of catheter-associated urinary tract infections 2009*. Infect Control Hosp Epidemiol, 2010. **31**(4): p. 319-26.
37. Saint, S., et al., *Are physicians aware of which of their patients have indwelling urinary catheters?* Am J Med, 2000. **109**(6): p. 476-80.
38. Meddings, J., et al., *Systematic review and meta-analysis: reminder systems to reduce catheter-associated urinary tract infections and urinary catheter use in hospitalized patients*. Clin Infect Dis, 2010. **51**(5): p. 550-60.
39. Saint, S., et al., *Condom versus indwelling urinary catheters: a randomized trial*. J Am Geriatr Soc, 2006. **54**(7): p. 1055-61.
40. Saint, S., et al., *Urinary catheters: what type do men and their nurses prefer?* J Am Geriatr Soc, 1999. **47**(12): p. 1453-7.

41. Niel-Weise, B.S. and P.J. van den Broek, *Urinary catheter policies for short-term bladder drainage in adults*. Cochrane Database Syst Rev, 2005(3): p. CD004203.
42. Stevens, E., *Bladder ultrasound: avoiding unnecessary catheterizations*. Medsurg Nurs, 2005. **14**(4): p. 249-53.
43. Heidenreich, A. and A. Thissen, *Urosepsis*, in *Urology at a Glance*, A.S. Merseburger, M.A. Kuczyk, and J.W. Moul, Editors. 2014, Springer Berlin Heidelberg. p. 47-52.
44. Tadesse, D.A., et al., *Antimicrobial drug resistance in Escherichia coli from humans and food animals, United States, 1950-2002*. Emerg Infect Dis, 2012. **18**(5): p. 741-9.
45. Cullen, I.M., et al., *The changing pattern of antimicrobial resistance within 42,033 Escherichia coli isolates from nosocomial, community and urology patient-specific urinary tract infections, Dublin, 1999-2009*. BJU Int, 2012. **109**(8): p. 1198-206.
46. Dennison, S.R., et al., *A novel form of bacterial resistance to the action of eukaryotic host defense peptides, the use of a lipid receptor*. Biochemistry, 2013. **52**(35): p. 6021-9.
47. Syed, M.A., et al., *Antibacterial effects of Tungsten nanoparticles on the Escherichia coli strains isolated from catheterized urinary tract infection (UTI) cases and Staphylococcus aureus*. New Microbiol, 2010. **33**(4): p. 329-35.
48. Lo, J., D. Lange, and B. Chew, *Ureteral Stents and Foley Catheters-Associated Urinary Tract Infections: The Role of Coatings and Materials in Infection Prevention*. Antibiotics, 2014. **3**(1): p. 87.
49. Chang, W.K., et al., *Triclosan-impregnated sutures to decrease surgical site infections: systematic review and meta-analysis of randomized trials*. Ann Surg, 2012. **255**(5): p. 854-9.
50. Stickler, D.J., G.L. Jones, and A.D. Russell, *Control of encrustation and blockage of Foley catheters*. Lancet, 2003. **361**(9367): p. 1435-7.
51. Chew, B.H., et al., *In-vitro activity of triclosan-eluting ureteral stents against common bacterial uropathogens*. J Endourol, 2006. **20**(11): p. 949-58.
52. Cadieux, P.A., et al., *Triclosan loaded ureteral stents decrease proteus mirabilis 296 infection in a rabbit urinary tract infection model*. J Urol, 2006. **175**(6): p. 2331-5.
53. Cadieux, P.A., et al., *Use of triclosan-eluting ureteral stents in patients with long-term stents*. J Endourol, 2009. **23**(7): p. 1187-94.
54. Wignall, G.R., et al., *The effects of triclosan on uropathogen susceptibility to clinically relevant antibiotics*. J Endourol, 2008. **22**(10): p. 2349-56.
55. Desai, D.G., et al., *Silver or nitrofurazone impregnation of urinary catheters has a minimal effect on uropathogen adherence*. J Urol, 2010. **184**(6): p. 2565-71.
56. Elwood, C.N., et al., *Understanding urinary conditioning film components on ureteral stents: profiling protein components and evaluating their role in bacterial colonization*. Biofouling, 2013. **29**(9): p. 1115-22.
57. Tunney, M.M. and S.P. Gorman, *Evaluation of a poly(vinyl pyrrolidone)-coated biomaterial for urological use*. Biomaterials, 2002. **23**(23): p. 4601-8.
58. Liu, X., et al., *Poly(N-vinylpyrrolidone)-modified surfaces for biomedical applications*. Macromol Biosci, 2013. **13**(2): p. 147-54.
59. Riedl, C.R., et al., *Heparin coating reduces encrustation of ureteral stents: a preliminary report*. Int J Antimicrob Agents, 2002. **19**(6): p. 507-10.
60. Tenke, P., et al., *Bacterial biofilm formation on urologic devices and heparin coating as preventive strategy*. Int J Antimicrob Agents, 2004. **23 Suppl 1**: p. S67-74.

61. Schierholz, J.M., et al., *Antimicrobial substances and effects on sessile bacteria*. Zentralbl Bakteriол, 1999. **289**(2): p. 165-77.
62. Lange, D., et al., *Uropathogen interaction with the surface of urological stents using different surface properties*. J Urol, 2009. **182**(3): p. 1194-200.
63. Nakatsuji, T. and R.L. Gallo, *Antimicrobial peptides: old molecules with new ideas*. J Invest Dermatol, 2012. **132**(3 Pt 2): p. 887-95.
64. Kitamura, T., J.E. Zerwekh, and C.Y. Pak, *Partial biochemical and physicochemical characterization of organic macromolecules in urine from patients with renal stones and control subjects*. Kidney Int, 1982. **21**(2): p. 379-86.
65. Choong, S.K., S. Wood, and H.N. Whitfield, *A model to quantify encrustation on ureteric stents, urethral catheters and polymers intended for urological use*. BJU Int, 2000. **86**(4): p. 414-21.
66. Jamal, M.A., et al., *In vivo biocompatibility and in vitro efficacy of antimicrobial gentamicin-coated central catheters*. Antimicrob Agents Chemother, 2015. **59**(9): p. 5611-8.
67. Tan, H., et al., *The use of quaternised chitosan-loaded PMMA to inhibit biofilm formation and downregulate the virulence-associated gene expression of antibiotic-resistant staphylococcus*. Biomaterials, 2012. **33**(2): p. 365-77.
68. Hazan, Z., et al., *Effective prevention of microbial biofilm formation on medical devices by low-energy surface acoustic waves*. Antimicrob Agents Chemother, 2006. **50**(12): p. 4144-52.
69. Price, C.T., I.R. Lee, and J.E. Gustafson, *The effects of salicylate on bacteria*. Int J Biochem Cell Biol, 2000. **32**(10): p. 1029-43.
70. Ouimet, M.A., et al., *Poly(anhydride-ester) and poly(N-vinyl-2-pyrrolidone) blends: salicylic acid-releasing blends with hydrogel-like properties that reduce inflammation*. Macromol Biosci, 2015. **15**(3): p. 342-50.
71. Gao, G., et al., *The biocompatibility and biofilm resistance of implant coatings based on hydrophilic polymer brushes conjugated with antimicrobial peptides*. Biomaterials, 2011. **32**(16): p. 3899-909.
72. Gao, G., et al., *Antibacterial surfaces based on polymer brushes: investigation on the influence of brush properties on antimicrobial peptide immobilization and antimicrobial activity*. Biomacromolecules, 2011. **12**(10): p. 3715-27.
73. Glinel, K., et al., *Antibacterial surfaces developed from bio-inspired approaches*. Acta Biomater, 2012. **8**(5): p. 1670-84.
74. Lo, J.C. and D. Lange, *Current and potential applications of host-defense peptides and proteins in urology*. Biomed Res Int, 2015. **2015**: p. 189016.
75. Jenssen, H., P. Hamill, and R.E. Hancock, *Peptide antimicrobial agents*. Clinical microbiology reviews, 2006. **19**(3): p. 491-511.
76. Hancock, R.E., *Cationic peptides: effectors in innate immunity and novel antimicrobials*. Lancet Infect Dis, 2001. **1**(3): p. 156-64.
77. Minardi, D., et al., *The antimicrobial peptide tachyplesin III coated alone and in combination with intraperitoneal piperacillin-tazobactam prevents ureteral stent Pseudomonas infection in a rat subcutaneous pouch model*. Peptides, 2007. **28**(12): p. 2293-8.
78. Fjell, C.D., et al., *Designing antimicrobial peptides: form follows function*. Nat Rev Drug Discov, 2012. **11**(1): p. 37-51.

79. Dubos, R.J., R.D. Hotchkiss, and A.F. Coburn, *The effect of gramicidin and tyrocidine on bacterial metabolism*. Journal of Biological Chemistry, 1942. **146**(2): p. 421-426.
80. Delves-Broughton, J., et al., *Applications of the bacteriocin, nisin*. Antonie van Leeuwenhoek, 1996. **69**(2): p. 193-202.
81. Fox, J.L., *Antimicrobial peptides stage a comeback*. Nat Biotechnol, 2013. **31**(5): p. 379-82.
82. Mangoni, M.L., *Host-defense peptides: from biology to therapeutic strategies*. Cell Mol Life Sci, 2011. **68**(13): p. 2157-9.
83. Baltzer, S.A. and M.H. Brown, *Antimicrobial peptides: promising alternatives to conventional antibiotics*. J Mol Microbiol Biotechnol, 2011. **20**(4): p. 228-35.
84. Hancock, R.E. and H.G. Sahl, *Antimicrobial and host-defense peptides as new anti-infective therapeutic strategies*. Nat Biotechnol, 2006. **24**(12): p. 1551-7.
85. Williams, R.L., et al., *Antimicrobial decapeptide KSL-W enhances neutrophil chemotaxis and function*. Peptides, 2012. **33**(1): p. 1-8.
86. Ali, A.S., et al., *Maintaining a sterile urinary tract: the role of antimicrobial peptides*. J Urol, 2009. **182**(1): p. 21-8.
87. Marr, A.K., W.J. Gooderham, and R.E. Hancock, *Antibacterial peptides for therapeutic use: obstacles and realistic outlook*. Curr Opin Pharmacol, 2006. **6**(5): p. 468-72.
88. Glaser, R., et al., *Antimicrobial psoriasin (S100A7) protects human skin from Escherichia coli infection*. Nat Immunol, 2005. **6**(1): p. 57-64.
89. Wimley, W.C., *Describing the mechanism of antimicrobial peptide action with the interfacial activity model*. ACS Chem Biol, 2010. **5**(10): p. 905-17.
90. Li, Y., et al., *Overview on the recent study of antimicrobial peptides: origins, functions, relative mechanisms and application*. Peptides, 2012. **37**(2): p. 207-15.
91. Salwiczek, M., et al., *Emerging rules for effective antimicrobial coatings*. Trends Biotechnol, 2014. **32**(2): p. 82-90.
92. Di Luca, M., G. Maccari, and R. Nifosi, *Treatment of microbial biofilms in the post-antibiotic era: prophylactic and therapeutic use of antimicrobial peptides and their design by bioinformatics tools*. Pathog Dis, 2014. **70**(3): p. 257-70.
93. Gee, M.L., et al., *Imaging the action of antimicrobial peptides on living bacterial cells*. Sci Rep, 2013. **3**: p. 1557.
94. Hilpert, K., et al., *Screening and characterization of surface-tethered cationic peptides for antimicrobial activity*. Chemistry & biology, 2009. **16**(1): p. 58-69.
95. Cassone, M., et al., *Scope and limitations of the designer proline-rich antibacterial peptide dimer, A3-APO, alone or in synergy with conventional antibiotics*. Peptides, 2008. **29**(11): p. 1878-86.
96. Chen, Y.Q., et al., *A cationic amphiphilic peptide ABP-CM4 exhibits selective cytotoxicity against leukemia cells*. Peptides, 2010. **31**(8): p. 1504-10.
97. Badosa, E., et al., *A library of linear undecapeptides with bactericidal activity against phytopathogenic bacteria*. Peptides, 2007. **28**(12): p. 2276-85.
98. Lundy, F.T., et al., *Antimicrobial activity of truncated alpha-defensin (human neutrophil peptide (HNP)-1) analogues without disulphide bridges*. Mol Immunol, 2008. **45**(1): p. 190-3.
99. Savoia, D., et al., *Synthesis and antimicrobial activity of dermaseptin S1 analogues*. Bioorg Med Chem, 2008. **16**(17): p. 8205-9.

100. Zhou, J., et al., *Sequence characterization and expression patterns of two defensin-like antimicrobial peptides from the tick Haemaphysalis longicornis*. Peptides, 2007. **28**(6): p. 1304-10.
101. Ahn, H.S., et al., *Design and synthesis of cyclic disulfide-bonded antibacterial peptides on the basis of the alpha helical domain of Tenecin 1, an insect defensin*. Bioorg Med Chem, 2008. **16**(7): p. 4127-37.
102. Ahn, H.S., et al., *Design and synthesis of novel antimicrobial peptides on the basis of alpha helical domain of Tenecin 1, an insect defensin protein, and structure-activity relationship study*. Peptides, 2006. **27**(4): p. 640-8.
103. Podda, E., et al., *Dual mode of action of Bac7, a proline-rich antibacterial peptide*. Biochim Biophys Acta, 2006. **1760**(11): p. 1732-40.
104. Zelezetsky, I., et al., *Identification and optimization of an antimicrobial peptide from the ant venom toxin pilosulin*. Arch Biochem Biophys, 2005. **434**(2): p. 358-64.
105. Palm, C., S. Netzereab, and M. Hallbrink, *Quantitatively determined uptake of cell-penetrating peptides in non-mammalian cells with an evaluation of degradation and antimicrobial effects*. Peptides, 2006. **27**(7): p. 1710-6.
106. Li, X., et al., *Antimicrobial functionalization of silicone surfaces with engineered short peptides having broad spectrum antimicrobial and salt-resistant properties*. Acta Biomater, 2014. **10**(1): p. 258-66.
107. Rapsch, K., et al., *Identification of antimicrobial peptides and immobilization strategy suitable for a covalent surface coating with biocompatible properties*. Bioconjug Chem, 2014. **25**(2): p. 308-19.
108. Yoshinari, M., et al., *Prevention of biofilm formation on titanium surfaces modified with conjugated molecules comprised of antimicrobial and titanium-binding peptides*. Biofouling, 2010. **26**(1): p. 103-10.
109. Lim, K., et al., *Development of a catheter functionalized by a polydopamine peptide coating with antimicrobial and antibiofilm properties*. Acta Biomater, 2015. **15**: p. 127-38.
110. Pasupuleti, M., A. Schmidtchen, and M. Malmsten, *Antimicrobial peptides: key components of the innate immune system*. Critical Reviews in Biotechnology, 2011. **32**(2): p. 143-171.
111. Afacan, N.J., et al., *Therapeutic potential of host defense peptides in antibiotic-resistant infections*. Curr Pharm Des, 2012. **18**(6): p. 807-19.
112. Perez Espitia, P.J., et al., *Bioactive Peptides: Synthesis, Properties, and Applications in the Packaging and Preservation of Food*. Comprehensive Reviews in Food Science and Food Safety, 2012. **11**(2): p. 187-204.
113. Luan, C., et al., *Recombinant expression of antimicrobial peptides using a novel self-cleaving aggregation tag in Escherichia coli*. Canadian journal of microbiology, 2014. **60**(3): p. 113-120.
114. Li, W., et al., *Fouling control in a submerged membrane-bioreactor by the membrane surface modification*. Journal of Applied Polymer Science, 2010. **115**(4): p. 2302-2309.
115. Feng, W., et al., *Methacrylate polymer layers bearing poly(ethylene oxide) and phosphorylcholine side chains as non-fouling surfaces: In vitro interactions with plasma proteins and platelets*. Acta Biomaterialia, 2011. **7**(10): p. 3692-3699.

116. Smith, R.S., et al., *Vascular Catheters with a Nonleaching Poly-Sulfobetaine Surface Modification Reduce Thrombus Formation and Microbial Attachment*. Vol. 4. 2012. 153ra132-153ra132.
117. Thissen, H., et al., *Clinical observations of biofouling on PEO coated silicone hydrogel contact lenses*. Biomaterials, 2010. **31**(21): p. 5510-5519.
118. Rodriguez-Emmenegger, C., et al., *Polymer Brushes Showing Non-Fouling in Blood Plasma Challenge the Currently Accepted Design of Protein Resistant Surfaces*. Macromolecular Rapid Communications, 2011. **32**(13): p. 952-957.
119. McArthur, S.L., et al., *Effect of polysaccharide structure on protein adsorption*. Colloids and Surfaces B: Biointerfaces, 2000. **17**(1): p. 37-48.
120. Meyers, S.R. and M.W. Grinstaff, *Biocompatible and bioactive surface modifications for prolonged in vivo efficacy*. Chem Rev, 2012. **112**(3): p. 1615-32.
121. Zhang, L., et al., *Zwitterionic hydrogels implanted in mice resist the foreign-body reaction*. Nat Biotech, 2013. **31**(6): p. 553-556.
122. Gabriel, M., et al., *Preparation of LL-37-grafted titanium surfaces with bactericidal activity*. Bioconjug Chem, 2006. **17**(2): p. 548-50.
123. Peyre, J., et al., *Co-grafting of amino-poly(ethylene glycol) and Magainin I on a TiO<sub>2</sub> surface: tests of antifouling and antibacterial activities*. J Phys Chem B, 2012. **116**(47): p. 13839-47.
124. Blin, T., et al., *Bactericidal microparticles decorated by an antimicrobial peptide for the easy disinfection of sensitive aqueous solutions*. Biomacromolecules, 2011. **12**(4): p. 1259-64.
125. Glinel, K., et al., *Antibacterial and antifouling polymer brushes incorporating antimicrobial peptide*. Bioconjug Chem, 2009. **20**(1): p. 71-7.
126. Laloyaux, X., et al., *Temperature-responsive polymer brushes switching from bactericidal to cell-repellent*. Adv Mater, 2010. **22**(44): p. 5024-8.
127. Lim, K., et al., *Immobilization Studies of an Engineered Arginine-Tryptophan-Rich Peptide on a Silicone Surface with Antimicrobial and Antibiofilm Activity*. ACS Applied Materials & Interfaces, 2013. **5**(13): p. 6412-6422.
128. Wang, Q., et al., *Self-Assembled Poly(ethylene glycol)-co-Acrylic Acid Microgels to Inhibit Bacterial Colonization of Synthetic Surfaces*. ACS Applied Materials & Interfaces, 2012. **4**(5): p. 2498-2506.
129. Vreuls, C., et al., *Biomolecules in multilayer film for antimicrobial and easy-cleaning stainless steel surface applications*. Biofouling, 2010. **26**(6): p. 645-656.
130. Muszanska, A.K., et al., *Antiadhesive polymer brush coating functionalized with antimicrobial and RGD peptides to reduce biofilm formation and enhance tissue integration*. Biomacromolecules, 2014. **15**(6): p. 2019-26.
131. Yu, K., et al., *Interaction of blood components with cathelicidins and their modified versions*. Biomaterials, 2015. **69**: p. 201-211.
132. Kurosaka, Y., et al., *A non-surgical rat model of foreign body-associated urinary tract infection with Pseudomonas aeruginosa*. Microbiol Immunol, 2001. **45**(1): p. 9-15.
133. Gilson, L., A. Kuo, and P.V. Dunlap, *AinS and a new family of autoinducer synthesis proteins*. J Bacteriol, 1995. **177**(23): p. 6946-51.
134. Dong, X., et al., *Superior Antibacterial Activity of Photochemical Synthesized Ag-CNT Composites and their Synergistic Effects in Combination with other Antimicrobial Agents*. J Nanomed Nanotechnol, 2015. **6**(279): p. 2.

135. Scott, M.G., M.R. Gold, and R.E. Hancock, *Interaction of cationic peptides with lipoteichoic acid and gram-positive bacteria*. Infect Immun, 1999. **67**(12): p. 6445-53.
136. Ginsburg, I., *Role of lipoteichoic acid in infection and inflammation*. The Lancet Infectious Diseases, 2002. **2**(3): p. 171-179.
137. Robert, E.W.H. and M.G. Scott, *The Role of Antimicrobial Peptides in Animal Defenses*. Proceedings of the National Academy of Sciences of the United States of America, 2000. **97**(16): p. 8856-8861.